Calhoun
Institutional Archive of the Naval Postgraduate School

Calhoun: The NPS Institutional Archive

DSpace Repository

Theses and Dissertations 1. Thesis and Dissertation Collection, all items

1955

Propeller excited bossing forces

Jenks, Albert L.; Metzer, Robert P.

Massachusetts Institute of Technology

http://hdl.handle.net/10945/14528

Downloaded from NPS Archive: Calhoun

DUDLEY
KNOX
LIBRARY

Calhoun is the Naval Postgraduate School's public access digital repository for research materials and institutional publications created by the NPS community. Calhoun is named for Professor of Mathematics Guy K. Calhoun, NPS's first appointed -- and published -- scholarly author.

Dudley Knox Library / Naval Postgraduate School
411 Dyer Road / 1 University Circle
Monterey, California USA 93943

http://www.nps.edu/library

PROPELLER EXCITED BOSSING FORCES

Albert L. Jenks, Jr.
and
Robert P. Metzger

Library
U. S. Naval Postgraduate School
Monterey, California

PROPELLER EXCITED BOSSING FORCES

by

ALBERT L. JENKS, JR., LIEUTENANT, U.S. NAVY

B.S., U.S. Naval Academy
(1949)

ROBERT P. METZGER, LIEUTENANT, U.S. NAVY

B.S., U.S. Naval Academy
(1947)

SUBMITTED IN PARTIAL FULFILLMENT
OF THE REQUIREMENTS FOR THE
DEGREE OF NAVAL
ENGINEER
at the
MASSACHUSETTS INSTITUTE OF
TECHNOLOGY
May, 1965

PROPELLER EXCITED BOSSING FORCES

by

Albert L. Jenks, Jr., Lieutenant, U.S. Navy
Robert P. Metzger, Lieutenant, U.S. Navy

Submitted to the Department of Naval Architecture and Marine Engineering on 20 May 1955 in partial fulfillment of the requirements for the degree of Naval Engineer.

ABSTRACT

The objective of this thesis has been the investigation of the influence of various design and operational parameters on the magnitude and phase relationship of propeller excited bossing forces. The investigation was confined to the hydrodynamically induced forces normal to the bossing.

A model bossing was installed upstream of a four-bladed Troost propeller in the test section of the MIT Marine Propeller Tunnel. The magnitudes of the forces were determined by comparison of the response of the bossing system as instrumentation readings with readings representing the application of known forces to the bossing. Phase relationships were obtained by combining angular measurements computed from the instrumentation readings with direct angular readings, taken by means of properly timed strobe lights.

The major conclusions of this investigation are:

(1) The hydrodynamically induced vibratory force normal to the bossing is a function of propeller thrust, water velocity, clearance, and bossing length.

(2) The generally accepted law of similitude for scaling bossing forces is substantially in error for the forces measured in this investigation.

(3) The phase angle relationship between the measured force and the propeller blade is relatively insensitive to clearance, but varies with propeller thrust and bossing length.

The major recommendations resulting from this thesis are:

25785

(1) Investigate the existing law of similitude,

(2) Verify the conclusion that the magnitude of the force is a function of the water velocity, and

(3) Investigate the effect of variable wake on the magnitude of the vibratory force and its phase angle.

Thesis Supervisor: Frank M. Lewis

Title: Professor of Marine Engineering

Cambridge, Massachusetts
20 May 1955

Secretary of the Faculty
Massachusetts Institute of Technology
Cambridge 39, Massachusetts

Dear Sir:

In accordance with the requirement for the Degree of Naval Engineer, we submit herewith a thesis entitled: "Propeller Excited Bossing Forces".

Respectfully yours,

ACKNOWLEDGEMENT

Without the patient guidance and engineering genius of Professor Frank M. Lewis, this investigation would not have been possible.

TABLE OF CONTENTS

Title — Page

I. Introduction 1

II. Apparatus 11

- General 11
- A. Propeller Tunnel 15
- B. Propeller 16
- C. Bossing 17
- D. Horizontal Arm 20
- E. Mounting 20
- F. Detector System 24
- G. Calibrator 30
- H. Phase System 37
- I. Speed Control 39

III. Procedure 42

IV. Results 49

V. Discussion of Results 62

VI. Conclusions 69

VII. Recommendations 71

VIII. Appendix 74

- A. Details of Procedure 75
  - 1. Determination of an Acceptable Calibration and Measure Procedure 75
  - 2. Details of Force Determination 87
  - 3. Details of Phase Angle Determination 95
- B. Sample Calculation 103
- C. Original Data and Calculations 109
- D. Bibliography 157

LIST OF FIGURES

		Page
I	Creation of Force	4
II	Propeller and Bossing in Test Section	12
III	Bossing System as Mounted in Test Section	13
IV	Propeller Testing Tunnel at M.I.T.	14
V	Bossing	18
VI	Bossing, Nose Piece, and Spacer Rings	12
VII	Horizontal Arm	21
VIII	Mountings	23
IX	Wiring Diagram of Detector Circuit	25
X	Detector	26
XI	Instrumentation Arrangement	27
XII	Calibrator	31
XIII	Lever Arms	33
XIV	Calibrator in Position for a Calibration Run	34
XV	Calibration Set-up	35
XVI	Calibrator in Position for a Measurement Run	38
XVII	Telescope Mounted in Test Section Window	38
XVIII	Propeller Tunnel Speed Control Circuit ...	40
XIX	Tuning Fork	34
XX	Force Determination	44
XXI	Plot of Force vs Thrust for Short Bossing	52
XXII	Plot of Force vs Thrust for Long Bossing..	53

LIST OF FIGURES
(continued)

Page

XXIII Plot of Force vs Clearance 54

XXIV Plot of Force vs Clearance, Semi-Log 55

XXV Plot of Force vs Thrust, Short Bossing with Variable Water Velocity 56

XXVI Plot of Force vs Water Velocity, Short Bossing 57

XXVII Bossing Clearance 88

XXVIII Force Measured 88

XXIX Force Sign Convention 89

XXX Phase Angle Relationships for Calibration and Measurement 97

XXXI Composite Phase Angle Diagram 98

XXXII Calibration Curve for Short Bossing, Clearance 1.00" 145

XXXIII Calibration Curve for Short Bossing, Clearance 1.00" 146

XXXIV Calibration Curve for Short Bossing, Clearances of 1.00", 2.00", 3.00" 147

XXXV Calibration Curve for Short Bossing, Clearances of 1.50", 2.25", 2.75" 148

XXXVI Plot of RPM vs Resultant Reading for Short Bossing, Clearance 2.00" 149

XXXVII Calibration Curve for Short Bossing, Clearance 2.00", Variable RPM 150

XXXVIII Calibration Curve for Short Bossing, Clearance 2.00", Variable RPM 151

XXXIX Calibration Curve for Short Bossing, Clearance 2.00", Variable RPM 152

LIST OF FIGURES (continued)

Page

XL Plot of J vs Thrust 153

XLI Calibration Curve for Long Bossing, Clearance 1.00", 1.25", 1.50" 154

XLII Calibration Curve for Long Bossing, Clearance, 1.50", 1.75", 2.00", 2.25", 2.50" 155

XLIII Calibration Curve for Long Bossing, Clearances of 2.50", 2.75", 3.00" 156

LIST OF TABLES

		Page
I	Calibration Run No. 1, Short Bossing, Clearance 1.00"	110
II	Calibration Run No. 2, Short Bossing, Clearance 1.00"	112
III	Measurement Run No. 1, Short Bossing, Clearance 1.00"	113
IV	Calibration Run No. 3, Short Bossing, Clearance 1.50"	114
V	Measurement Run No. 2, Short Bossing, Clearance 1.50"	115
VI	Measurement Run No. 3, Short Bossing, Clearance 1.75"	116
VII	Calibration Run No. 4, Short Bossing, Clearance 2.00"	117
VIII	Calibration Run No. 4, Short Bossing, Clearance 2.00"	119
IX	Measurement Run No. 8, Short Bossing, Clearance 2.00"	121
X	Calibration Run No. 5, Short Bossing, Clearance 2.25"	122
XI	Measurement Run No. 4, Short Bossing, Clearance 2.25"	123
XII	Measurement Run No. 5, Short Bossing, Clearance 2.50"	124
XIII	Calibration Run No. 6, Short Bossing, Clearance 2.75"	125
XIV	Measurement Run No. 6, Short Bossing, Clearance 2.75"	126
XV	Calibration Run No. 7, Short Bossing, Clearance 3.00"	127

LIST OF TABLES (continued)

Page

XVI Measurement Run No. 7, Short Bossing, Clearance 3.00" 128

XVII Measurement Run No. 9, Short Bossing, Clearance 2.00" 129

XVIII Measurement Run No. 10, Short Bossing, Clearance 2.00" 130

XIX Calibration Run No. 8, Long Bossing, Clearance 1.00" 131

XX Calibration Run No. 9, Long Bossing, Clearance 1.50" 132

XXI Calibration Run No. 10, Long Bossing, Clearance 2.00" 133

XXII Calibration Run No. 11, Long Bossing, Clearance 2.50" 134

XXIII Calibration Run No. 12, Long Bossing, Clearance 3.00" 135

XXIV Measurement Run No. 11, Long Bossing, Clearance 1.00" 136

XXV Measurement Run No. 12, Long Bossing, Clearance 1.25" 137

XXVI Measurement Run No. 13, Long Bossing, Clearance 1.50" 138

XXVII Measurement Run No. 14, Long Bossing, Clearance 1.75" 139

XXVIII Measurement Run No. 15, Long Bossing, Clearance 2.00" 140

XXIX Measurement Run No. 16, Long Bossing, Clearance 2.25" 141

XXX Measurement Run No. 17, Long Bossing, Clearance 2.50" 142

LIST OF TABLES
(continued)

Page

XXXI Measurement Run No. 18, Long Bossing, Clearance 2.75" 143

XXXII Measurement Run No. 19, Long Bossing, Clearance 3.00" 144

XXXIII Summary of Phase Angles for Short Bossing 58

XXXIV Summary of Phase Angles for Long Bossing 59

XXXV Summary of Phase Angles and Forces 60

XXXVI Comparison of Force by Law of Similitude .. 61

I. INTRODUCTION

A. GENERAL.

Theoretically for any system to vibrate at other than its natural frequency a driving force constitutes a necessary condition. The resultant vibration is a function of the frequency and magnitude of the driving or exciting force. Any periodic force acting externally or internally on the system may constitute the excitation. Considering a ship underway as the system the possible sources of excitation are numerous. The magnitude of a majority of these driving forces are such, or can be made such, that they are negligible. The rotating propeller constitutes a source of excitation which is of substantial magnitude. In geared-turbine and electric drive vessels this form of excitation is predominant and in many cases the sole source of vibration from a practical standpoint.

Propeller excited vibrations may be subdivided into two distinct groups: (1) those of once per revolution frequency which result from propeller unbalance and (2) those of blade frequency. (Blade frequency equals the number of propeller blades times the shaft speed.) Observations and previous investigations have shown that

the excitation frequency of ship hull vibrations is that of blade frequency. Further reference to propeller excited vibrations will be to excitation of blade frequency unless specified otherwise.

The propeller forces exciting hull vibrations are caused by hydrodynamic forces acting on the propeller alone and/or by the interaction of the hydrodynamic forces acting on the propeller, hull, and appendages. In general, it has been established that the excitation forces of blade frequency are transmitted to the vessel by means of: (1) shaft bearing and (2) hydrodynamically generated pressure fluctuations acting directly on the hull or its appendages.

To clearly define the source of excitation of the blade frequency vibrations,the total vibratory force acting on a vessel is separated into bearing forces and surface forces. The surface force is more completely defined by specifying the surface upon which it acts. For example, a single screw vessel may have hull surface and rudder surface forces while the twin screw vessel may have, in addition, bossing surface forces or strut surface forces. Sometimes, the hull surface forces are referred to as hull suction forces.

The bearing forces are caused principally by the wake variation across the propeller disc. From past investigations it has been generally concluded that in

both single and twin screw vessels the bearing forces are a minor source of hull vibration. The hull surface forces in single screw vessels or the bossing surface forces, if bossing are fitted, in twin screw vessels are the predominant sources of excitation.

A reasonable theoretical solution to the problem of calculating the surface forces is non-existant. A qualitative explanation of the creation of this surface force is based on the concept of circulation. Referring to Fig. 1, in position (1) the circulation is entirely around the blade element as shown. This causes a negative pressure on the forward face and a positive pressure on the after or driving face of the propeller blade. As the blade element approaches the bossing or hull surface there is a shift in the circulation to some path as shown in position (2). The shift in circulation is caused by the introduction of the structure in the path of circulation. The change in circulation is accompanied by a tangential momentum change. To produce this change a force acts on the system of hull and propeller. As the blade moves past the structure the circulation is restored to its original value with an accompanying reversal of momentum and force. Thus, a periodic force is imparted to the hull and the propeller. The forces imparted directly to the hull are the surface forces. Those imparted to the propeller result in bearing forces.

FIGURE I

CREATION OF FORCE

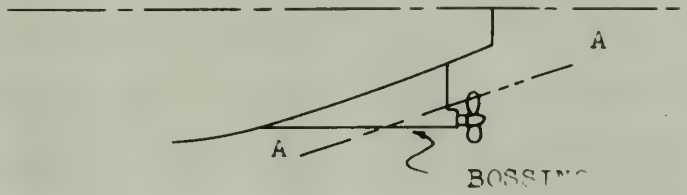

SECTION A-A

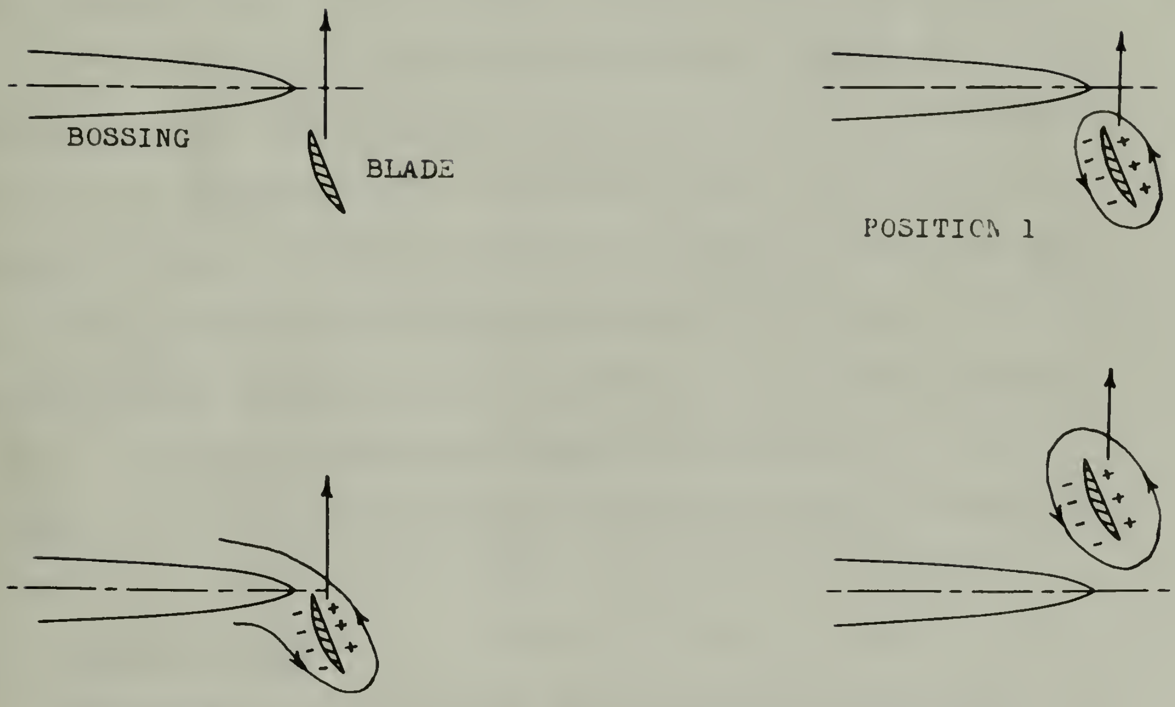

POSITION 1

POSITION 2

POSITION 3

The composition of the actual periodic force system described above is not definitely known but is seen to be a complex system. In order to permit an experimental analysis of the force system it is necessary to replace the actual system with a simplified force system which is considered to be practically equivalent. In adopting such a system only the blade frequency vibrations are considered. In the past investigations an equivalent system consisting of six components was adopted: vertical, transverse, and longitudinal forces and couples about the vertical, transverse, and longitudinal axes. From past work it has been seen that the predominant components are the vertical and horizontal forces and the couple about the longitudinal axis. It should be emphasized that these components of the adopted system are nominal, simple harmonic forces which are nearly equivalent to the actual total force system. Thus, it seems entirely feasible to reduce the entire problem of propeller excited vibrations to individual investigations of predominant equivalent force components acting on one of the known sources of vibration, i.e. bossing surface, hull surface, rudder surface, or bearings.

B. PREVIOUS WORK

In the past four basic approaches have been used to determine information regarding propeller excited hull vibrations. The basic approaches are: (1) electrical analogy,

(2) full scale shipboard measurements, (3) self propelled model testing, and (4) propeller tunnel investigations.

Professor F. M. Lewis has computed the pressure variations on an infinite plane wall, parallel to the propeller axis by an electrical analogy(10)*. The analogy consisted of magnetic measurement of the field strength of an electrical model of a propeller in which current varying conductors replaced vortex filaments. From the basic data, pressure contours could be plotted and these in turn integrated to determine the magnitude of the total vibratory force. It is also possible by this method to deduce the total mean longitudinal component of the pressure, which should correspond to the thrust deduction. This method provides the order of magnitude of the forces only. The broad assumption required for solution of the problem exclude the possibility of refined results.

The literature available on ship vibration indicates that numerous shipboard vibratory measurements have been made(19),(18),(4). The purpose of many of these investigations has been to correlate data for verification of the design formulas used in the calculations of the natural frequency of the hull strusture. The shipboard vibratory investigations in which the ob-

---

* Numbers in parentheses refer to References.

jective was to determine information regarding the source and magnitude of the excitation forces are few. Measurements of the vertical excitation forces on the OLD COLONY MARINER were made in 1952 and on the GOPHER MARINER at a later date.(11) Obviously, some shipboard measurements are necessary to establish laws of similitude so that model testing will be of significance, but full scale basic research is impractical.

Professor Lewis conducted research on the propeller excited vibration problem by means of self-propelled models under the sponsorship of the Society of Naval Architects and Marine Engineers in the early 1930's(10). A continuation of this work, again by the use of self-propelled models, has been conducted recently under the sponsorship of Panel H-8 of the Society of Naval Architects and Marine Engineers(11). Practically all of the information available on this subject is a result of this research with the self-propelled models. The system employed consists of a hull balance system. An adjustable vibration generator and a vibration detector are mounted on the model. The magnitude and direction of the vibratory force applied to the model by the vibration generator is controllable. The procedure would be to run the model at the desired advance coefficient, adjust the vibration generator to give a zero output from the vibration pick-up, and then interpret the vibration generator settings to calculate the vibratory

excitation force. The vibration detector (pick-up) can be adjusted to respond to either vertical, transverse, or torsional motion. This approach to the problem has yielded good results but has many disadvantages from an operational standpoint. The employment of self-propelled models is expensive, cumbersome, and requires some type of ship model tank facilities.

The basic approach to the problem which is the most convenient experimentally is that of a propeller tunnel investigation. Two methods have been employed in the propeller tunnel approach: (1) measurement of forces, (2) measurement of pressures. To the authors' knowledge there is no published information indicating that propeller tunnel investigations of propeller excited vibrations have been conducted at other than Massachusetts Institute of Technology. Five theses have been written concerning different phases of propeller excited vibrations since 1941. Pinkerton and Arnold(14) and Reece and Lansdowne(15) measured, directly, the vibratory force acting on a scale model of a ship's bossing. The three remaining theses measured the pressure field in various locations near the rotating propeller. Ellis and Henderson(7) measured the pressure distribution on a model bossing and integrated the pressure contours over the area of the bossing to find the total bossing surface force. Dinsmore and Hooper(6)

measured the pressure field on a flat surface directly above the propeller simulating the ship's hull. The pressure contours couldbe integrated to find the hull surface forces. McClure and Mavor(13) used, what was essentially, a pressure probe to measure pressure at various locations in an attempt to define the pressure field surrounding the propeller. All these methods involved tedious data reduction techniques, such as analysis of cathode ray oscilloscope presentations, graphical harmonic analysis, and graphical integration of pressure contours. As a result of these time consuming data reduction methods the amount of useful information and systematic testing has actually been extremely small.

C. OBJECTIVE.

The importance of reducing hull vibrations in all types of vessels needs no emphasis. Before vibration free designs can be made it is necessary to understand the mechanism of propeller excitation and to understand this mechanism additional research is necessary. The current technical interest in this problem is evidenced by(11) and the fact that a research program is now at the David Taylor Model Basin under the general advice of Research Panel H-8 of the Society of Naval Architects and Marine Engineers.

From an examination of the scope of the problem and the results of previous investigations it becomes apparent that a complete understanding of the design parameters affecting propeller excitation and their relative importance is lacking. By employment of a propeller tunnel it should be possible to investigate separately the various sources of excitation and their relationships to design or operational parameters. As discussed earlier an equivalent force system consisting of nominal simple harmonic forces may be employed and therefore each excitation source can be examined for the simple harmonic forces constituting the equivalent system. For example, an investigation of the bossing surface forces could be confined to the force normal to the bossing. A model bossing has recently been designed and developed at the Marine Propeller Tunnel at the Massachusetts Institute of Technology for use in such an investigation.

The objectives of this thesis are: (1) to assemble a satisfactory detector system for measurement of the vibratory forces normal to the bossing, (2) to arrive at an acceptable method of system calibration, and (3) to investigate as many of the variables affecting the magnitude of the vibratory forces as time permitted.

II. DESCRIPTION OF APPARATUS

GENERAL

The measurement of the vibratory force normal to the bossing was made by placing a cast aluminum bossing upstream of the propeller in the test section of the propeller tunnel. See Figures II, III, and IV. The hydrodynamically induced vibratory forces cause a rotational displacement of the bossing. This displacement is proportional to the magnitude and frequency of the excitation or vibratory force normal to the bossing. The motion of the bossing is transmitted through a hollow steel shaft to the horizontal arm and finally, by means of a vertical rod, to the moveable coil of the detector unit.See Figure III. The horizontal arm and bossing are clamped to the center portion of the hollow steel shaft which is clamped at its ends to the inside of the propeller tunnel. The dimensions of the hollow shaft are such that it responds only to the applied moment, resulting in an angular displacement or twist of the shaft with negligible bending.

The relative motion of the moveable coil in the detector, with respect to the field of a fixed energized

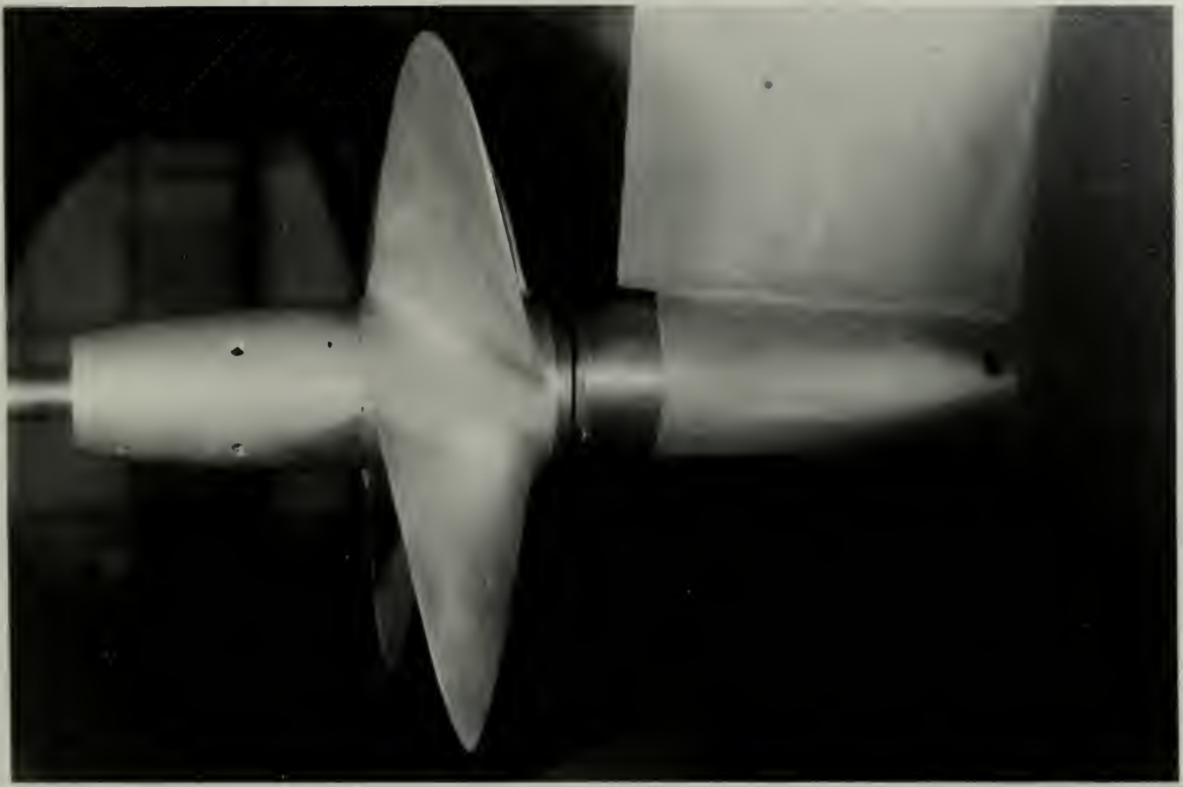

Fig. II. Propeller and Bossing mounted in test section of tunnel. (Note hole in bossing at 0.7 radius for attachment of wire from calibrator. One inch spacer is attached to bossing.)

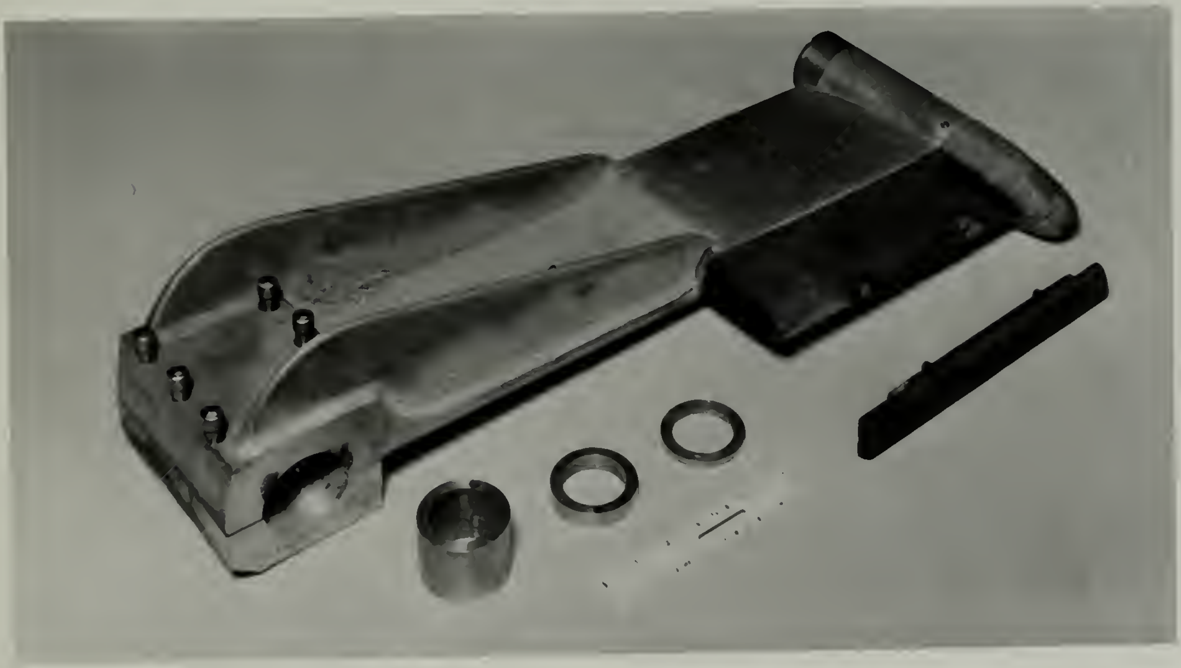

Fig. VI. Bossing, nose pieces, and spacer rings. (One inch spacer attached.)

FIGURE III

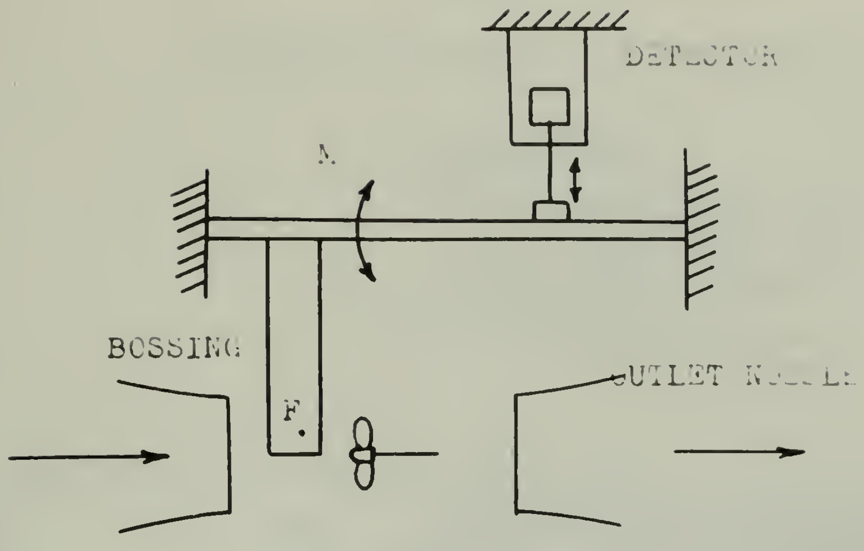

TEST SECTION

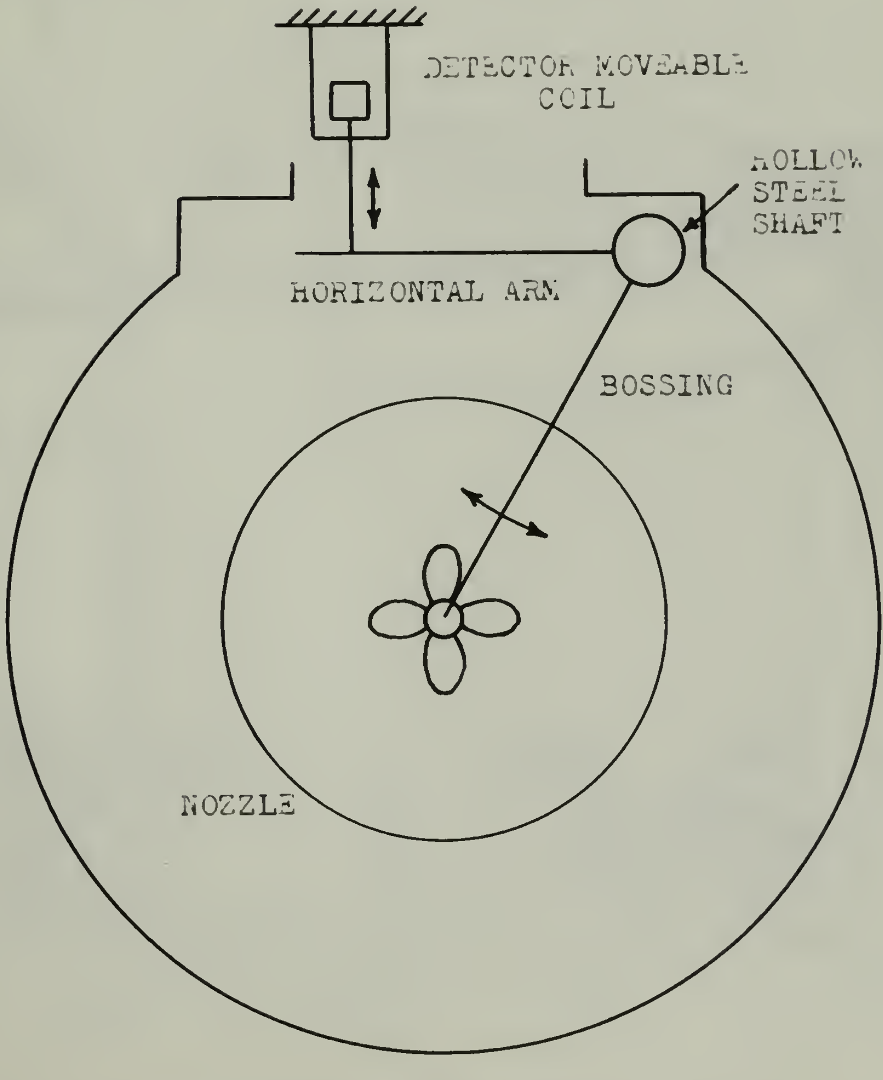

LOOKING UPSTREAM FROM OUTLET NOZZLE

FIGURE IV

PROPELLER TESTING TUNNEL AT M. I. T.

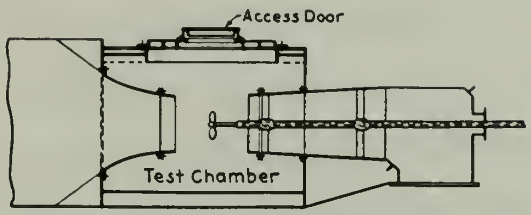

Vertical Cross-Section Through Nozzle

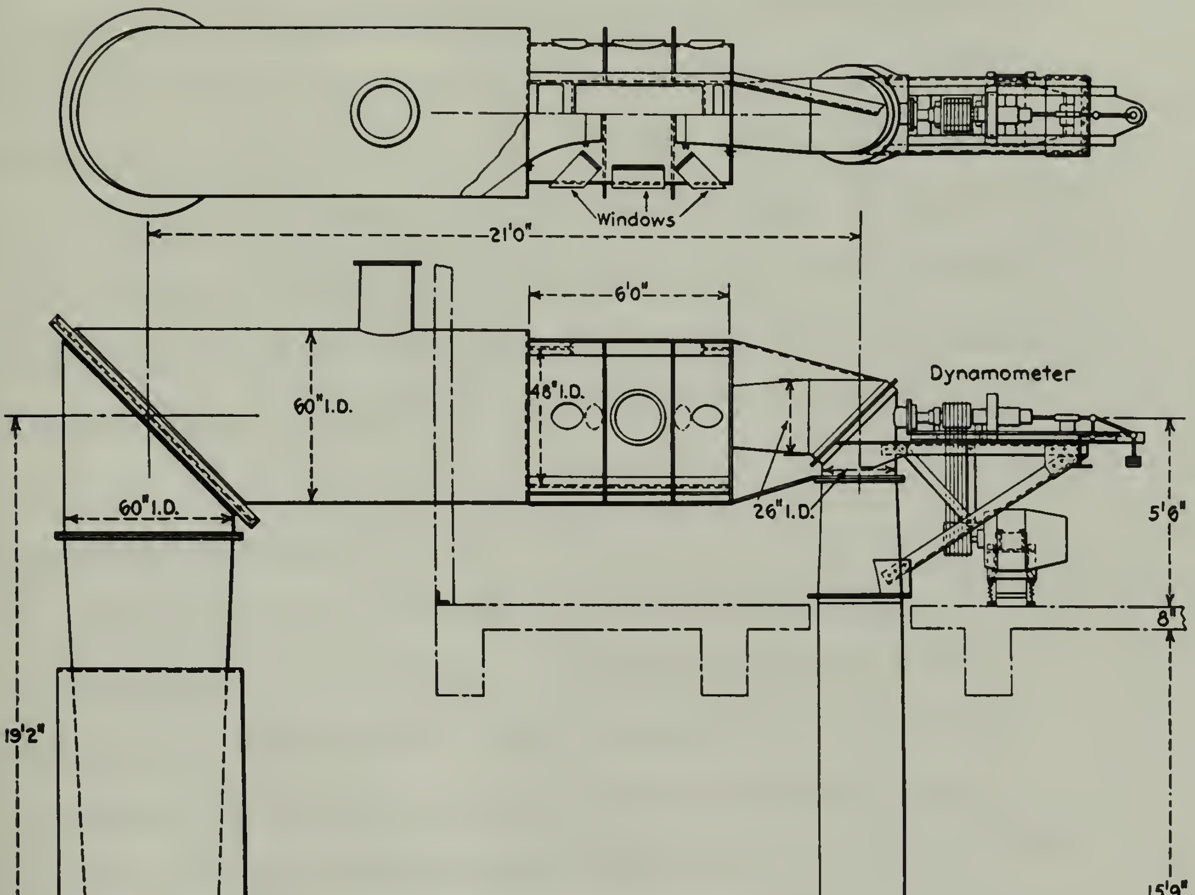

coil, results in the generation of a voltage proportional to the velocity of the moveable coil. If simple harmonic motion is assumed, this voltage is also proportional to the displacement of the bossing. The output of the detector, after amplification, is used to energize the moveable coil of an AC galvanometer. This instrument is essentially a wattmeter in which the magnetizing coil is energized by the output of a sine wave generator. The magnitude of the unknown force and its phase relationship to the propeller blade position is determined by comparison of the resultant galvanometer deflections with readings representing forces of known magnitude. Such known forces and deflections are plotted as calibration curves.

A. PROPELLER TUNNEL

The tests were made at the Massachusetts Institute of Technology, in the marine propeller tunnel, which is described in detail in(9) and illustrated in Fig. IV. In general, it consists of a closed circuit of large diameter tubing, through which water is circulated by an impeller located in the bottom, horizontal leg. The upper leg includes a test chamber in which the propeller is run. Water enters the test chamber through a converging nozzle twenty inches in diameter at its outlet. The propeller is driven by a shaft entering the test chamber through the

receiving nozzle. Speed control of both the water velocity and the propeller is by the Ward-Leonard System. A single 100-horsepower induction motor drives three generators, one for the impeller, one for the dynamometer, and one for excitation. A 75-horsepower motor drives the impeller and a 40-horsepower motor drives the dynamometer.

Water velocity in the test section is measured by using the differential pressure in the inlet nozzle. This pressure differential is transmitted to a gage containing a heavy hydrocarbon which has been calibrated by pitot tube measurements. Propeller revolutions are determined by an electric clock counter mechanism and torque is measured by reading the angular twist in a calibrated shaft. Thrust measurements are determined by a weighted balance arm in 30-pound increments while the differentials are converted into oil pressure and are read on a mercury column.

B. PROPELLER

The propeller used throughout the investigation was a twelve inch model of a 22-foot Troost merchant type propeller designed for an ore carrier. It has the following characteristics:

Material: Cast Aluminum
Diameter: 11.82 inches
No. of Blades: 4
Pitch Ratio (p/d): 0.957
Mean Width Ratio: 0.248
Blade Thickness Fraction: 0.05

C. BOSSING

The bossing consists of an aluminum casting fitted with detachable wooden nose pieces for varying its length and shape. See Fig. VI. The cast aluminum portion has been machined and hand filed to the dimensions shown in Fig. V.

As shown in Figs. V and VI the aluminum portion consists of three different shapes or sections: the hub section, airfoil section, and channel section. The hub or cylindrically shaped section houses a removable, spherically seated bearing designed to support a propeller shaft extension if used. The bossing and bearing are so designed that it is possible to vary the clearance between the airfoil section of the bossing and the propeller while the bearing remains fixed in relation to the propeller shaft extension. This is accomplished by attaching cylindrical spacer rings to lengthen the hub portion of the bossing. When the clearance is varied between the propeller and the bossing the spacers are inserted to maintain a constant clearance between propeller hub and bossing hub whether the bearing is in use or not. The forward or leading edge of the hub is fitted with a removable, wooden fair-water or nose piece. Fig. VI shows the bossing, several spacer rings and the wooden nose pieces.

C. BOSSING

The bossing consists of an aluminum casting fitted with detachable wooden nose pieces for varying its length and shape. See Fig. VI. The cast aluminum portion has been machined and hand filed to the dimensions shown in Fig. V.

As shown in Figs. V and VI the aluminum portion consists of three different shapes or sections: the hub section, airfoil section, and channel section. The hub or cylindrically shaped section houses a removable, spherically seated bearing designed to support a propeller shaft extension if used. The bossing and bearing are so designed that it is possible to vary the clearance between the airfoil section of the bossing and the propeller while the bearing remains fixed in relation to the propeller shaft extension. This is accomplished by attaching cylindrical spacer rings to lengthen the hub portion of the bossing. When the clearance is varied between the propeller and the bossing the spacers are inserted to maintain a constant clearance between propeller hub and bossing hub whether the bearing is in use or not. The forward or leading edge of the hub is fitted with a removable, wooden fair-water or nose piece. Fig. VI shows the bossing, several spacer rings and the wooden nose pieces.

FIGURE V

BOSSING

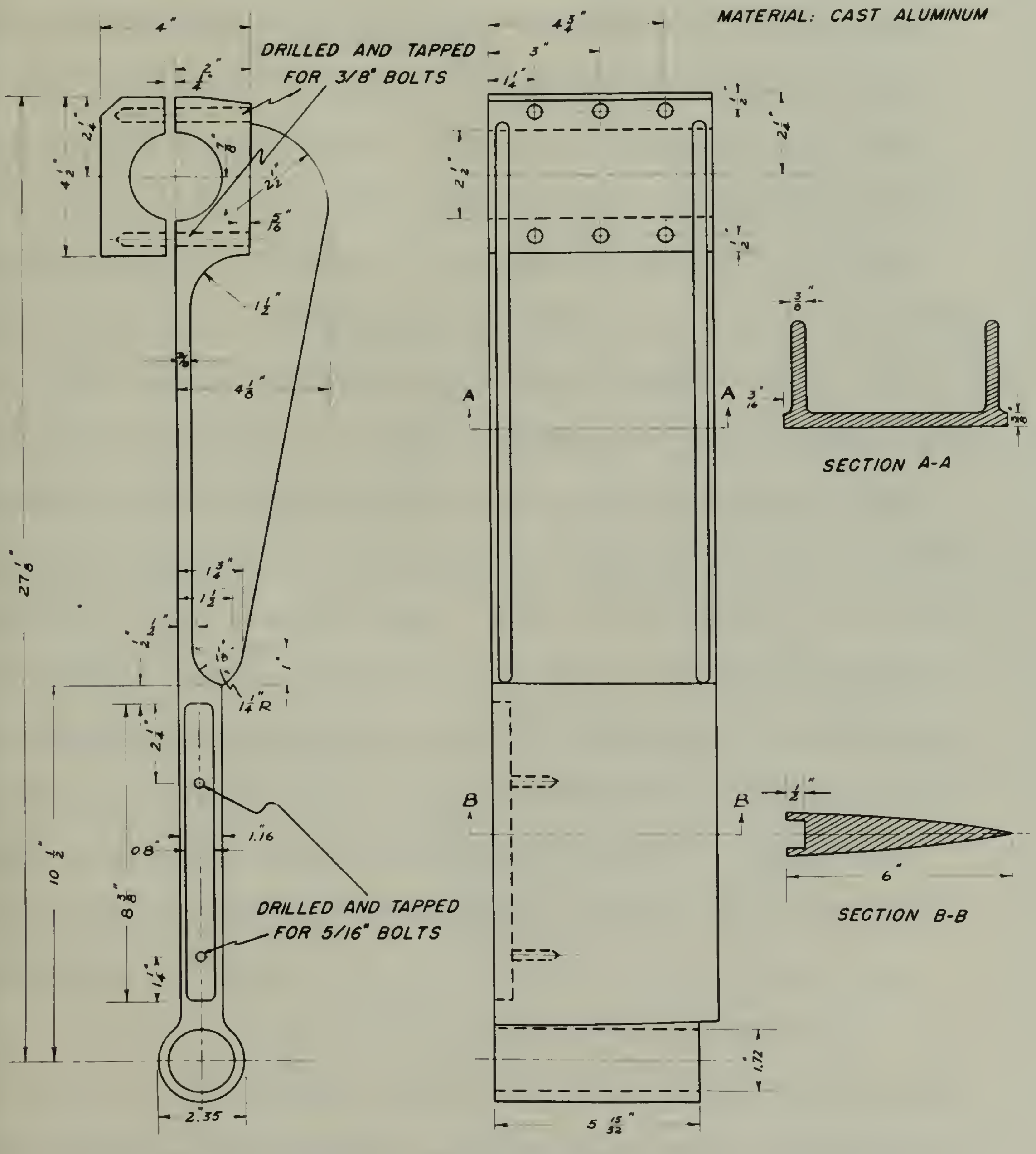

The airfoil or hydrofoil section extends from the hub to the channel section. The length of the airfoil section is such that with the bossing positioned in the test chamber of the propeller tunnel it extends radially beyond the water jet between the two nozzles. The aluminum portion of the airfoil section takes the form of the U.S. Navy Standard Strut Section. The forebody, as previously mentioned, consists of wooden nose pieces of various lengths, which complete the streamlined shape of the airfoil section. For these investigations two such pieces were employed. The first, or long nose piece, represents the forebody of the Navy Standard Strut Section, giving the bossing an overall length of 9-3/8 inches. The second, or short nose piece, has a semi-circular cross-section of diameter equal to the thickness of the aluminum bossing at the forward edge. Thus it represents the minimum overall length possible with this aluminum afterbody. In subsequent discussions any reference made to the long bossing is to be interpreted as referring to the aluminum casting with the long nose piece attached. Similarly, the short bossing is the aluminum section with the short nose piece in place.

For the section of bossing outside the flow a modified channel shape is used to maintain maximum stiffness with minimum weight. At the upper end, provision is made for clamping the bossing to the hollow steel shaft. See Fig. V.

D. HORIZONTAL ARM

The horizontal arm is mounted transversely near the top of the propeller tunnel as shown in Fig. III. It is clamped to the hollow steel shaft at approximately the center of the propeller tunnel hatch. The angular displacement of twist of the steel shaft causes a rotation of the horizontal arm and a resulting vertical displacement of the unclamped end, where it is connected to the moveable coil of the detector. The linkage between the moveable coil of the detector and the horizontal arm is a 3/8-inch rod with a rigid coupling for easy disassembly.

The arm is an aluminum casting, having an I-beam cross section to give maximum stiffness with minimum weight. The casting has been machined to the dimensions shown in Fig. VII for clamping to the hollow steel shaft.

E. MOUNTING

Both the horizontal arm and the bossing were clamped to a hollow steel shaft having an inside diameter of 2-1/4 inches, an outside diameter of 2-1/2 inches, and a length of 30 inches. Dimensioning of the steel shaft was such as to provide a large bending stiffness with suitable torsional stiffness for the magnitude of forces anticipated. The shaft was rigidly clamped to the inside top of the propeller tunnel test section at two points each approximately thirteen inches

FIGURE VII

HORIZONTAL ARM

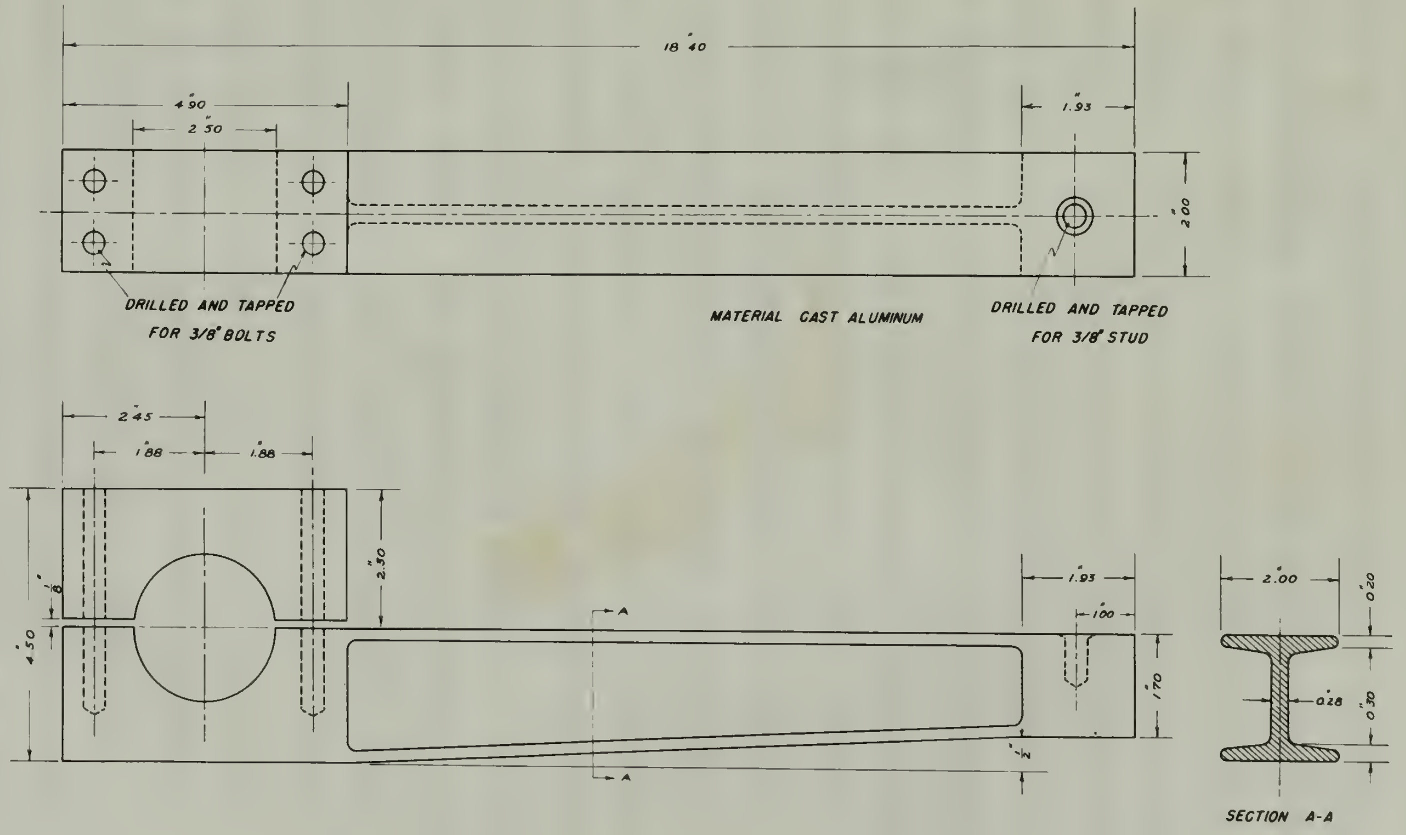

from the point where the horizontal arm was mounted. See Fig. III.

The shaft was clamped in two cast bronze mountings, machined to the dimensions shown in Fig. VIII. The bronze mountings are bolted to the inside top of the propeller tunnel test section and so positioned that the hollow steel shaft is parallel to the propeller shaft. Once installed, the cast bronze mountings and the hollow steel shaft remained in the propeller tunnel throughout the investigation. The horizontal arm was permanently clamped to the hollow steel shaft in the desired location just below the propeller tunnel hatch. Thus the horizontal arm, hollow steel shaft, and bronze mountings remained in position throughout the investigation. The bossing was shifted to various locations on the hollow steel shaft and removed from the test section whenever required and/or at the completion of a day's work. The detector and calibrator were clamped to the propeller tunnel hatch coaming for easy removal and in the case of the calibrator, ease of relocation to the control panel. See Figs. XIV and XVI. The positions of the detector unit and the calibrator were carefully marked to facilitate exact relocation.

In addition to the bossing system mounting as described above, the propeller mounting and the mounting for the frictionless bearing pulley should be mentioned.

MOUNTINGS

MATERIAL: CAST BRONZE

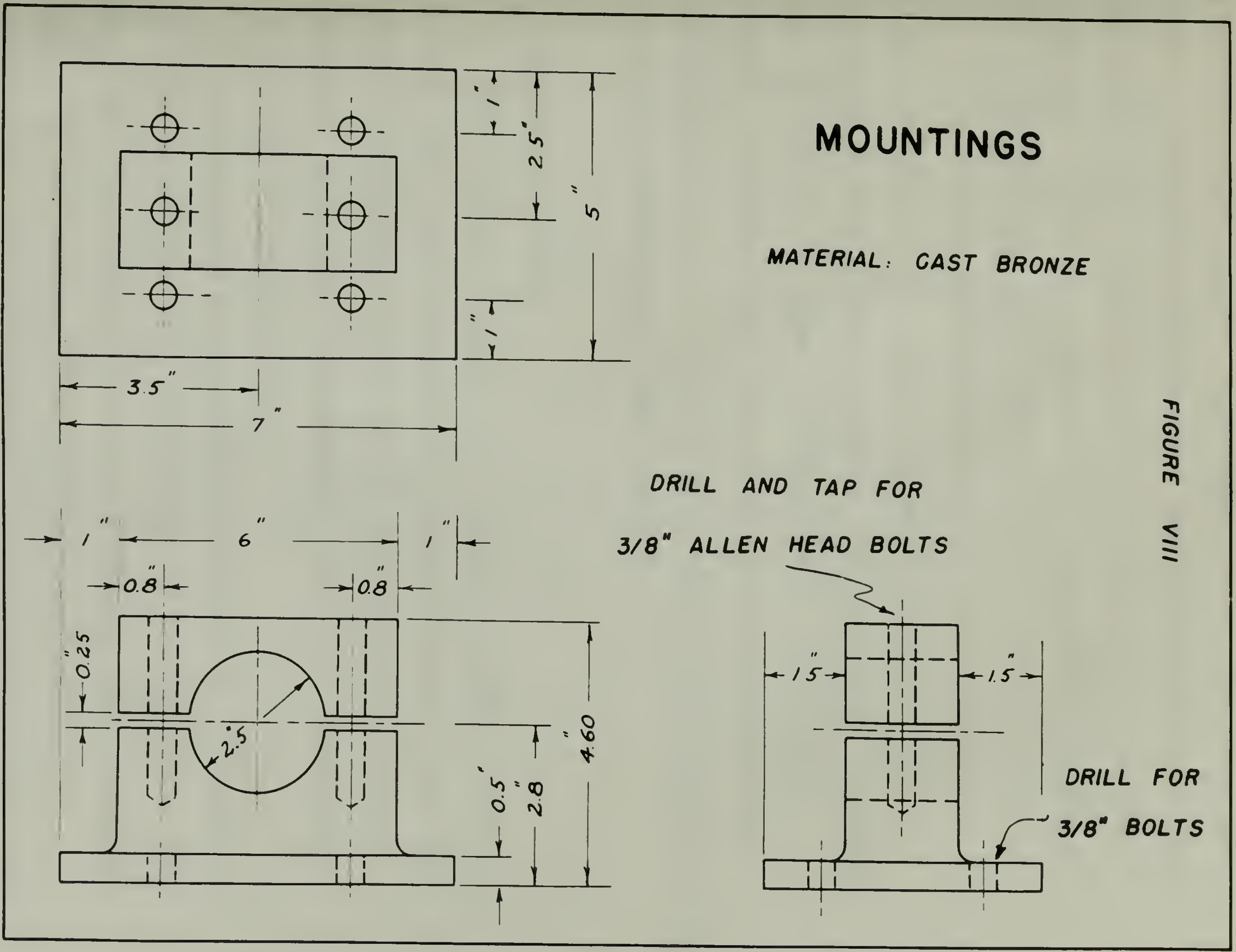

FIGURE VIII

Propeller mounting refers to keying the propeller to the propeller shaft for the measurement runs. The important point is that the propeller and propeller shaft were carefully marked to insure correct angular mounting of the propeller. This was required for the method employed in determining phase angle relationships. See Appendix A.

The frictionless bearing pulley was mounted in such a location as to insure normal attachment of the calibration wire to the bossing. See Fig. XV. A channel beam was bolted between the two nozzles of the test chamber. See Fig. IV. The pulley was then mounted on the channel in such a fashion that removal and reinstallation was easily accomplished when desired.

F. DETECTOR SYSTEM

The wiring diagram of the detector system is shown in Fig. IX. From the writing diagram it can be seen that the instrumentation consisted of five major components: detector, amplifier, galvanometer, sine wave generator, and cathode ray oscilloscope.

The detector is described in detail in (10) and illustrated in Fig. X. It consists of a fixed coil, (E), energized by a lead acid storage battery, and a moveable coil, (F), containing 8000 turns of No. 36 enameled copper wire. The moveable coil is positioned within the

FIGURE IX

WIRING DIAGRAM OF DETECTOR CIRCUIT

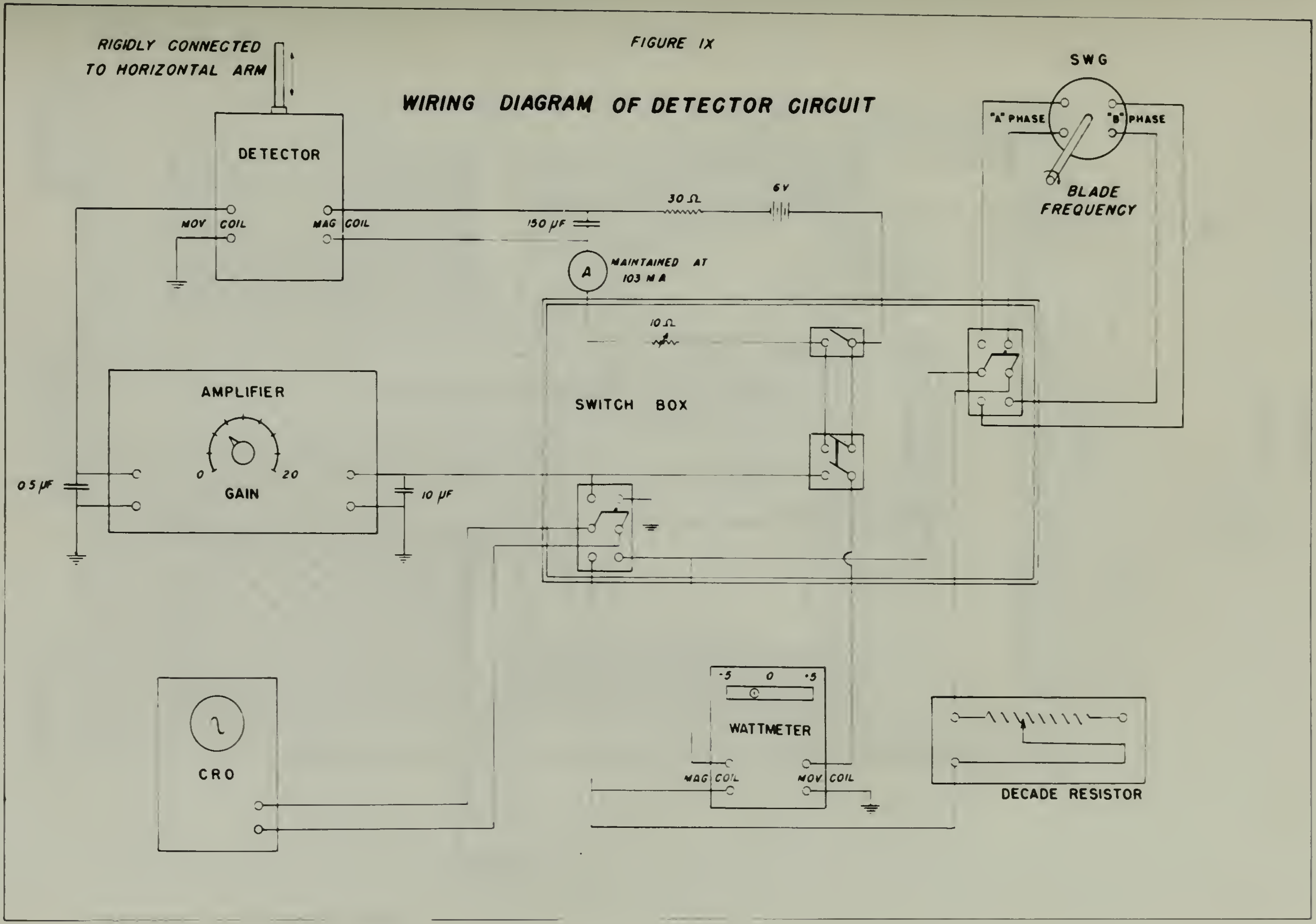

FIGURE X

DETECTOR

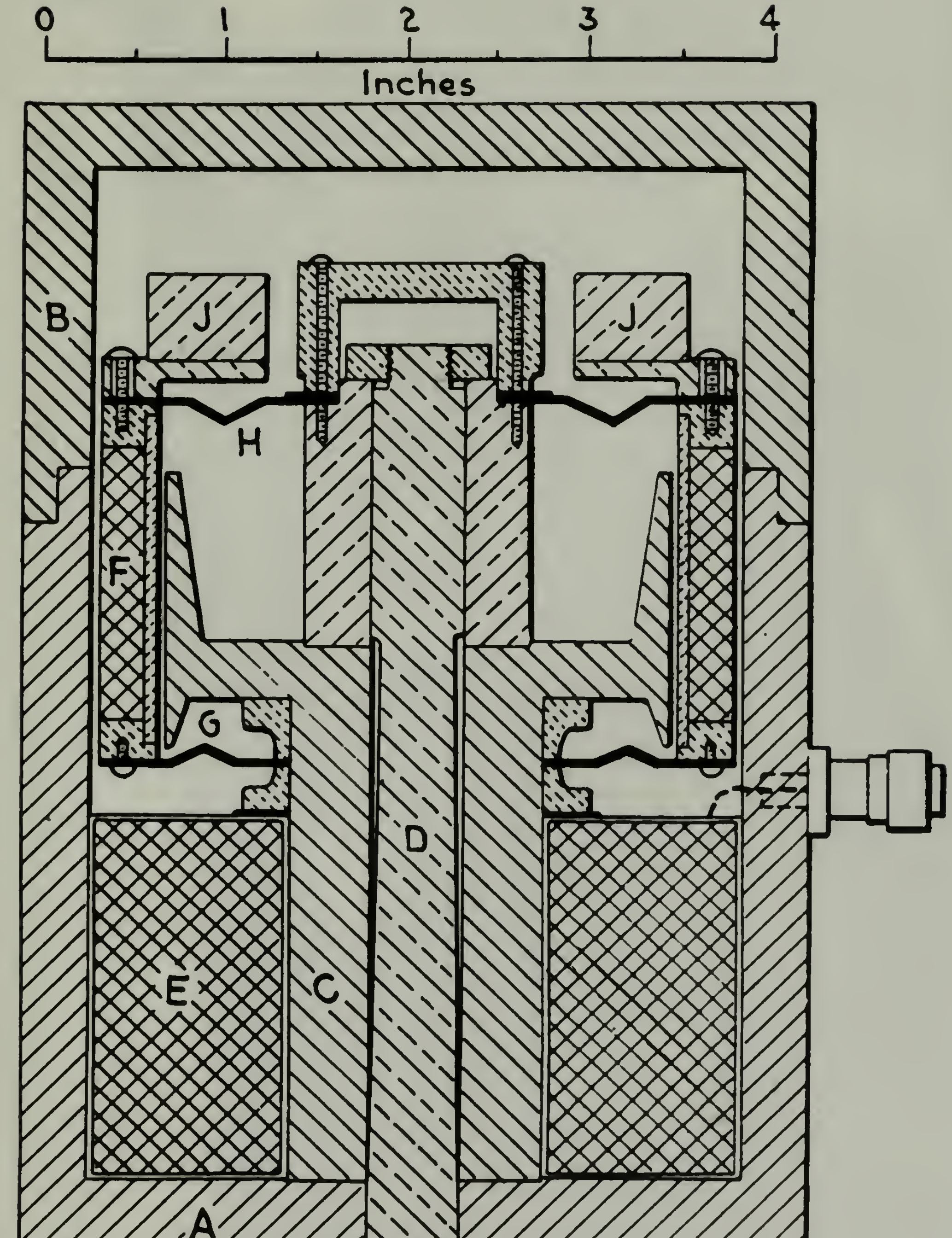

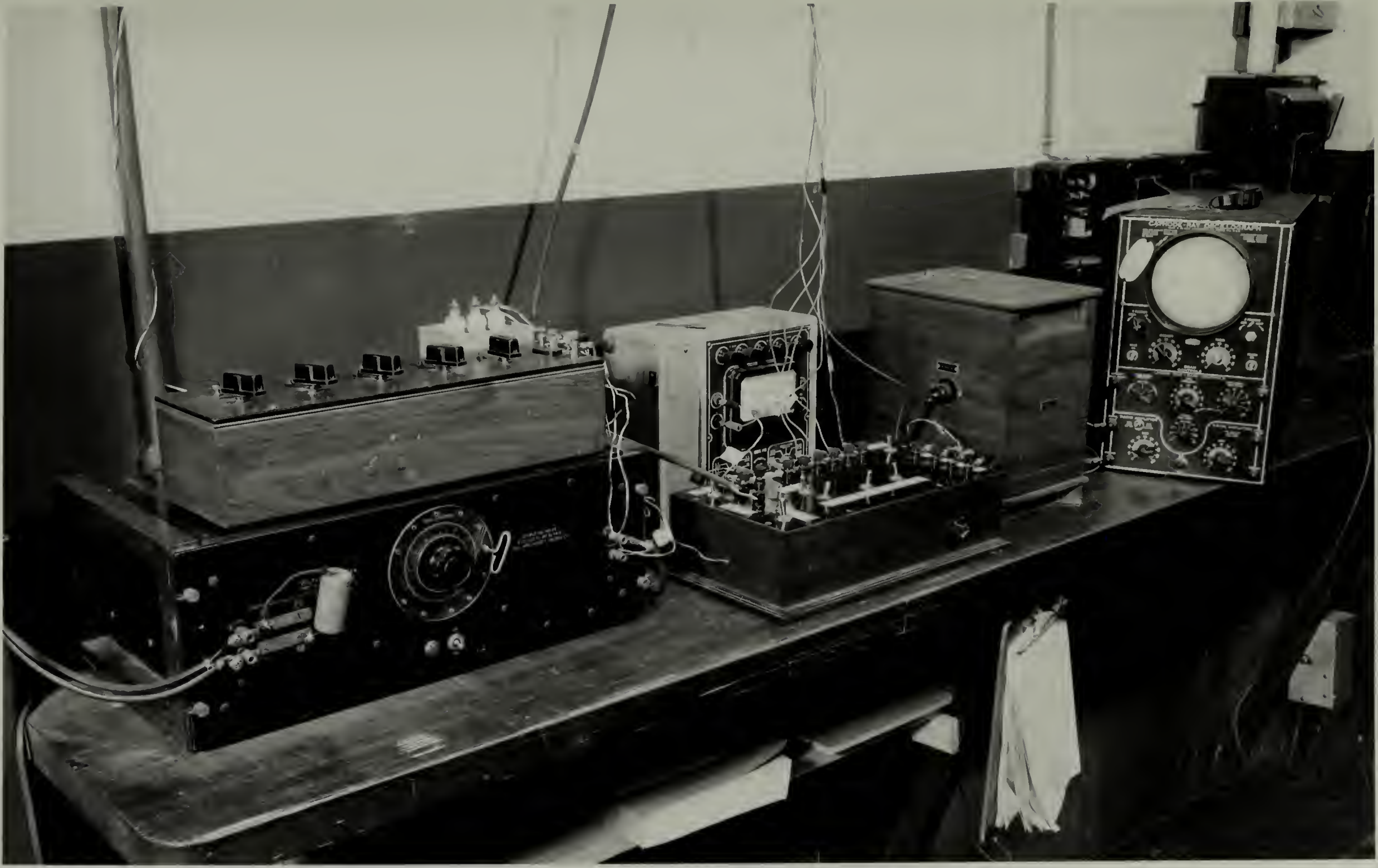

Fig. XI. Instrumentation Arrangement.

detector case by a pair of spring bronze flexures and is connected to the horizontal arm by a three-eighths inch rod as shown in Fig. III. The detector shown in Fig. X was modified to accommodate the three-eighths inch rod by replacing (J) with a cone-shaped piece and drilling a hole in the center of the case top. Energizing the fixed coil forces flux in the air gap between (A) and (C). Motion of the moveable coil therefore generates a voltage proportional to its velocity and the flux linkages.

Amplification of the detector signal was accomplished by means of a General Radio Co. voltage amplifier having the following characteristics:

Serial No.: 102

Model: 714A

Constant Gain: 20-6000 cps.

Mid-Band Gain: 910 maximum with variable gain control. Gain control dial subdivided into 20 divisions.

The output of the amplifier was fed to the moveable coil of a galvanometer. This galvanometer was manufactured by the Rubicon Company of Philadelphia, Pa. In the years following its purchase, Professor F.M. Lewis redesigned the galvanometer so that it is now best described as an alternating current galvanometer or a very sensitive wattmeter. The magnetizing coil of the galvanometer was

energized by a sine wave generator whose voltage output was a function of speed. Since the calibration runs were made at shaft speeds corresponding to those of measurement runs the only variable supplied to the galvanometer was the amplified detector signal. The galvanometer as modified actually performed as a wattmeter and read EI cosβ. A 110-6 volt transformer was used as a supply for the light source of the galvanometer.

The sine wave generator employed was model No. F-16, manufactured by The Electric Indicator Co. of Stamford, Conn. It is rated at 1.3 volts per 100 rpm and has two outputs which are 90° out of phase. This permitted reading EI cosβ, and EI cos $(\beta + 90°)$ or EI sinβ with the galvanometer. EI cosβ was designated as the A reading of the galvanometer and EIsinβ as the B reading. The angle was designated β_1 or β_2 corresponding to a calibration run or a measurement respectively.

The wiring diagram indicates that the amplifier output was also fed to a cathode ray oscilloscope. The cathode ray oscilloscope was used to monitor the circuit. It could be switched to either the output of the sine wave generator or the amplifier. During the runs it was kept on the amplifier output and thus permitted a visual presentation of the signal generated in the detector and served as a warning system for malfunctioning of the equip-

ment or circuit. Figure XI shows the amplifier, galvanometer, cathode ray oscilloscope, and switch box as used during the investigation. The switch box merely provided a convenient mounting for the various switches which were installed in the detector circuit for ease and flexibility of operation.

G. CALIBRATOR

Figure XII shows the principal dimensions of the calibrator and Figure XIV shows the calibrator in position for a calibration run. This mechanism was used to calibrate the entire system so that the galvanometer reading could be related to the magnitude of the hydrodynamically induced vibratory forces. Basically, the calibration mechanism was designed to apply an excitation force of known magnitude and frequency to the bossing at a position assumed to correspond to the point of application of the actual vibratory force.

The calibrator consists of a cam actuated lever arm which is driven at four times propeller speed by shafting geared to the dynamometer. Connected to the lever arm is a wire-spring combination which in turn is connected to the bossing. The wire is normal to the bossing at a point whose distance from the propeller shaft axis is equal to 0.7 of the propeller radius. Longitudinally the point is located approximately two inches from the trailing edge of the bossing. See Fig. II.

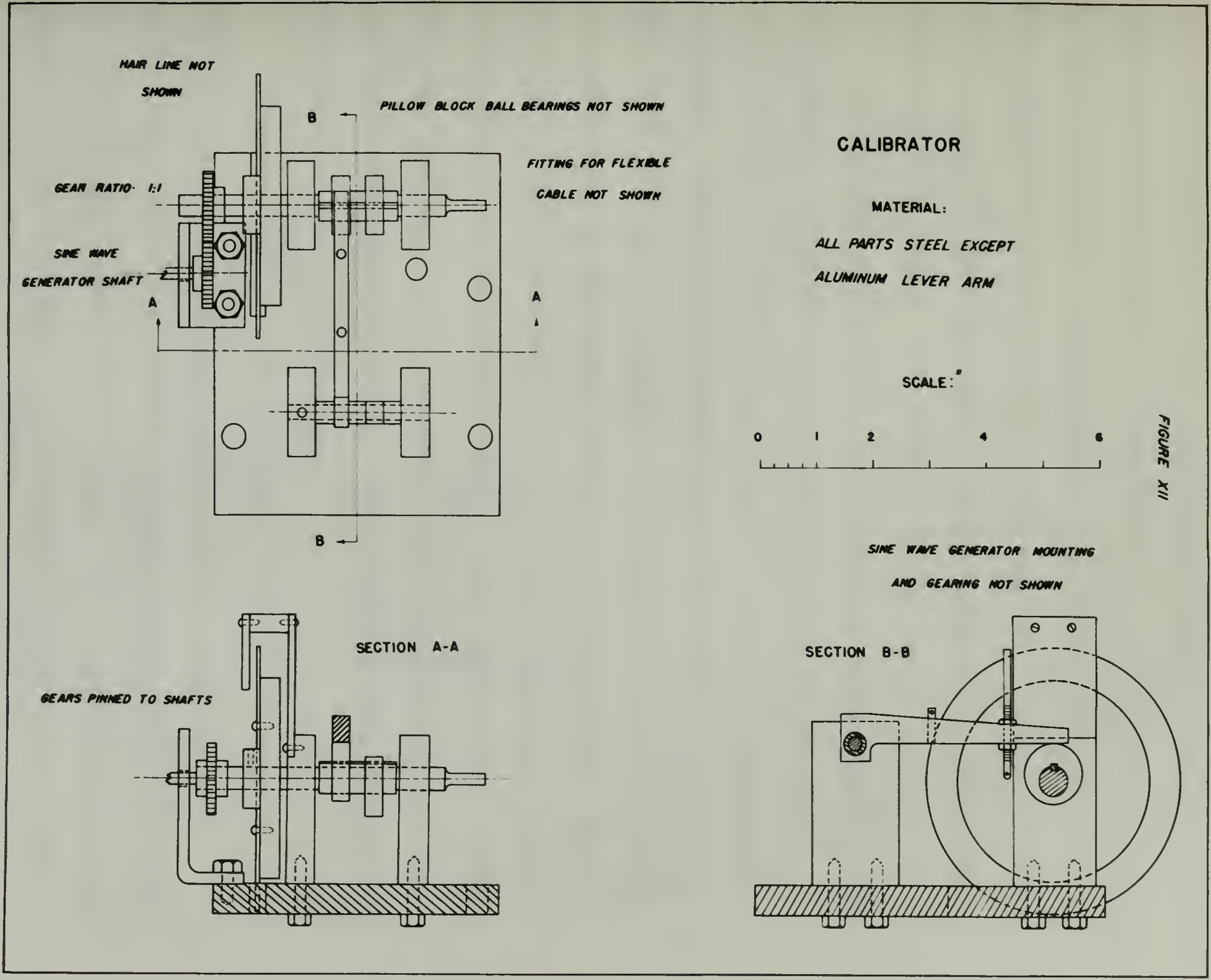
HAIR LINE NOT SHOWN
B
PILLOW BLOCK BALL BEARINGS NOT SHOWN
FITTING FOR FLEXIBLE CABLE NOT SHOWN
GEAR RATIO· 1:1
SINE WAVE GENERATOR SHAFT
A
A
B
CALIBRATOR
MATERIAL:
ALL PARTS STEEL EXCEPT
ALUMINUM LEVER ARM
SCALE: "
0
1
2
4
6
SINE WAVE GENERATOR MOUNTING AND GEARING NOT SHOWN
SECTION A-A
GEARS PINNED TO SHAFTS
SECTION B-B

FIGURE XII

Rotation of the cam shaft causes a sinusoidal displacement of the lever arm and consequently a sinusoidally varying elongation of the wire-spring combination. An excitation force equal in magnitude to the spring constant of the wire-spring combination times its elongation is thus applied to the bossing. The cam has a total throw of one-quarter inch causing a displacement of 3/32 inches at the point of wire attachment to the lever arm.

To minimize flexural and torsional vibration of the cam shaft, a flywheel was attached to the shaft and a second cam was installed adjacent to first but 180° out of phase. Each cam actuated two lever arms, held in contact with the cam by springs. Only one of the four arms was connected to the wire running to the bossing. See Figs. XII, XIII, and XIV. It was found during the early calibration runs that the effect of the three extra lever arms was negligible in reducing torsional vibration, and they were therefore removed. This explains the additional cam shown in the illustrations.

Figure XIV is a photograph of the calibrator in position on the propeller tunnel hatch coaming for a calibration run. The various springs shown were attached directly to the lever arm by means of a tension regulating spindle. The wire then led from the spring to the point of attachment on the bossing. See Fig. XV. The wire used

FIGURE XIII

LEVER ARMS

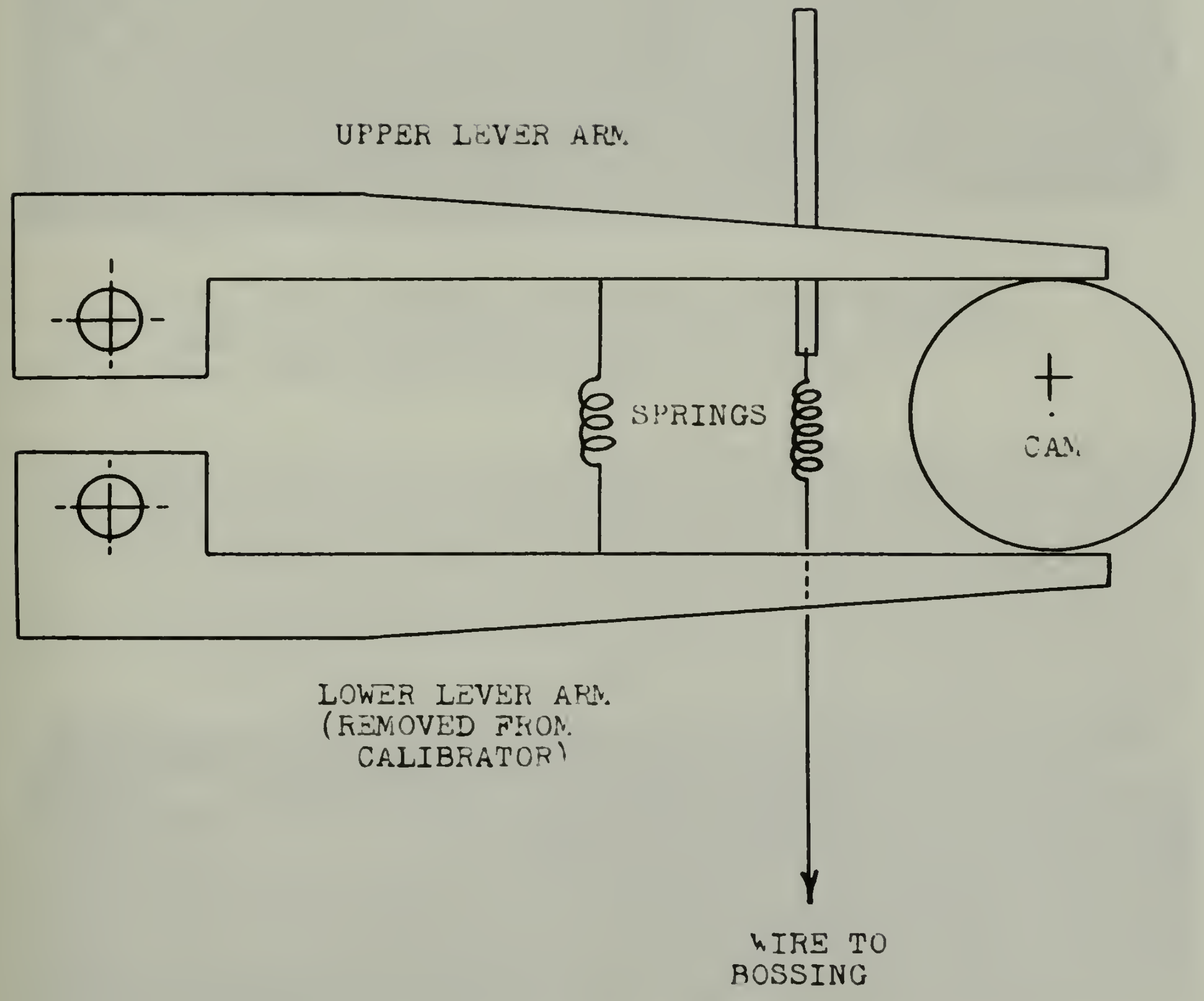

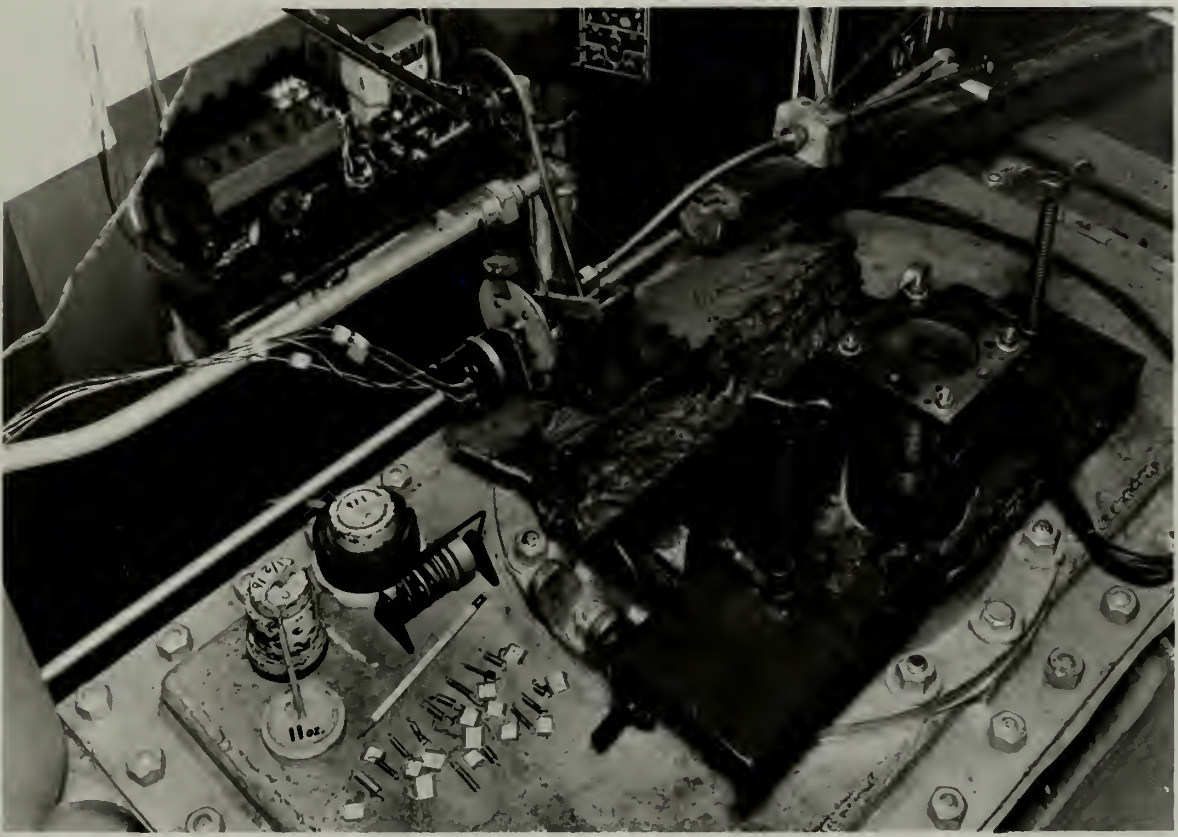

Fig. XIV. Propeller tunnel hatch showing detector mounting and calibrator in position for a calibration run. Note calibrating springs in foreground.

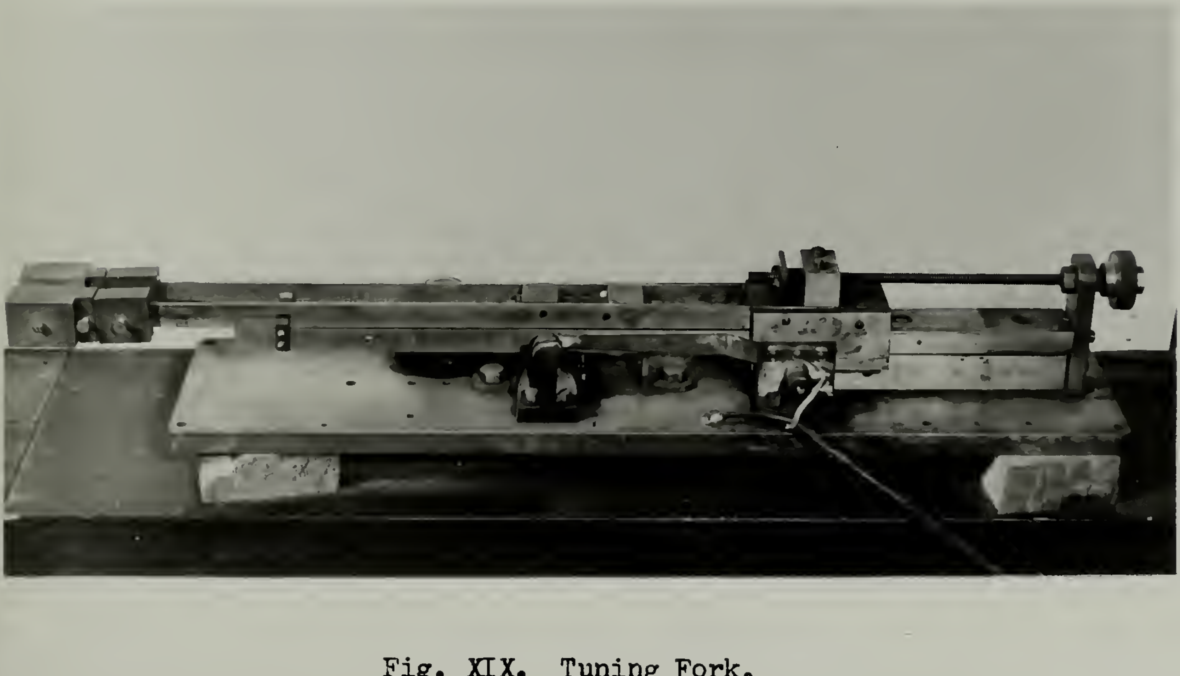

Fig. XIX. Tuning Fork.

FIGURE XV

CALIBRATION SET-UP

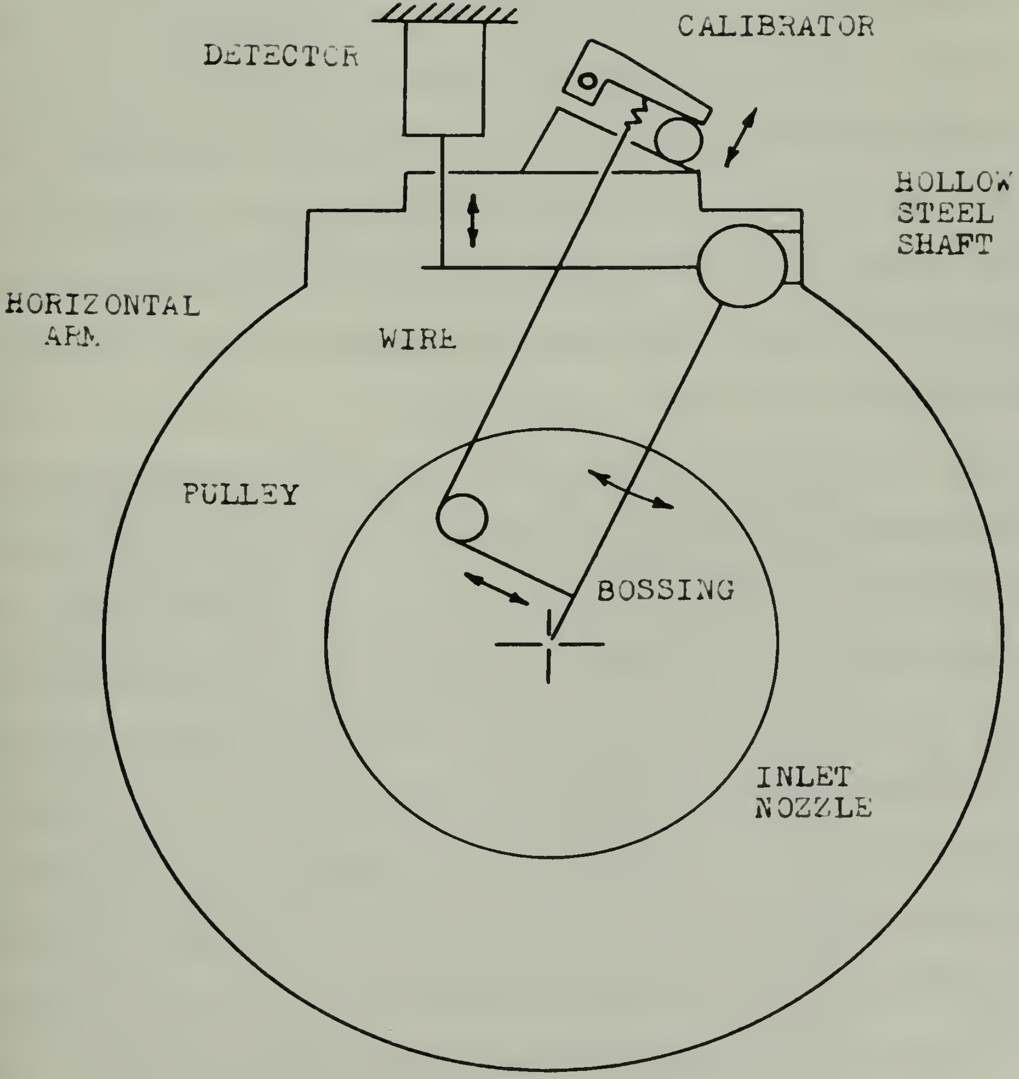

LOOKING UPSTREAM TOWARD THE INLET NOZZLE

was 0.010 in. diameter piano wire. It was directed normal to the bossing surface by using a pulley with frictionless bearings positioned as shown in Fig. XV. Care was taken to insure that the wire had no kinks in order to maintain as nearly as possible a linear wire-spring combination.

As seen in the illustrations of the calibrator, the sine wave generator was mounted on the same base as the cam shaft and geared directly to the cam shaft. The only purpose in using a geared drive was to avoid an alignment problem between the cam shaft and the sine wave generator shaft. The flywheel, in addition to reducing torsional vibrations, provided a suitable location for the mounting of an indicator card used in phase angle determinations. The hair line and indicator card were adjusted so that a 0° reading on the card represented the high point of the actuating cam. This relationship is discussed in the Appendix. However, it should be mentioned here that the calibrator was designed in the above manner to provide flexibility of the system in physical positioning. As a packaged unit it was easily moved to a new location above the tunnel control panel during the actual measurement runs without disturbing the angular relationships between the sine wave generator phases, indicator card, and cam.

As originally designed the calibrator unit, when in position for a calibration run, was driven by a long flexible cable geared to the dynamometer shaft. Excessive torsional vibration made it necessary to use a solid shaft with short flexible cables at each end. See Fig. XIV. The gearing was four to one at the driven end so that the long shaft and cam shaft (calibrator) rotated at four times propeller shaft speed. When the calibrator was relocated above the control panel for measurement runs one of the short flexible cables was used to drive the calibrator from the same gears on the dynamometer shaft. Figure XVI shows the calibrator unit in position above the control panel for a measurement run.

H. PHASE SYSTEM.

Determination of the phase relationship between the time of occurrence of the measured force and the propeller blade position with respect to the trailing edge of the bossing is described in detail in the Appendix. The procedure consisted of determining three angles. Two of these angles were calculated directly from the galvanometer readings; one from the calibration runs and one from the measurement runs. The third angle was read directly on the calibrator indicator card during the measurement runs.

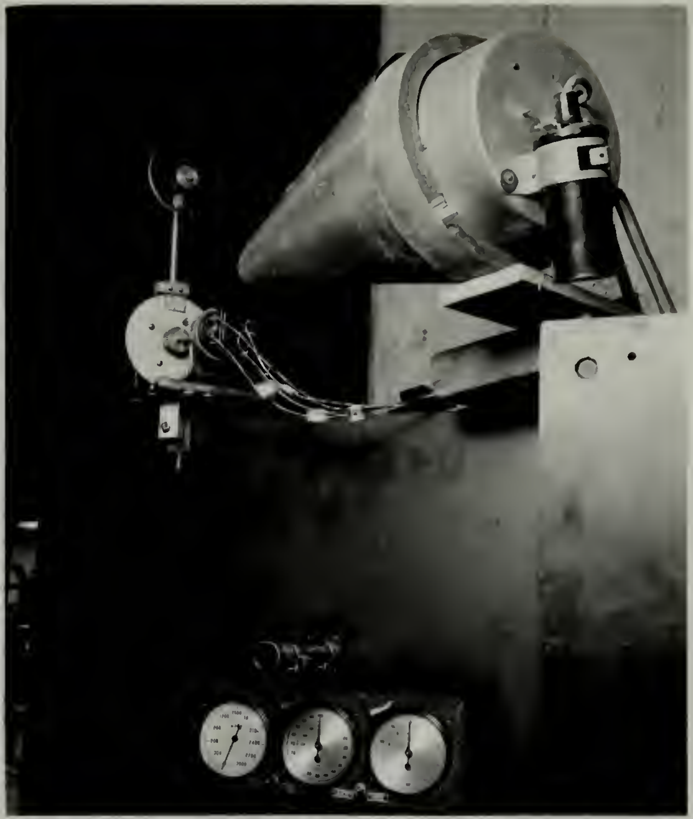

Fig. XVI. Calibrator and Strobe light in position for a measurement run.

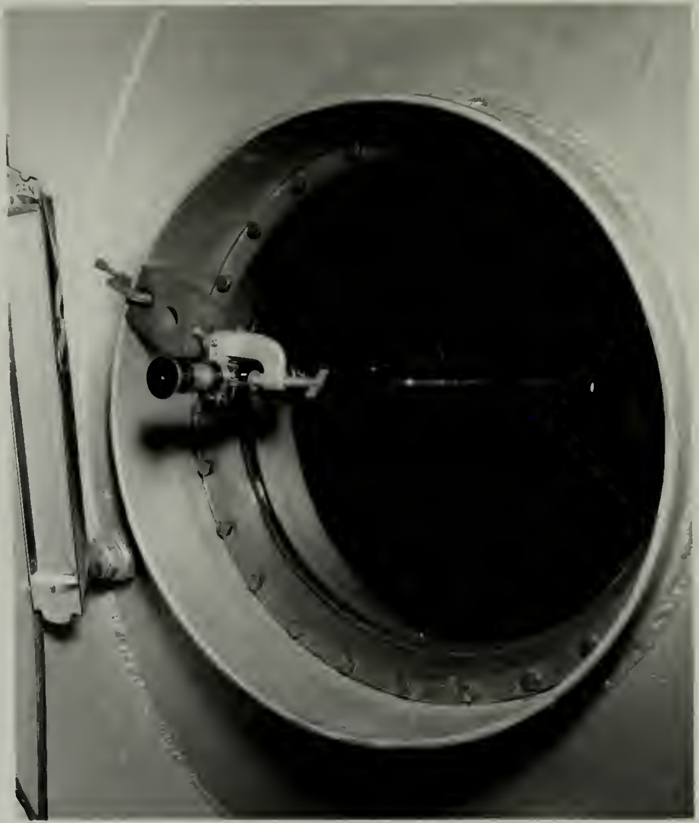

Fig. XVII. Telescope mounted in test section window.

Essentially, then, the phase system consisted of the galvanometer, the indicator card on the flywheel of the calibrator, the phaser for timing of the strobe lights and a telescope. The telescope was mounted in a side window of the propeller tunnel as shown in Fig. XVII and used to correctly time firing of the strobe lights. One strobe light was mounted at a window in the test section and the other on the control panel for reading the indicator card. Both lights fired simultaneously.

I. TUNNEL SPEED CONTROL

For all constant speed runs, the propeller shaft was operated at a speed corresponding to a frequency close to the natural frequency of the bossing system. Increased sensitivity in force detection together with satisfactory phase angle determination was attained by operating the system just off the resonant peak. Such a frequency required that the control of the propeller shaft speed be extremely accurate. The principle of the Wenner speed controller was utilized.

The speed control circuit is discussed in detail in(10). Basically, speed control was obtained within very narrow limits by means of an adjustable frequency tuning fork acting in the motor field circuit as shown in Fig. XVIII. The tuning fork actually consists of a pair of tuning forks of different lengths and con-

FIGURE XVIII

TUNNEL SPEED CONTROL CIRCUIT

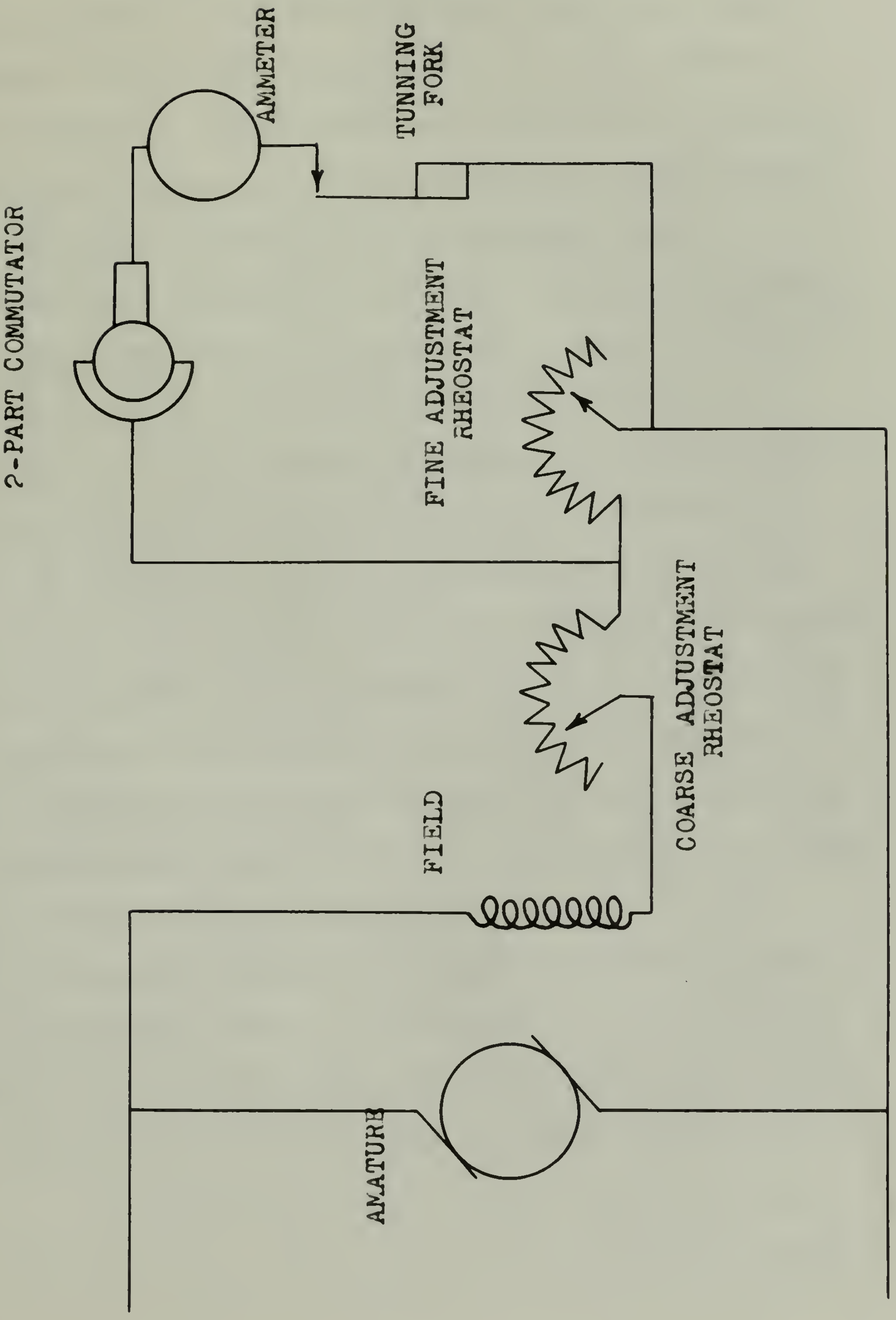

sequently of different frequencies, mounted one over the other. The pair of forks were designed so that the relative position of the two could be varied by a screw adjustment. Clips near the ends constrain the forks to vibrate together. Rough frequency adjustment is attained by attaching weight sets to the fork tips. Finer adjustment is achieved by varying the adjustment screw.

A two-part commutator is geared to the dynamometer shaft. The commutator is constructed so that the circuit is closed for half a revolution and open for half a revolution. In series with the commutator is the tuning fork make-and-break contact maker which is adjusted so that it is closed for half a vibration and open for the other half. If the tuning fork and commutator are running in step the second field rheostat will be short circuited for a portion of each revolution. The field current will attain a certain value dependent upon the phase relation of the tuning fork and commutator. If the load or voltage changes the commutator speed, and therefore the phase relationship, the field current will then vary to return it to the desired value. A galvanometer in the circuit, mounted on the control panel, provides visual indication of synchronism of the commutator and tuning fork.

III. PROCEDURE

Once the instrumentation and method of calibration were considered to be operationally acceptable, the procedure consisted of three basic steps which were repeated for each condition investigated. These were: (1) calibration, (2) measurement and (3) force and phase angle determination. Before the investigation could proceed, however, it was necessary to investigate the effects of certain variables, correct design defects, and obtain reproducible data. Since this initial procedure is confined to only the beginning of the investigation it will be omitted here and discussed instead in the Appendix.

Calibration consisted of applying a force of known magnitude and frequency to the bossing and recording the response of the system as galvanometer deflections. This was accomplished by using the calibrator described in Section II and a variety of wire-spring combinations. The wire from the calibrator was attached to the bossing at a position which was assumed to be the point of application of the hydrodynamically induced vibratory force. A variety of springs was used with the calibrator cover-

ing a range of forces from approximately 0.25 lbs. to 1.10 lbs. Enough wire-spring combinations were used to clearly define calibration curves of resultant galvanometer deflections vs. force.

Once the desired spring was attached between the calibrator lever arm and the wire to the bossing, it was necessary to set the initial tension and determine the magnitude of the force which would be applied to the bossing. The initial tension was set by placing the desired weight on the weight pan and then adjusting the length of the wire-spring combination (the elongation of the spring) until the lever arm just lifted from the low point of the cam. See Figs. XVI and XX. The magnitude of the force applied to the bossing through the wire-spring combination was measured by adding weights to the weight pan until the lever arm just lifted off the high point of the cam. The weight pan was then disconnected from the lever arm and the tunnel run at the required speed. If the calibration was to be at a constant propeller speed, the tuning fork speed control circuit was used. For variable speed runs the tuning fork was disconnected. This procedure was repeated for a number of wire-spring combinations, the number used being determined by the number required to define a calibration curve. The end result of a calibration run was a plot of resultant galvanometer deflection readings against force.

FIGURE XX

FORCE DETERMINATION

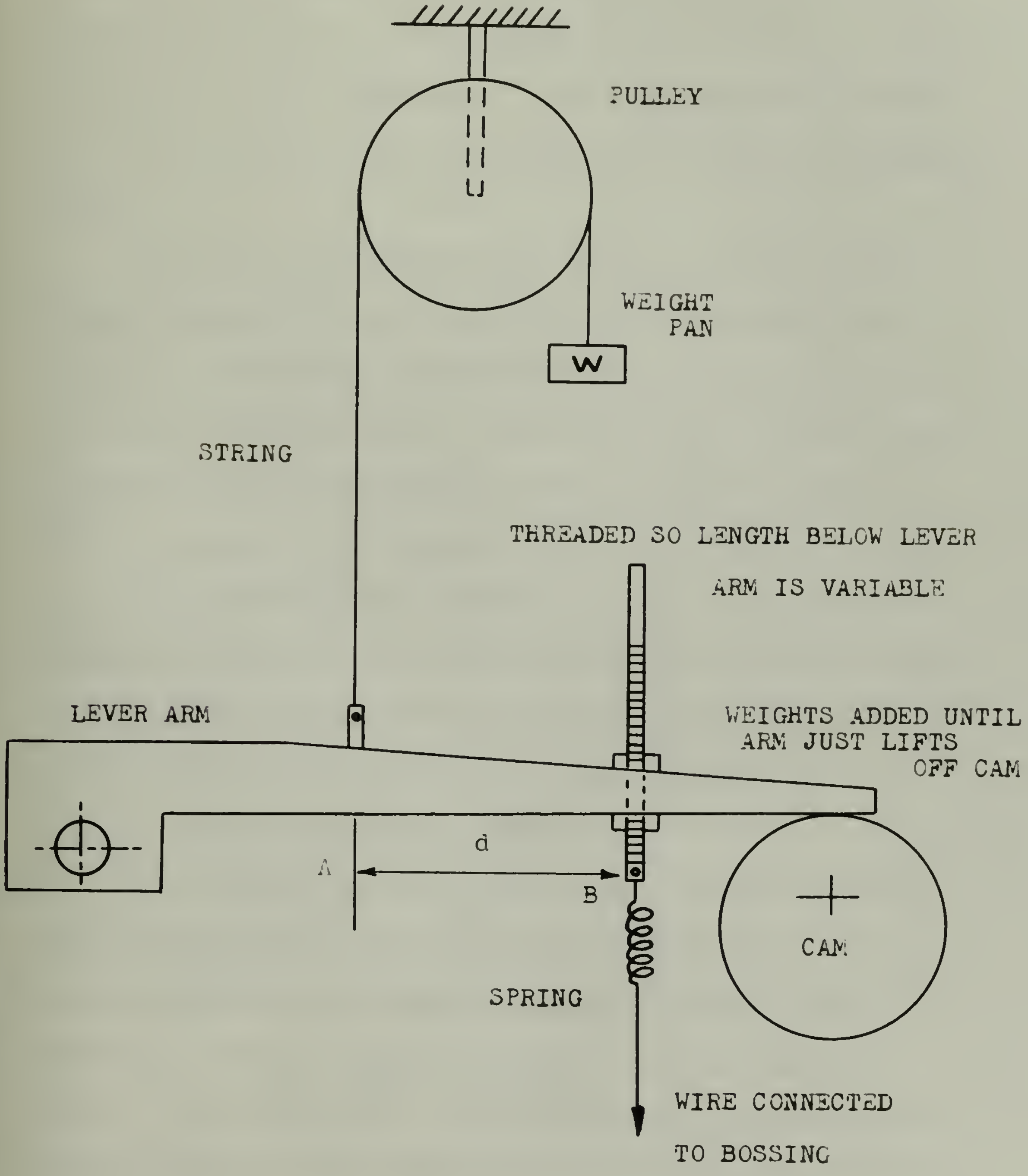
PULLEY
WEIGHT PAN
W
STRING
THREADED SO LENGTH BELOW LEVER ARM IS VARIABLE
LEVER ARM
WEIGHTS ADDED UNTIL ARM JUST LIFTS OFF CAM
A
d
B
CAM
SPRING
WIRE CONNECTED TO BOSSING

The response of the entire system was a function of the magnitude and frequency of the applied force and the natural frequency of the bossing. The natural frequency of the bossing system varied with clearance between the propeller and bossing, and the length of the nose piece used. Therefore, the calibration runs had to be made under the same conditions as the measurement runs.

For the measurement runs the wire of the wire-spring combination was removed from the bossing, the propeller installed, and the calibrator relocated on the tunnel control panel. See Fig. XVI. For the major portion of the investigation the propeller speed was held constant by the tuning fork speed control circuit and the water velocity changed to give the desired thrust variations. The remainder of the data was taken with either constant water velocity and variable RPM, or constant thrust and variable combinations of propeller RPM and water velocity.

In addition to recording the galvanometer deflection readings, as in the calibration runs, it was necessary to record propeller speed, thrust, water velocity, and the angle α, as read on the indicator card of the calibrator. The method of measuring propeller speed, thrust and water velocity is described in Section II.

The angle α is defined as the phase angle between the time the generating line of an arbitrarily selected propeller blade coincides with the trailing edge of the bossing, and the time the calibrator cam causes the maximum positive force to be applied to the bossing during calibration. The propeller shaft was marked so that the generating line of the chosen blade coincided with the trailing edge of the bossing when the cross hairs of the telescope were aligned with the mark. See Fig. XVII. During the measurement runs the timing of the strobe lights was adjusted until the scribe mark on the propeller shaft coincided with the telescope cross hairs. The angle α was then read on the calibrator indicator card.

Once both the calibration and measurement runs had been comoleted for a desired condition of investigation, the magnitude of the hydrodynamically induced force could be determined together with its phase relationship to the propeller blade position. From the galvanometer readings recorded during the calibration runs, resultant galvanometer readings and the angle β_1 were computed:

$$\text{Resultant reading} = \sqrt{\text{A reading}^2 + \text{B reading}^2}$$

$$\beta_1 = \tan^{-1} \frac{\text{Breading}}{\text{Areading}}$$

The resultant readings were plotted against the forces

which produced them to give a curve of force vs. resultant galvanometer readings for the particular set of conditions employed.

The resultant galvanometer readings and the angle β_2 for the measurement runs were computed in a similar manner. The calibration curve was then entered with resultant readings and the magnitude of the forces determined. The phase relationship between the time of occurrence of the measured vibratory force and the time the propeller blade generating line coincided with the trailing edge of the bossing was then calculated. This relationship is represented by the angle γ, which is defined as the phase angle between the time the generating line of the arbitrarily selected propeller blade coincides with the trailing edge of the bossing and the occurrence of the measured hydrodynamically induced force normal to the bossing. The relationship for determination of γ is:

$$\angle\gamma = \beta_2 - (\beta_1 + \alpha)$$

where the following convention was adopted for β_1 and β_2 quadrant determination:

A reading	B reading	Angle
+	+	0 - 90°
-	+	90 - 180°
-	-	180 - 270°
+	-	270 - 360°

A detailed description of the methods of force determination, phase angle determination, and the method of calculation is given in the Appendix.

IV. RESULTS

The results of this investigation are best presented in graphical and tabular form. Figures XXI and XXII illustrate the variation of the vibratory force with thrust and clearance. Clearance values used refer to the clearance between the propeller leading edge and the bossing trailing edge at 0.7 radius. Since the propeller blade is slightly raked (8°), actual clearance varies from one-quarter inch at 0.2 radius to one and one-half inches at the blade tip. In examining these figures it should be remembered that the variation in thrust was obtained by a variation in water velocity at a constant propeller speed. It should also be pointed out that the normal operating point of the propeller used would correspond to a thrust of approximately 21 lbs.

Figure XXIII shows the variation in vibratory force with clearance for a thrust of 21 lbs. This figure clearly illustrates the affect of bossing length as well as clearance on the magnitude of the induced vibratory forces. Figure XXIV is the same information as Figure XXIII plotted on semi-log coordinates. It

should be emphasized here that Figs. XXII and XXIII are for one particular set of conditions. For example, these figures are for a thrust of 21 lbs. and a propeller speed of 548 RPM.

Figure XXV is another plot showing the variation of force with thrust for a particular value of clearance. However, in this figure water velocity was held constant and the propeller speed varied to obtain the desired thrust values. The upper curve was taken directly from Fig. XXI for purposes of comparison.

Figure XXVI is plotted using values obtained from Fig. XXV and illustrates the variation of force with water velocity.

The phase angle relationships resulting from the investigation are summarized in Tables XXXIII and XXXIV. The values of the phase angles for each measurement run are included on the measurement tables which appear in the Appendix. These tables show the maximum variation in the phase angle for the thrust range used at each value of the clearance. In addition, the value of the angle is given for a thrust of 21 lbs. which, as previously mentioned, corresponds to the average operating point of the propeller.

Table XXXV is a summary of the magnitude of the vibratory force and its phase angle relationships. The

force value has been reduced to a percentage of the thrust at the operating point.

The generally accepted law of similitude for bossing forces states that for equal values of the advance coefficient, J, the forces vary as the ratio of the propeller speed squared. ($F_2 = F_1(\frac{N_2}{N_1})^2$). Table XXXVI is an illustration of the values computed by this law as compared to the measured values. The table also gives the values computed by the same basic relationship but using a power of 2.75 rather than 2.00.

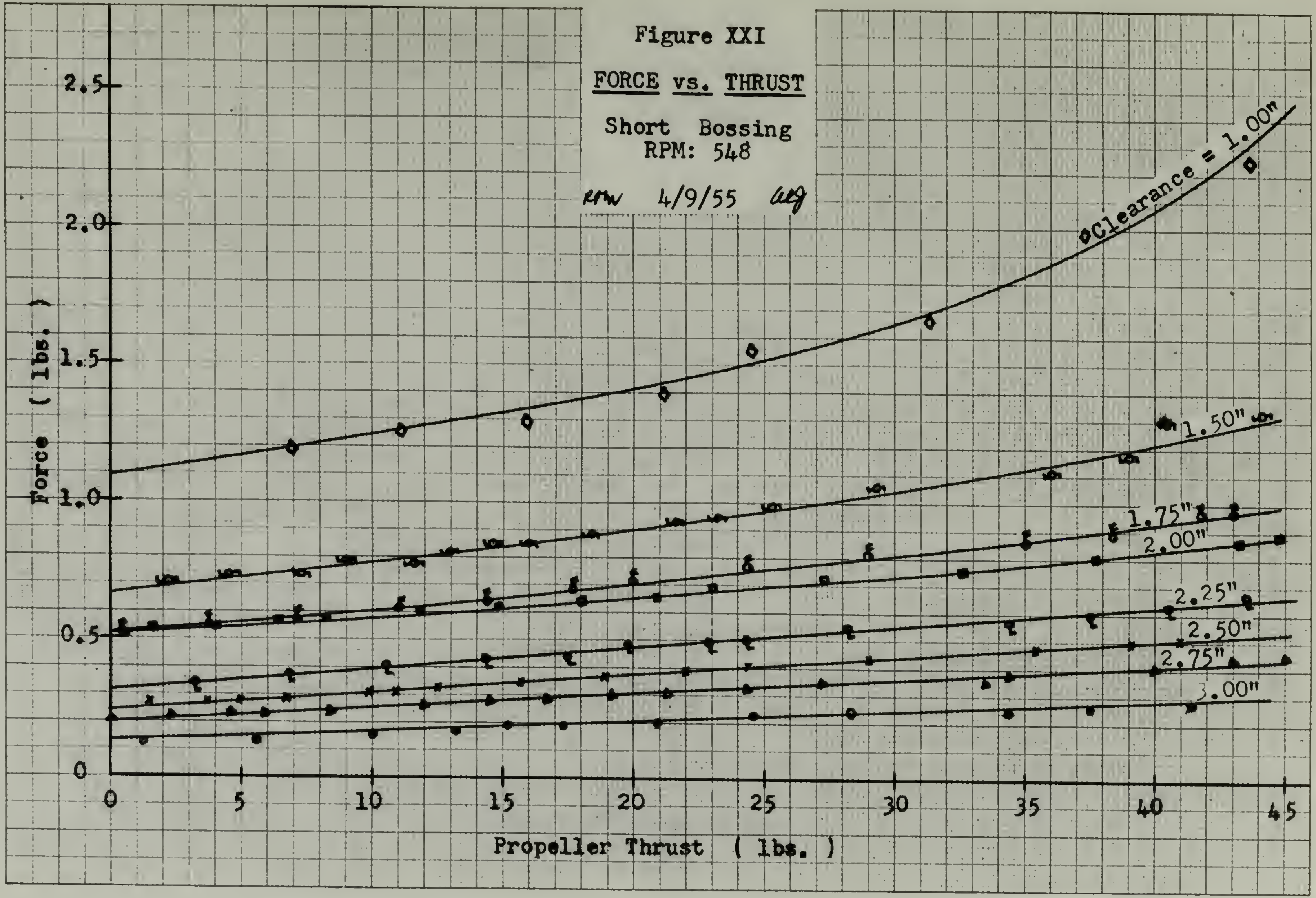

Figure XXI

FORCE vs. THRUST

Short Bossing
RPM: 548

RMW 4/9/55 alg

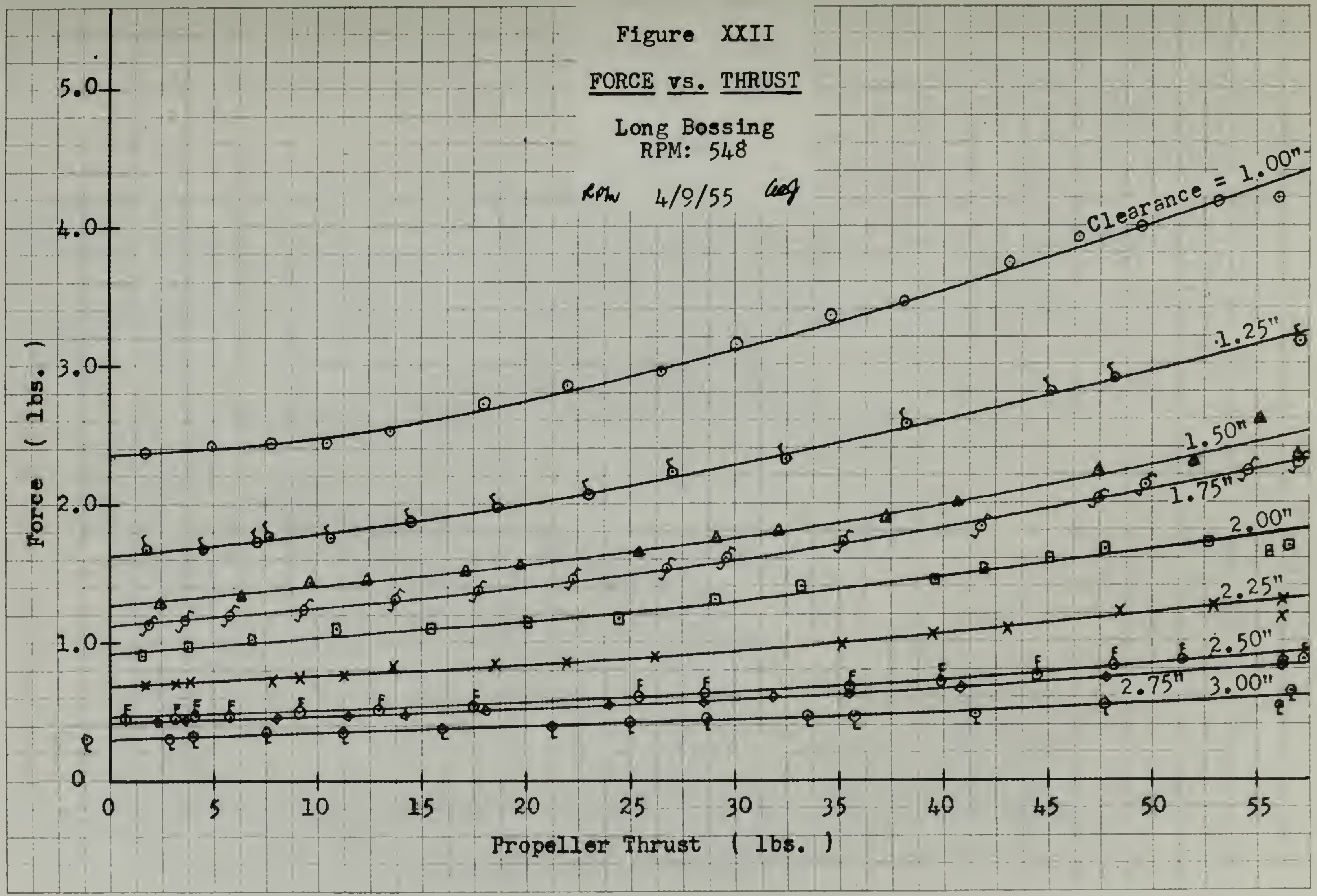

Figure XXII

FORCE vs. THRUST

Long Bossing
RPM: 548

RPW 4/9/55

Figure XXIII

FORCE vs. CLEARANCE

RPM: 548

RPW 4/9/55

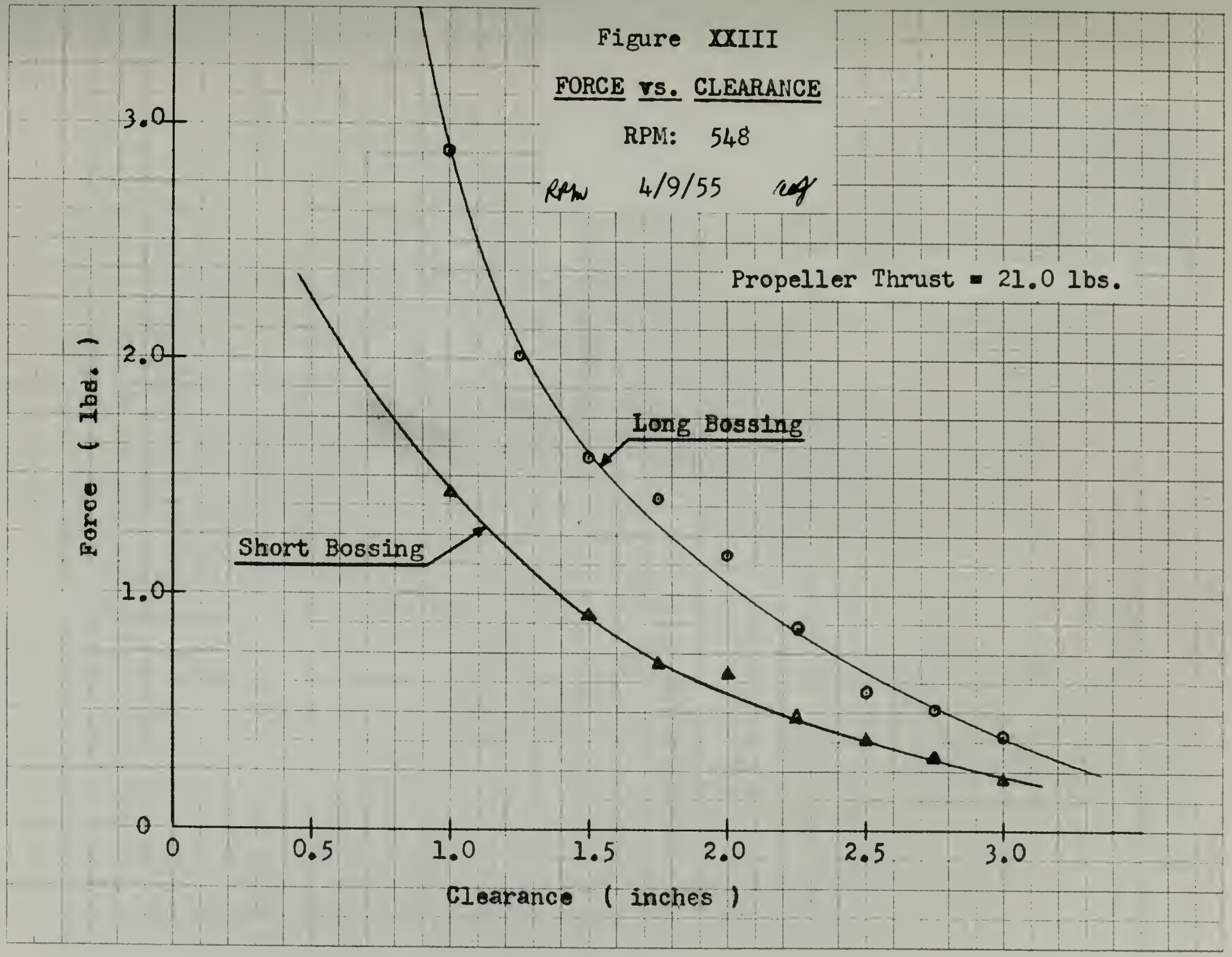

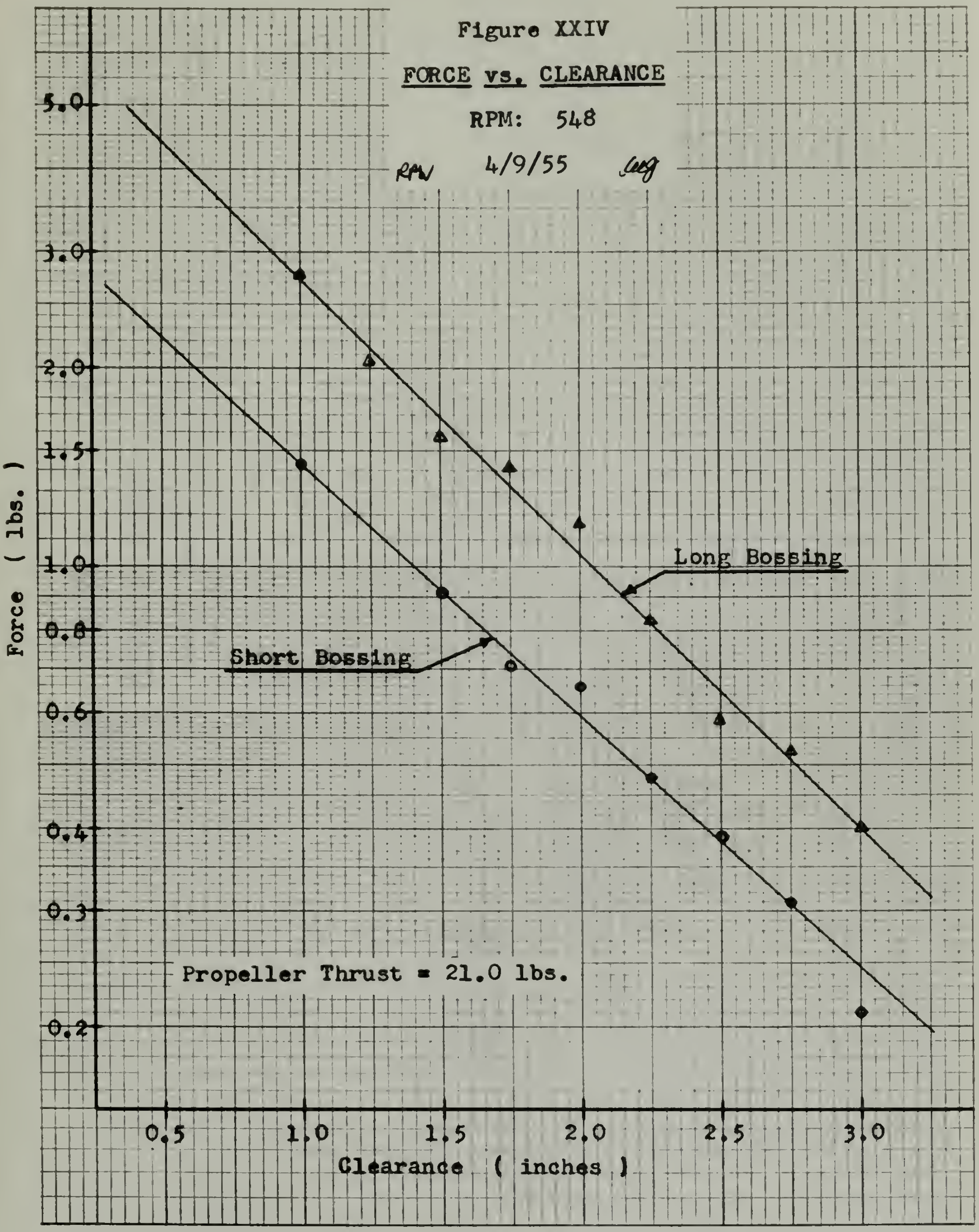

Figure XXIV

FORCE vs. CLEARANCE

RPM: 548

4/9/55

Figure XXV

FORCE vs. THRUST

Short Bossing
Clearance: 2.00"

RPW 4/9/55 aeg

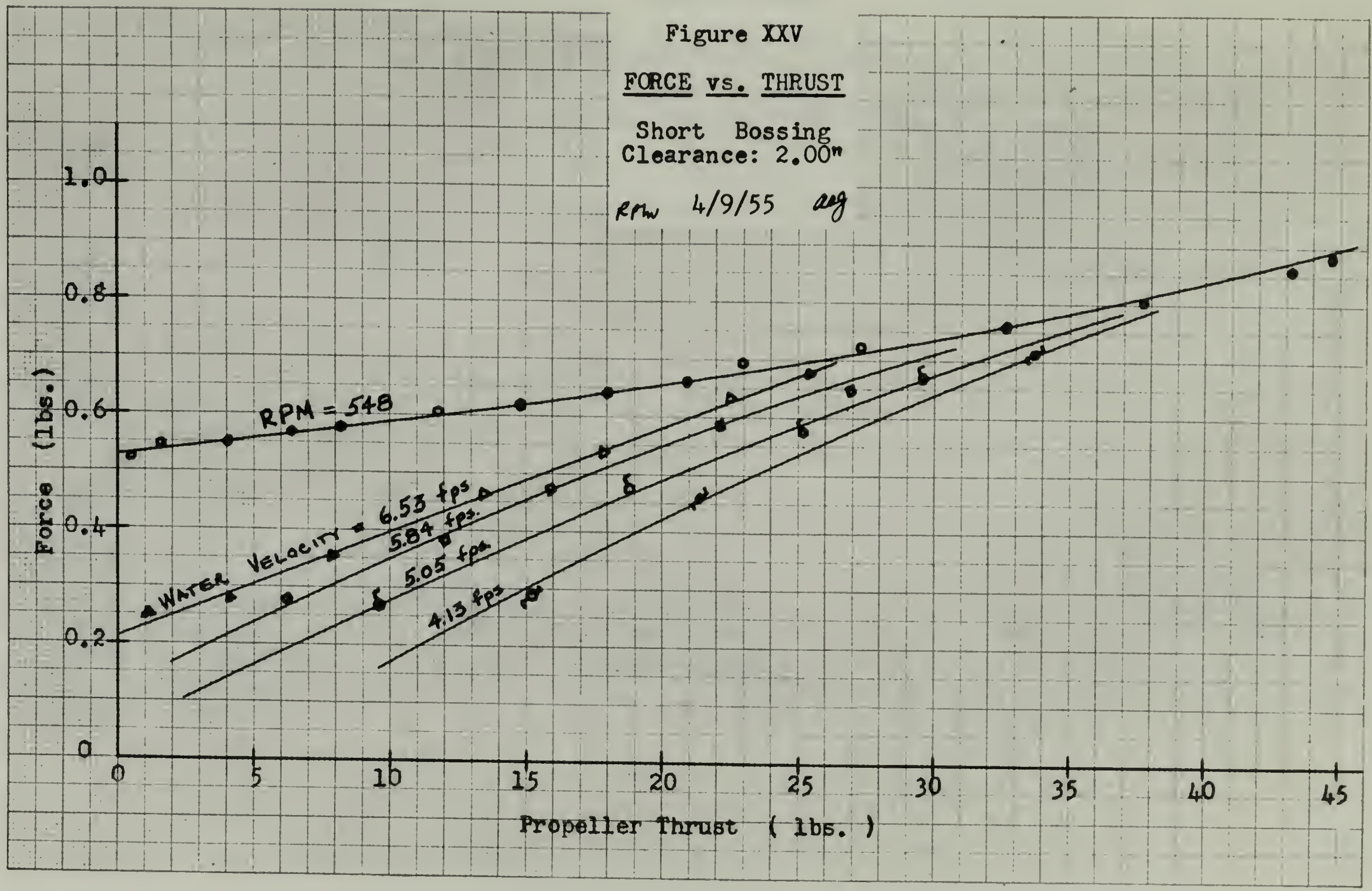

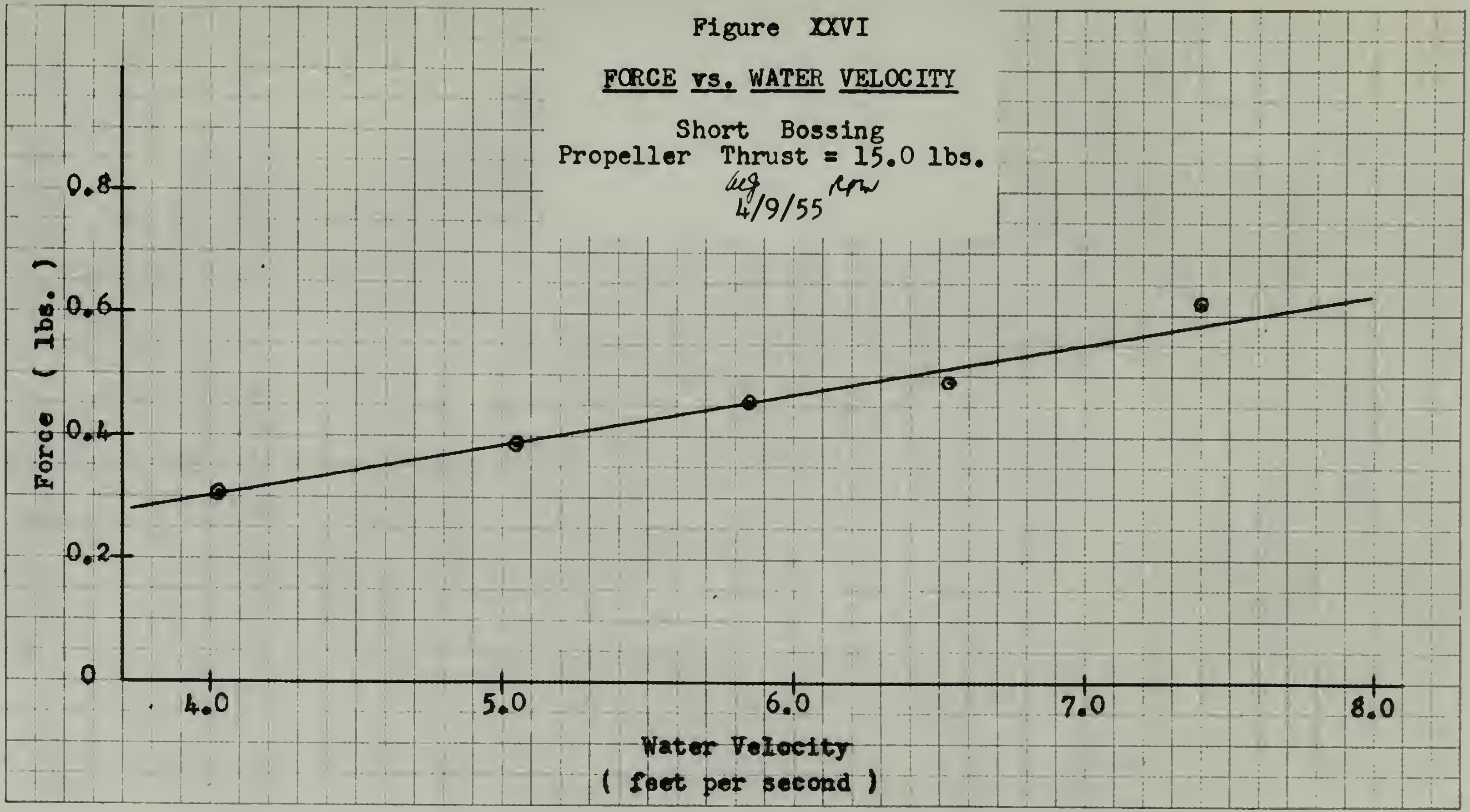

Figure XXVI

FORCE vs. WATER VELOCITY

Short Bossing
Propeller Thrust = 15.0 lbs.
wg rpw
4/9/55

TABLE XXXIII

Summary of Phase Angle γ

for Short Bossing

Clearance	Clearance / Prop. Diam.	γ_{min} (-)	γ_{max} (-)	$\Delta\gamma$	$\gamma_{T=21 \text{ lbs.}}$ (-)	$\gamma_{T=21 \text{ lbs.}}$ (+)
inches		deg	deg	deg	deg	deg
1	0.085	31.0	37.6	6.6	35.0	10.0
1.50	0.127	29.9	33.1	3.2	30.8	14.2
1.75	0.148	30.3	34.3	4.0	31.1	13.9
2.00	0.169	not computed				
2.25	0.190	31.5	34.4	2.9	32.5	12.5
2.50	0.211	32.5	37.3	4.8	34.8	10.2
2.75	0.232	33.5	37.6	4.1	35.4	9.6
3.00	0.250	30.8	35.6	4.8	32.0	13.0

Av. $\Delta\gamma = 4.34°$

NOTE: γ_{min} generally corresponds to high thrust values.

γ_{max} generally corresponds to low thrust values.

$\Delta\gamma_{max}$ is maximum variation.

By Definition $+\gamma$ is the phase angle by which the force leads the propeller blade.

TABLE XXXIV

Summary of Phase Angle γ

for Long Bossing

Clearance	$\frac{\text{Clearance}}{\text{Prop. Diam.}}$	$\gamma_{min.}$ (+)	$\gamma_{max.}$ (+)	$\Delta\gamma$	$\gamma_{T=21\ lbs.}$ (+)
inches		deg	deg	deg	deg
1	0.085	23.9	26.0	2.1	25.1
1.25	0.106	24.9	26.1	1.2	25.9
1.50	0.127	24.3	26.1	1.8	26.0
1.75	0.148	22.9	23.9	1.0	23.8
2.00	0.169	22.9	24.5	1.6	24.5
2.25	0.190	21.9	24.3	2.4	24.0
2.50	0.211	21.9	23.5	1.6	23.0
2.75	0.232	21.6	25.5	3.9	25.0
3.00	0.250	22.2	25.9	3.7	25.2

Av. $\Delta\gamma = 2.14°$

NOTE: γ_{min} generally corresponds to high thrust values.

γ_{max} generally corresponds to low thrust values.

$\Delta\gamma_{max}$ is maximum variation.

By Definition $+\gamma$ is the phase angle by which the force leads the propeller blade.

TABLE XXXV

Summary of Force and Phase Angle

Thrust = 21 lbs. RPM = 548

	SHORT BOSSING				LONG BOSSING		
Clearance	$\frac{\text{Clearance}}{\text{Prop. Diam.}}$	Force	% Thrust	γ (+)	Force	% Thrust	γ (+)
inches		lbs		deg	lbs		deg
1.00	0.085	1.43	6.82	10.0	2.78	13.22	25.1
1.25	0.106	----	----	----	2.03	9.68	25.9
1.50	0.127	0.91	4.33	14.2	1.58	7.52	26.0
1.75	0.148	0.71	3.48	13.9	1.42	6.77	23.8
2.00	0.169	0.66	3.14	----	1.16	5.53	24.5
2.25	0.190	0.48	2.38	12.5	0.84	4.00	24.0
2.50	0.211	0.38	1.81	10.2	0.58	2.76	23.0
2.75	0.232	0.31	1.48	9.6	0.52	2.48	25.0
3.00	0.250	0.21	1.00	13.0	0.40	1.91	25.2

NOTE: By Definition $+\gamma$ is the angle by which the force leads the propeller blade.

TABLE XXXVI

Comparison of Measured Values With Law of Similitude

J	Thrust	Force measured	N	$(N_2/N_1)^2$	Force computed by square law	$(N_2/N_1)^{2.75}$	Force computed by 2.75 law
v/nd	lbs.	lbs.	RPM		lbs.		lbs.
0.58	28.9	0.655	530	1.49	0.56	1.73	0.657
0.58	18.7	0.38	434				
0.62	22.3	0.535	496	1.49	0.46	1.727	0.535
0.62	15.2	0.31	407				
0.65	27.8	0.680	547	2.00	0.510	2.60	0.662
0.65	18.5	0.460	473	1.49	0.382	1.73	0.441
0.65	13.2	0.255	387				
0.70	25.0	0.670	568	1.66	0.590	2.015	0.720
0.70	19.9	0.550	506	1.32	0.470	1.47	0.523
0.70	13.5	0.355	440				
0.77	15.2	0.490	516	1.66	0.440	2.015	0.534
0.77	11.8	0.385	462	1.25	0.330	1.366	0.362
0.77	9.4	0.265	400				
0.85	7.2	0.345	468	1.25	0.340	1.366	0.368
0.85	6.4	0.270	418				

V. DISCUSSION OF RESULTS

The factual statement of the results of this investigation has been presented in the preceding section. The purpose of this section is to discuss these results in order that they may be correctly interpreted and properly evaluated.

It has not been the purpose of this thesis to develop a new theory or to disprove existing theories, but rather to cast additional light on the mechanism of propeller excited vibratory forces. In an attempt to increase the existing factual knowledge of the phenomena, the influence of various parameters on the magnitude and phase angle of the vibratory force have been studied. In order that the results of these studies may be a significant contribution it becomes necessary to indicate their validity by an examination of the techniques employed in their determination. It is also imperative to re-emphasize some of the more subtle points which may be overlooked in analysis of the factual results.

The best method of insuring accurate interpretation of the measurement data was by comparison with calibration data corresponding in magnitude to the measurements. In

determining the variation of vibratory force with thrust, it was impossible to use this method for all measurement runs, particularly in the analysis of data taken with the long bossing (long nose piece). (Fig. XXII). Forces obtained using the short nose piece, with the exception of 1" clearance data, were taken directly from either directly plotted or interpolated (1.75" and 2.5") calibration curves. (Figs. XXXV and XXI). The method employed for a clearance of 1.0 inch is considered valid although is recognized to be not as direct as having a calibration covering the ranges of measured force. For clearances of 1.75 and 2.50 inches the interpolation between existing calibration curves was linear. As shown in Fig. XXIV these two points are slightly off the straight line representing the variation of force with clearance. Closer correspondence of the data would have been obtained had a logrithmic interpolation been made between existing calibration curves. The ideal solution, of course, would have been the preparation of a separate calibration curve for each individual spacer arrangement. The overall error resulting from such calibration interpolation, however, is seen to be small, and therefore the procedure is considered justifiable.

Of the total of nine clearance runs made with the long nose piece, only four (2¼"-3") were possible to analyze directly from calibration curves.

Time did not permit a data reduction technique similar to that employed for a clearance of 1 inch with the short bossing. For the determination of forces measured which were outside the range of the calibration data, it was necessary to assume that the calibration curves were straight lines. This assumption permitted force determination for any galvanometer deflection by mere application of the calibration curve slope.

In addition, data for clearances of 1.25, 1.75, 2.25, and 2.75 inches for the long bossing were reduced by logrithmic interpolation between existing calibration curves. It should be noted that the calibration curves, as drawn, do not always intersect at the origin. (Figs. XLII and XLIII). The initial procedure and preliminary calibrations indicated that the galvanometer scale was not linear and, therefore, the calibration curves of resultant galvanometer readings vs. force possessed slight curvature. This was demonstrated in the short bossing calibration curves.

This discussion should emphasize that certain errors were accepted in the reduction of the data for the long bossing which were not present in the short bossing analysis. If it is assumed that the values of the force determined for clearances of 2.5" and 3.0" are correct, since they were derived directly from cal-

ibration curves, the slope of the long bossing curve in Fig. XXIV could be reduced to a value corresponding to that of the short bossing. This would indicate that the values at smaller clearances as plotted, are high. If the calibration curves were of a shape similar to those of the short bossing these values would be smaller, and better agreement would exist between the slopes of the two curves. Despite these small discrepancies, the qualitative results indicate conclusively that for the longer bossing the magnitude of the force is at least 1.5 times as great as that for the corresponding conditions with the short bossing.

The curves of vibratory forces vs. clearance could be more clearly defined by measurement at clearances of less than 1 inch. The propeller selected for this investigation was designed with 8° rake so that a clearance of one inch at the 0.7 radius was the minimum value obtainable.

During the initial procedure and the exploratory runs it was discovered that lateral vibration of the wire-spring combination introduced a small error in the magnitude of the calibration force. The initial tension of the wire was increased to reduce this vibration, and several forms of dampers were used. These proved to be unsatisfactory, however, and were removed. Thus a small

but constant error existed for all data runs due to the lateral vibration of the wire-spring combination. The magnitude of this error is considered negligible for forces exceeding 0.4 lbs., but may be of some significance at lower values of force which correspond to the greater clearances.

Preliminary runs to determine the influence of certain parameters on the proposed calibration method revealed that self-excitation of the bossing system by the water was possible. The magnitude of the vibration varied directly with the water velocity while the frequency remained constant at the natural frequency of the bossing system. To increase the sensitivity of the detector system the investigation was conducted, for the most part, near the resonant peak. Thus the operating frequency corresponded closely to that of the natural frequency of the system and, therefore, the frequency of self-excitation. When compared with the vibratory forces, the influence of this phenomenon was found to be small at the water velocities anticipated. However small, it is possible that some slight error could have been introduced, particularly at low thrust values for the greater clearance runs.

Operation of the bossing system near the resonant peak made propeller speed control extremely critical.

Errors of 2 and 3 RPM in propeller speed caused relatively large errors in the magnitude of the measured force. To insure that such errors were kept to a minimum, constant attention had to be directed toward speed control. The magnitude of the errors introduced is felt, for the most part, to be negligible. However, this was only possible through constant adjustment of the speed control system. It is felt that the quantity of data taken could have been roughly doubled had speed control not been such a problem, either by having a more positive means of speed control available or by operating the system further from the resonant frequency.

Figure XXV illustrates the results of an investigation to determine the influence of water velocity on the vibratory force and to confirm the existing laws of similitude. For a constant value of thrust, the data clearly demonstrates the increase in the induced vibratory force with an increase in the water velocity past the bossing.

Correlation of this data was impossible with the existing laws of similitude, i.e. $F_2 = F_1(\frac{N_2}{N_1})^{2.00}$. As demonstrated in Table XXXVI, however, if the exponent of 2.00 is increased to 2.75, the results are in better agreement. It is suspected that the amplifier in the circuit was operating at or slightly below the linear

range of frequency vs. gain for these data runs. With a decrease in RPM the curves would drop off more sharply than they should. Thus the possibility exists that the effect represented here is somewhat exaggerated. The overall discrepancy is felt to be small, however, and qualitatively the data is valid.

Tables XXXIII and XXXIV are a summary of the phase angle relationships for the vibratory force. In calculating the values of the phase angle it was necessary to use measurements at a particular gain setting since it was found that the angle β_1 varied with gain. This was thought to be the results of operating the amplifier in the non-linear frequency range. The phase angle β_1 also varied in magnitude throughout a calibration run, but to a much lesser extent. Since a constant value of β_1 is essential for the evaluation of the phase angle γ, the average value of β_1 for each calibration run was used. For phase angle determination where the calibration curves had been derived by interpolation it was necessary to interpolate between the β_1 values also. It is felt that the phase angle relationships are of the correct order of magnitude but are subject to small errors which were introduced by the calculation procedure employed.

VI. CONCLUSIONS

1. The induced vibratory force normal to the bossing is a function of the following variables:

   (a) Propeller thrust.

   (b) Water velocity.

   (c) Clearance between propeller blade and bossing.

   (d) Length of bossing.

2. For a constant value of propeller speed the vibratory force as a function of clearance may be represented by the following relationship:

$$F_2 = F_1 \epsilon^{-\mu(C_2 - C_1)}$$

where, F_2 and F_1 are the vibratory forces

μ is the slope of the semi-log plot of force vs. clearance, and

C_1 and C_2 are the clearances in inches at 0.7 radius.

3. The law of similitude for vibratory forces normal to the bossing corresponds more closely to the following relationship:

for $J_2 = J_1$

$$F_2 = F_1\left(\frac{N_2}{N_1}\right)^{2.75}$$

where F_1 and F_2 are the forces and N_1 and N_2 are the corresponding propeller speeds.

4. For design purposes a clearance equal to 1/3 the propeller diameter is recommended to minimize vibratory forces.

5. The phase angle, γ, defined as the angle between the time the generating line of an arbitrarily selected propeller blade coincides with the trailing edge of the bossing, and the occurrence of the measured hydrodynamically induced force normal to the bossing, is:

(a) Independent of the clearance between propeller and bossing, and

(b) A function of the bossing length and propeller thrust.

VII. RECOMMENDATIONS

A. Redesign of Apparatus and Changes to Instrumentation:

1. Design a new calibrator capable of applying a force of at least 5 lbs. to the bossing and operating at much higher speeds.

2. Design a chain or geared drive for the increased capacity calibrator to eliminate torsional vibrations at higher loadings. The drive end of the system should be at the tunnel end of the dynamometer shaft. The new calibrator may still use a short flexible cable drive in the measurement run position.

3. Design a damper to eliminate lateral vibration of the spring-wire combination used for calibrating the system. In reducing lateral vibrations this damper should not be permitted to interfere with application of the calibrator force to the bossing.

4. Obtain a propeller with no rake in order to reduce minimum propeller clearances.

5. Obtain a voltage amplifier which is linear down to 10 cps; i.e. gain is independent of frequency down to 10 cps.

6. Devise a system which insures positive propeller tunnel speed control to within .5 RPM with little or no manual adjustment necessary. This may be accomplished by modification to the tuning fork circuit described herein.

7. Obtain an alternating current galvanometer or similar measuring instrument with a linear reading scale.

8. Rewind moveable coil of detector unit to give a larger number of turns. This will permit greater sensitivity and allow operation away from the resonant peak.

B. For Future Investigations:

1. Confirm assumption that vibratory force is applied at a distance from the propeller shaft corresponding to the 0.7 radius of the propeller. The possibility exists of accomplishing this by the use of strain gages.

2. Investigate the presently accepted law of similitude to confirm the results of this investigation.

3. Investigate more thoroughly the affects of bossing length on the induced force by running at least two additional series, each with different nose pieces.

4. Investigate more thoroughly the influence of water velocity on the induced vibratory forces.

5. Confirm the phase angle relationship established in this thesis by additional investigation.

6. Investigate the influence of wake distribution on the magnitude and phase angle of the induced vibratory forces.

7. An alternate solution to the problem of designing a larger capacity calibrator and chain drive would be to use a smaller diameter propeller.

8. Utilize the bossing bearing installed in the hub to investigate bearing forces of blade frequency induced using similar parameters as in this thesis.

VIII. APPENDIX

APPENDIX A

Detailed Procedure

1. Determination of an acceptable calibration and measurement procedure.

After the bossing system and the instrumentation were assembled and before the calibration and measurement runs could be commenced, many small, time-consuming problems had to be solved. The solution to these problems influenced the procedure finally adopted and therefore constitute a part of the initial procedure. The initial procedure may be subdivided into three groups of problems or investigations: (1) those concerning instrumentation, (2) those concerning the mechanical aspects of the bossing system as employed and (3) the effects of certain variables.

The instrumentation problems were actually simple in nature but are included for future reference. The amplifier characteristics were unknown at the start of the investigation. The major characteristics of the amplifier which were considered to be important were frequency response, linearity and amplification. These were determined by various techniques in the De Forrest Experimental Stress

Analysis Laboratory. A plot was made on semi-log paper of gain vs. gain dial setting with gain as the log coordinate. The plot was a straight line between settings of 6 to 11 inclusive, increased suddenly at settings of 5-1/2 and 11-1/2, and was curved above 12 and below 5. In order to utilize the relationship between gain and gain dial settings it was necessary to restrict the settings used between the values of 6 and 11. A plot was made of gain vs. frequency for various gain dial settings in order to determine the linear range of frequency response. A constant gain was obtained from approximately 20 cps to 6000 cps. Since 20 cps corresponds to a propeller speed of 300 RPM, if a four-bladed propeller is used, 300 RPM was considered to be the lowest possible shaft speed. Actually, it was found later in the investigation that with the amplifier in the detector circuit (Fig. IX) the linear range did not extend much below 35 cps. Thus the amplifier characteristics as originally determined restricted the flexibility of the measurement system to propeller speeds greater than 300 RPM, and gain dial settings of 6 to 11 inclusive.

Despite the fact that the linear range as originally measured was found to extend to as low as 20 cps, trouble was experienced with the phase angle relationships. It was found that the phase shift within the amplifier varied with gain. This probably was a result of operating at a

frequency which was in the non-linear range of the amplifier. This condition was recognized early in the investigation. To correct it an amplifier of a lower frequency range was required. Such an amplifier was not available so the angles β_1 and β_2 became functions of the gain dial setting.

Being restricted to gain dial settings of 6 to 11 inclusive, it was necessary to decrease the magnitude of the galvanometer inputs by some other method when necessary to get on-scale readings. To accomplish this a resistance decade box was connected in series with the sine wave generator input to the galvanometer. Since the galvanometer multiplies the amplified detector output and the sine wave generator input together, a reduction in the sine wave generator input reduces the galvanometer sensitivity for a given detector output. Thus, the decade box functioned as an additional sensitivity control. The amount of resistance to use in a series of runs was usually established by making a preliminary measurement run to determine the magnitude of the signals to be expected. This was done because it was highly desirable to make both the measurement run and the calibration run at the same gain dial setting and thus avoid unduly complicated methods of data reduction.

The magnitude of the signal generated in the detector unit is a function of the velocity of the moveable coil and its flux linkages. The amount of flux linkage was controlled by the current in the fixed coil (E of Fig. X). Any fluctuations in this current would cause variations in the sensitivity of the detector system. Originally a 1.5 volt dry cell battery was used to energize this coil and was found to be unsatisfactory because its terminal voltage could not be maintained constant. To maintain the current in the fixed coil constant a lead acid storage battery was used. A variable resistor and ammeter were placed between the battery and the coil so that a constant current could be insured. An automobile battery charger was used to keep the storage battery in a constant state of charge.

During the early calibration runs a great deal of trouble was experienced with the reproducibility of data. The reasons for such difficulties were two-fold in that they arose from both instrumentation and mechanical sources. During the original calibration runs the galvanometer zero setting was arbitrarily chosen to facilitate acquiring on-scale readings. It was discovered that the response of the galvanometer to a signal of fixed magnitude and frequency was a function of the zero setting. In other words, the galvanometer was found to be non-linear.

After this discovery the same zero setting was used throughout the investigation and carefully checked at frequent intervals.

As previously mentioned, the bossing system operated in most conditions just off the resonant peak to give increased sensitivity. During the preliminary calibration runs the propeller shaft speed was checked at frequent intervals and corrected occasionally to the desired value. Subsequent measurements revealed that the response of the system was extremely critical with respect to propeller shaft speed and that the speed was not held constant enough by frequent manual adjustments. The tuning fork speed control circuit as described in Section II was then adopted. The tuning fork held the speed within approximately 1 RPM.

The first determinations of the phase angle γ relating the propeller blade position and the occurrence of the measured vibratory force revealed another instrumentation problem. It was possible to calculate two values of γ depending upon which phase of the sine wave generator appeared first in the time domain of the measurement system. By using a once per revolution contact maker and the cathode ray oscilloscope, it was established that the arbitrarily designated A reading preceded B reading in the measurement system used. This

fact controls the definitions of β_1 and β_2 and the make-up of the phase angle determination method employed. Although a small problem, it is representative of the ones which lead to time delays in discovery and correction.

At the same time instrumentation troubles were being corrected and modified, the problems concerning the mechanical aspects of the bossing system were discovered. Preliminary calibration runs quickly showed the calibrator mechanism as originally designed and driven had to be modified to eliminate torsional vibrations. These torsional vibrations affected the calibration method in several ways. Since the sine wave generator was driven by the calibrator shaft, the torsional oscillations caused an unsteady sine wave generator output. Thus the sine wave generator input to the galvanometer was unsteady causing the galvanometer readings to oscillate. In addition, torsional vibration of the calibrator cam shaft produced a vibratory force whose frequency did not correspond to that of the hydrodynamically induced force, and therefore could not be used for construction of a representative calibration curve. The calibrator, when in position for a calibration run, was originally driven by a long flexible cable geared to the dynamometer shaft at the thrust meter end. To reduce the torsional vibration to an acceptable level, the major portion of

the flexible cable was replaced by a solid steel shaft. The shaft was mounted on a long 4" x 4" wooden beam and supported by bronze bearings. Short pieces of flexible cable were used at each end of the solid shaft. Figure XVI shows part of the shaft and one of the short flexible cables connected to the calibrator. It should be mentioned here that the three extra arms on the calibrator had a negligible effect in reducing vibration and were removed during the initial phase of the investigation.

Although the torsional vibration was greatly reduced by using the solid steel shaft, it still persisted. It was discovered that the alignment of the calibrator cam shaft and the sine wave generator shaft was not true. The two shafts had been coupled together with a solid steel coupling to prevent slippage and to preserve the phase angle relationships. To eliminate the alignment problem the sine wave generator was moved to one side and identical gears were pinned to each shaft. This is the reason for the sine wave generator gear drive.

In one of the many attempts to obtain reproducible data it was found that the sensitivity of the measurement system varied with the exact location of the detector unit. This was caused by rubbing of the moveable coil on the inside of the detector case. As seen in Fig. X the clearance between the moveable coil and the side is ex-

tremely small. Therefore, unless the vertical rod connecting the horizontal arm to the moveable coil of the detector was correctly aligned, rubbing occurred and consequently greatly varying detector sensitivities resulted. To eliminate this variable the correct position of the detector unit was found and carefully marked to insure a reproducible location and thus a constant sensitivity. In addition the detector casing was remachined to a larger internal diameter to provide greater clearance around the moveable coil. The final remedial measures taken in obtaining reproducible data focused themselves about the wire used between the calibrator lever arm and the bossing during the calibration runs. The wire which was originally selected for this function was black iron wire, of 1/32 inch diameter. In selecting this wire, calculations were made to determine the influence of the weight of the wire on the spring constants of the springs used, and, on the time lag between the time the cam reached the high point and the time the bossing received the application of this maximum force. Both of these effects were calculated to be negligible. Initially, the force applied to the bossing by a particular spring was determined by measuring the elongation of the spring alone as a function of the required elongation force. These measurements were made for each

spring individually. It had been calculated that the spring constant of the wire was infinite compared to that of the spring and was therefore negligible. This method was found to be completely unsatisfactory. The first corrective step was to replace the wire then in use with 0.010" diameter steel piano wire. The use of piano wire reduced the number of kinks and small bends which ordinary wire inherently possesses. In addition, it reduced the spring action of the wire on the pulley, used to guide the wire to the bossing. This replacement of the original wire with piano wire still did not completely solve the problem of reproducible data. The system used to determine the force applied to the bossing was inadequate. Using the initial system the elongation of the wire was assumed to be zero, and the displacement of the bossing and pulley was assumed to be zero when the force was applied. The method finally adopted took these variables into account by determining the force applied to the bossing with the bossing and calibrator system assembled and the wire-spring combination attached in the exact manner in which it was to be used for calibration. The method is described in detail in the following section on force determination.

With adoption of the piano wire for the wire-spring combination another problem was inherited:

lateral vibration of the wire in the span between the lever arm and the pulley. See Fig. XV. It was found that the amount of lateral vibration of the wire was a function of the initial tension applied to the wire-spring combination. The amount of lateral vibration affected the magnitude of the force applied to the bossing. By increasing the initial tension lateral vibrations were greatly reduced although not eliminated. Several attempts were made to eliminate these vibrations by using different types of dampers. The dampers not only tended to reduce the lateral vibration but also the longitudinal vibration and consequently, the magnitude of the force applied to the bossing. The effect of the lateral vibration at higher initial tensions was felt to be almost negligible when the precision of the overall assumptions were reconsidered. For this reason, rather than use some type of damper which would further complicate the calibration system, a small but constant error was accepted.

With an operationally acceptable system of measurement and calibration, there remained the problem of evaluating the effects of certain parameters on the calibration technique. Several of these have been mentioned in connection with the instrumentation and mechanical aspects of the initial procedure. The one remaining parameter to be mentioned is that of water

velocity. The calibration technique employed assumed the effect of water velocity to be negligible on the response of the bossing. It was found, however, that the bossing was sensitive to variations in water velocity. The phenomenon is similar to that of the self-excitation of airplane wings commonly known as wing flutter. The frequency of the vibration was constant but its amplitude was found to increase with increasing water velocity. A shift from the long nose piece to the short nose piece was accompanied by a shift in the frequency of the self excited vibration. The frequency measured coincided closely to the calculated natural frequency of the bossing system. This meant that the water velocity would affect the response of the system to a given force and frequency. To reduce this effect to a negligible quantity it was decided to accept a reduced sensitivity and operate away from the natural frequency of the bossing. Poor performance of the calibrator mechanism at propeller speeds greater than 625 RPM placed an upper limit on the frequency. (625 RPM corresponds to a calibrator speed of 2500 RPM). The lower limit was established at approximately 350 RPM because of the amplifier characteristics. A propeller shaft speed of 548 RPM was therefore selected as the basic speed at which a large portion of the investi-

gation was conducted. At this propeller speed it was found that the water velocities required to cover the desired range of thrusts were sufficiently low to have a negligible effect on the system response. A small error is introduced at the higher water velocities but these correspond to negative thrust values which were not of interest in this investigation.

From this it can be seen that many assumptions have been made as to the magnitude of various sources of error. Refinement of the instrumentation, bossing system, calibration and measurement techniques could go on endlessly. As many refinements were made as considered compatible with the time allowed for the thesis. Whether more refined measurements would have been consistent with the basic assumptions used to permit the investigation is questionable.

2. Details of Force Determination:

Determination of the magnitude of the hydrodynamically induced vibratory force, was accomplished by preparation of a series of calibration curves. The response of the system to a vibratory force was a function of the frequency of the excitation force and the natural frequency of the bossing system. The frequency of the excitation force corresponds to four times the propeller shaft speed and, consequently, calibration was required for each speed used. The natural frequency of the bossing system was found to be a function of clearance and bossing length, i.e. which nose piece and spacer ring combination was in use. The term clearance refers to the distance between the propeller and bossing and the term length to the dimension parallel to the direction of water flow. See Fig. XXVII. The clearance between the propeller and bossing was varied by lengthening the cylindrical or hub section of the bossing. Lengthening was accomplished by inserting brass spacers at the after end of the cast aluminum hub section. See Fig. VI and Fig. XXVII. This additional weight altered the natural frequency of the bossing and thus the natural frequency of the entire bossing system comprising the bossing, hollow steel shaft, and horizontal arm. Addition of the brass spacers was accompanied by relocation of the point

FIGURE XXVII

BOSSING CLEARANCE

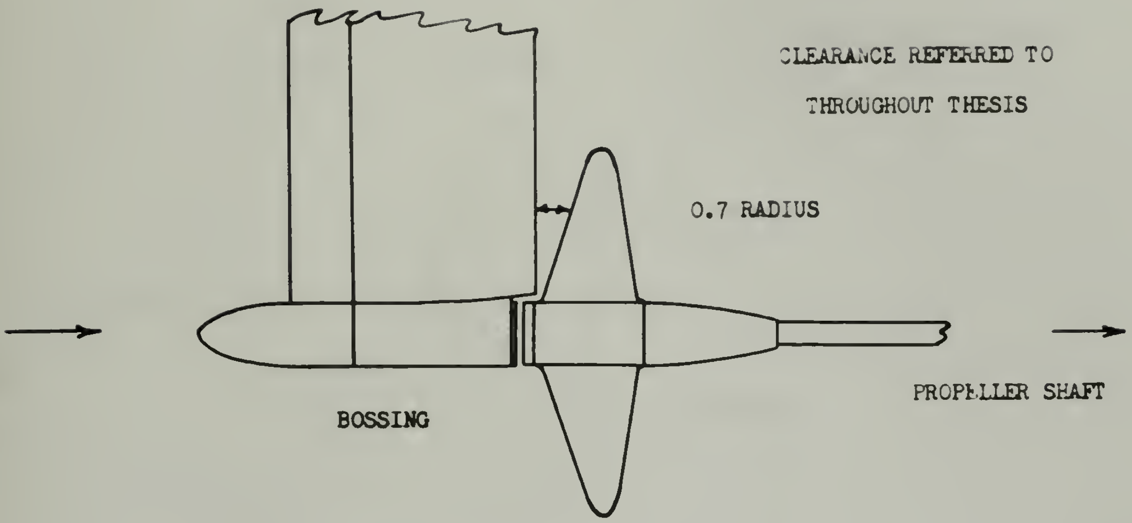

FIGURE XXVIII

FORCE MEASURED

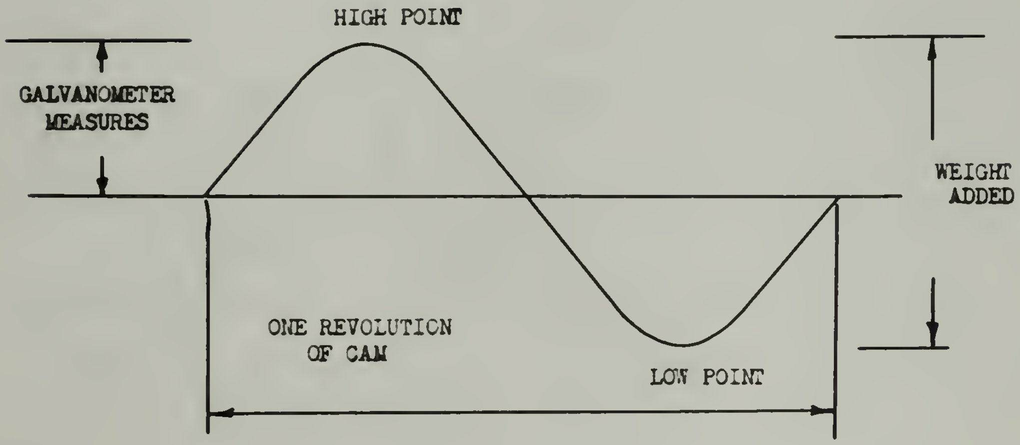

FIGURE XXIX

FORCE SIGN CONVENTION

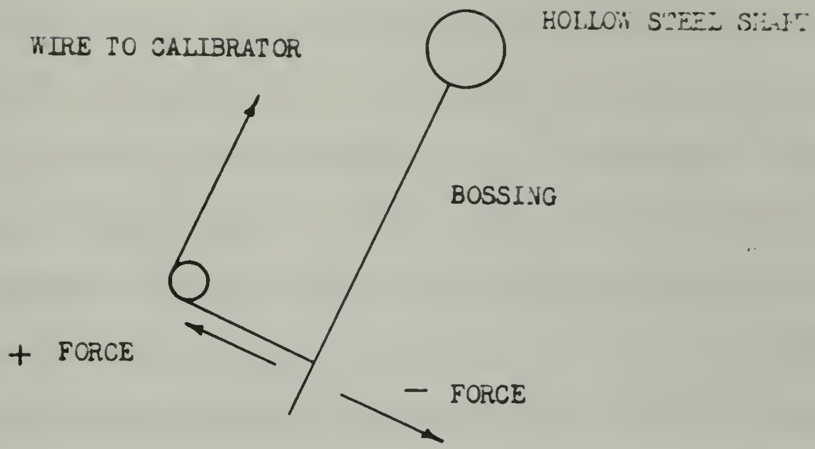

FOR CALIBRATION

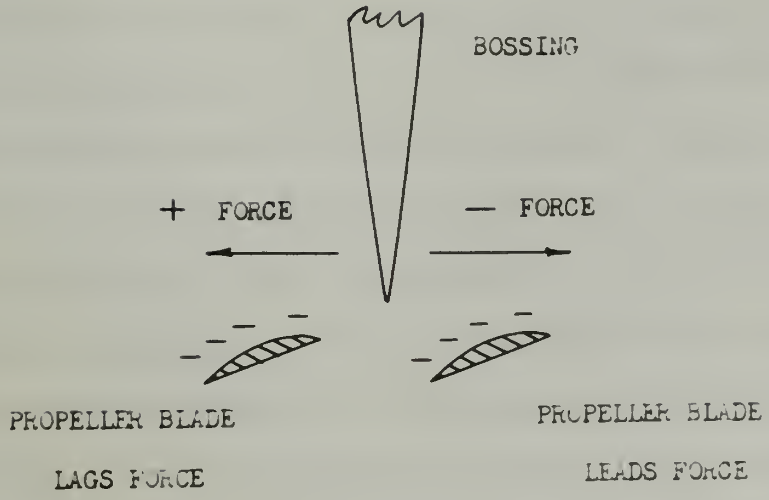

FOR MEASUREMENT

of attachment of the bossing to the hollow steel shaft. As a result the point of application of the alternating twisting moment was changed and this in turn changed the angular displacement of the hollow steel shaft and horizontal arm for a given vibratory force. For this reason it was necessary to calibrate the system for each clearancee investigated and each length of bossing used. The shift in natural frequency of the bossing with a variation in length resulted from the fact that the inertia of the entrained water varies as the square of the bossing length.

Calibration was accomplished by means of the calibrator described in Section II. The appropriate nose piece and the piano wire were fastened to the bossing before it was placed in the test section. The bossing was placed at the desired location in the test section dependent upon the clearance under investigation. The propeller was not attached to the propeller shaft during the calibration runs because it was necessary to run the dynamometer shaft at the correct speed. This was necessary since the calibrator shaft was driven by the dynamometer. The piano wire was then run through a pulley with frictionless bearings to the calibrator where it was attached to the lever arm by means of a small helical spring. An assortment of springs provided a good range of spring constants. With the lever arm at the low point of the cam the initial tension was set by putting the desired

weight on the weight pan and then adjusting the length of the wire-spring combination until the lever arm just lifted off the cam. This amounted to varying the initial elongation of the spring. See Fig. XX. The same initial tension or force was applied to each spring depending upon stiffness. Having adjusted the initial tension to the desired value, the cam was rotated 180° to the high point. Weights were then added to the weight pan until the lever arm just lifted off the cam. This additional weight was the force applied to the bossing when corrected for the distance (d) between A and B in Fig. XX, the angle between the weight pan string and the arm, and the actual amplitude measured. See Fig. XXVIII.

Although the same springs and same diameter piano wire were used repeatedly for the various calibration runs, the spring constant was determined independently for each run.

Having determined the magnitude of the weights required, the weights were removed from the weight pan and the weight pan string removed from the lever arm. The propeller shaft was then run at the desired RPM and the galvanometer readings, A reading and B reading, recorded. The above process was then repeated for a sufficient number of springs to determine a calibration curve of force vs. resultant galvanometer reading, R reading.

See sample calculations and a typical calibration curve.

The next phase of the procedure consisted of actual force measurements. Having sufficient data to plot a calibration curve the wire-spring combination was removed from the bossing, the propeller keyed to the propeller shaft in the marked angular position (see details of phase angle determination), and the calibrator relocated on the control panel. See Fig. XVI.

The results of previous investigations indicated that the magnitude of the bossing force was mainly a function of two variables: thrust and clearance. Consequently, for each set of conditions, measurements were made for a wide range of thrusts; from above the operating point to approximately zero. At the desired values of thrust the galvanometer readings were recorded and reduced to the corresponding force by means of the calibration curves.

Early calibration runs revealed that the maximum force which could be applied to bossing by the calibrator was approximately 1.1 lbs. (See Discussions of Results). Because the magnitudes of the forces were well above 1.1 lbs. for 1" clearances with the short bossing, and the calibration curves showed the system to be non-linear, it was necessary in this case to use a different cali-

bration technique. From this it should not be concluded that the bossing system was non-linear, but rather the measurement system; in particular the galvanometer or amplifier. For this reason the magnitude of the force could not be determined by linear extrapolation of the 1" calibration curve.

A calibration curve was made in the usual manner with the calibrator for an amplifier gain setting of 10. The measurements were made with an amplifier gain setting of 6. In addition to taking the calibration data with a gain setting of 10, data was recorded for gain settings from 6 to 11 inclusive. Lines of constant force were then plotted on semi-log paper with an ordinate of resultant galvanometer reading and an abscissa of gain setting. From this, lines of constant resultant reading were plotted using an ordinate of force and an abscissa of gain setting. The average slope of the constant resultant galvanometer readings was measured. The relationship to determine the magnitude of the force at other gain settings was found to be $F = F_o \epsilon^{\mu(D_o - D)}$, where D_o and D are the amplifier gain settings, and μ is the slope. (For the 1" clearance runs $F_6 = F_{10} \epsilon^{4\mu}$). In other words, with the resultant galvanometer readings from the actual measurement runs, the force, F_{10}, is determined from the calibration curve. But the resultant

readings were taken with a gain setting of 6, therefore, it is necessary to run along a constant resultant reading line to a gain setting of 6 and read the force F_6. The data for a clearance of 1" with the short bossing was the only data reduced in this manner. The magnitude of the forces for the other runs with the short bossing could be determined directly from a calibration curve.

The method employed to determine the magnitude of the forces when the long bossing was employed differed from that described above. These forces were much greater than had been anticipated inasmuch as it was originally considered that the bossing with the short nose piece attached was "very long" in comparison with the propeller diameter, chord lengths, etc. Consequently, the calibration runs were made in a manner similar to those used with the short nose piece at clearances greater than 1". For most clearances the forces measured were larger than 1.1 lbs. and therefore too large to be taken directly from the calibration curves. Linear extrapolation was therefore employed to reduce this data. The method is described in detail in the section on Sample Calculations.

3. Details of Phase Angle Determination

Phase angle determination involved the evaluation of four phase angles and the relationship between these angles. In this calculation all the phase angles are referred to the indicator card which is attached to the flywheel of the calibrator mechanism and rotates at four times propeller shaft speed. The four angles are defined as follows:

$$\beta_1 = \tan^{-1} \frac{B_{rdg_1}}{A_{rdg_1}}$$

(Subscript one refers to calibration and two to measurement.)

$$\beta_2 = \tan^{-1} \frac{B_{rdg_2}}{A_{rdg_2}}$$

α = the phase angle between the time the generating line of an arbitrarily selected propeller blade coincides with trailing edge of the bossing and the time the calibrator cam applies the maximum positive force to the bossing during calibration.

γ = the phase angle between the time the generating line of the arbitrarily selected propeller blade coincides with the trailing edge of the bossing and the occurrence of the measured hydrodynamically induced force normal to the bossing. A positive force acts in the same direction as the maximum calibrator force; i.e. in the same direction as the calibrator wire pulls on the bossing.

λ = the phase angle between the time of occurrence of the measured signal to the galvanometer and the applied bossing force; either calibrator or measured, since this angle was assumed to be constant.

δ = the phase angle between the time of occurrence of the A reading to the galvanometer and the time the calibrator cam applies the maximum positive force to the bossing.

The indicator card was attached to the calibrator flywheel so that a zero reading corresponded to the high point of the cam, or application of the maximum positive calibrator force. The time delay between extension of the spring and application of the force at the bossing was calculated to be negligible.

For convenience in the determination of β_1 and β_2 the following sign convention was adopted:

A reading	B reading	Angle
+	+	0 - 90°
-	+	90 - 180°
-	-	180 - 270°
+	-	270 - 360°

From Fig. XXXI the following relationship can be determined:

Figure XXX

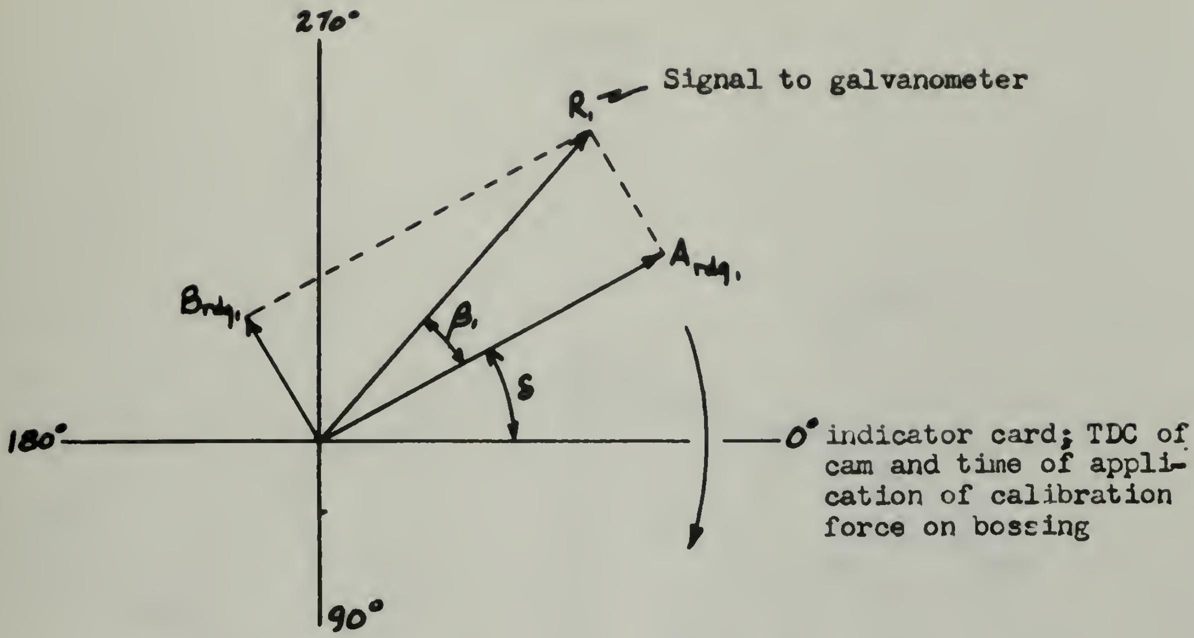
270°
R1
Signal to galvanometer
Brdg1
Ardg1
β1
δ
180°
0° indicator card; TDC of cam and time of application of calibration force on bossing
90°

PHASE DIAGRAM FOR CALIBRATION RUNS

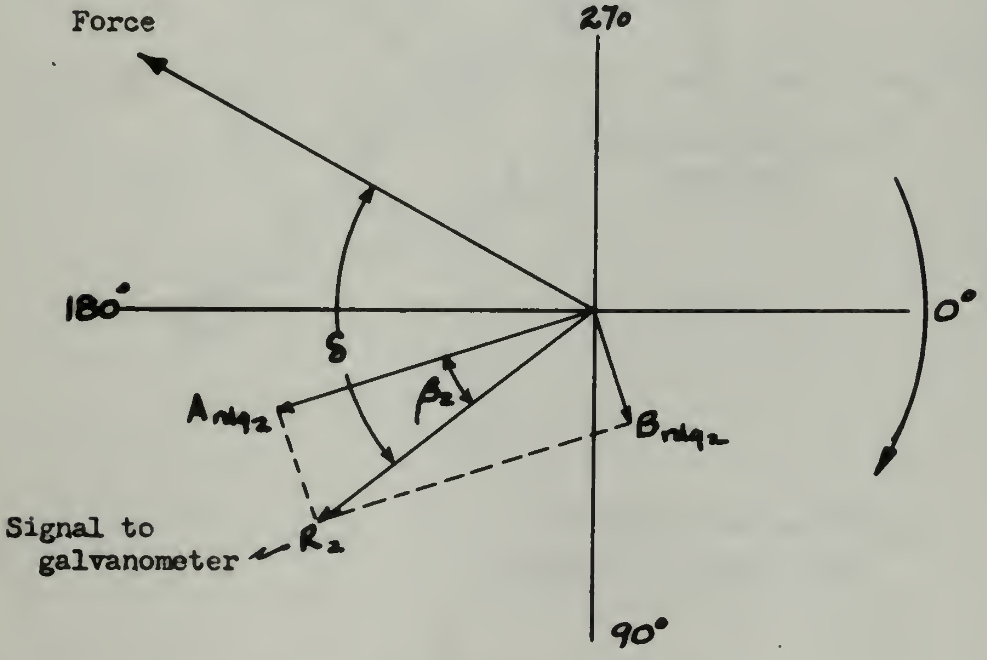

PHASE DIAGRAM FOR MEASUREMENT RUNS
(with negative readings)

Figure XXXI

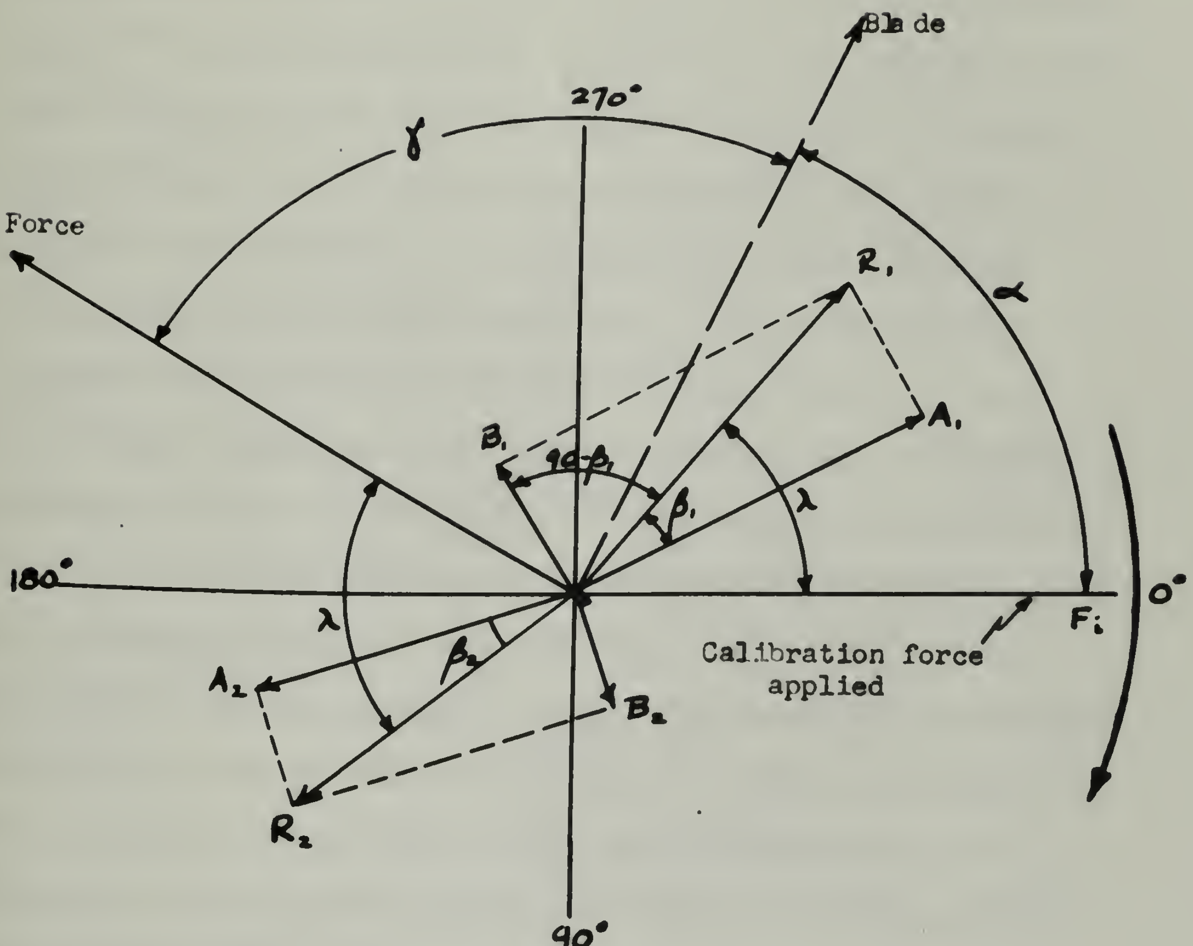

Derived from combining diagrams of Figure XXX

$$\gamma = 180 + \beta_2 - (\beta_1 + \delta)$$

or with the sign convention

$$\gamma = \beta_2 - (\beta_1 + \delta).$$

Since the above relationship has been referred to the indicator card which rotates at four times propeller speed, γ has to be divided by four to determine the relationship between force, propeller blade position and bossing. The angle is determined when the generating line of the propeller blade is in line with the trailing edge of the bossing. Therefore, on the phase diagram the bossing corresponds to the blade position. The force can be thought of as a rotating force vector rotating at four times shaft speed or at calibrator speed. The horizontal component of the force vector is the force applied to the bossing. For the case illustrated the measured force lags the propeller blade position by $\gamma°$. Since the force measured is in the negative sense, the positive force will lead the propeller blade by $\frac{180 - \gamma°}{4}$. When referred to the propeller blade and bossing this means that the positive force occurs before the propeller blade reaches the position where the generating line and the trailing edge of the bossing coincide.

The method of measurement employed assumed the phase angle λ to be constant. δ, the angle between phase A of the sine wave generator and the high point

of the cam was also constant since the sine wave generator and cam shaft were geared together. Consequently, β_1 was theoretically a constant as long as the sine wave generator and cam shaft were not displaced angularly by uncoupling. The calibrator being a packaged unit permitted movement from the propeller tunnel hatch where it was used for calibration, to a new location during the measurement runs. For propeller shaft speeds of 548 RPM which corresponds to 36.5 cps, it was found that the angle λ was a function of the amplifier gain. As a result the angle β_1 had to be as a function of gain setting. The galvanometer reads EI cos β, or EI cos $(\beta + \pi/2)$ dependent upon which sine wave generator output is used in conjunction with the amplified signal from the detector. A switch permitted rapid switching of the sine wave generator input to the galvanometer from phase A to phase B. The A reading corresponds to the galvanometer reading with phase A of the sine wave generator as an input to the galvanometer; a measure of EI cos (β_1). The B reading corresponds to the galvanometer reading with phase B as the input; a measure of EI sin β_1. Therefore, the signal to the galvanometer or resultant reading is:

$$\text{Resultant rdg} = \sqrt{(A_{rdg})^2 + (B_{rdg})^2}$$

$$= \sqrt{(EI)^2 \cos^2\beta_1 + (EI)^2 \sin^2\beta_1}$$

$$= \sqrt{(EI)^2 (\sin^2\beta_1 + \cos^2\beta_1)} = EI$$

$$\tan \beta_1 = \frac{B_{rdg}}{A_{rdg}} \qquad \text{or } \beta_1 = \tan^{-1} \frac{B_{rdg}}{A_{rdg}}$$

The resultant readings and β_1 were easily determined for each calibration run. In a similar manner for each measurement run, a resultant reading could be computed together with β_2.

The phase angle, α, as previously defined was determined by means of the indicator card and two strobe lights. The generating line of an arbitrarily selected propeller blade was marked on the blade at the tip. The propeller was then placed on the propeller shaft in the test section of the tunnel and the propeller and shaft marked so that the propeller was always returned to the same angular location on the shaft after each removal. The marked propeller blade was then aligned with the trailing edge of the bossing and the propeller shaft marked so that the mark coincided with the cross hairs of a small telescope mounted outside the test chambe window. See Fig. XVII. By means of the phaser for

timing of the strobe-lights, the strobe lights could be phased so that they "stopped" the propeller shaft when the scribe mark lined up with the cross hairs in the telescope (blade in line with bossing). A second strobe light, fired simultaneously with the first, was used to read the indicator card. The phase angle, α, was read directly from the card since 0° corresponded to the high point of the cam. Using the relationship $\Delta\gamma = \beta_2 - (\beta_1 + \alpha)$ and the sign convention for determination of the quadrant β_1 and B_2, the phase angle between force and blade position was determined.

APPENDIX B

SAMPLE CALCULATIONS

As discussed in Section III, analysis of the major portion of the data recorded involved three basic divisions: (1) calibration, (2) measurement, and (3) phase angle determination. To illustrate the calculations sequence, each step will be taken individually, using arbitrary data:

A. Calibration:

Data recorded:

Spring No. R
Initial Tension: 4 lbs., 11 oz.
Weight: 3 lbs., 100 gms.
RPM: 548
Gain Setting: 6
Resistance: 1000 ohms
$A_{reading}$ -1.39
$B_{reading}$ -1.48

To obtain the force applied to the bossing by the wire-spring combination, the weight added to the weight pan is converted by a ratio of lever arms and the cosine of the angle of attachment of the weight pan string to the lever arm:

Force per one-half revolution of the cam $= \frac{3 \text{ lbs. } 100 \text{ gms.}}{2} \cos 83°23'$

$$= \frac{3.2205}{2} \times 0.99$$

$$= 1.596 \text{ lbs.}$$

This value represents the total change in force on the bossing while the cam travels through twice the amplitude. The excitation force, then, is just half of this value:

$$\text{Force} = 0.798 \text{ lbs.}$$

Since the galvanometer deflection readings recorded represent two perpendicular vectors, the resultant deflection:

$$R_{rdg}^{2} = A_{rdg}^{2} + B_{rdg}^{2}$$

$$= (1.39)^2 + (1.48)^2$$

$$R_{rdg} = 2.02$$

With these two calculated values, a point on the calibration curve is determined for this set of data.

For use in the phase determination, β_1, must be determined. By definition:

$$\beta_1 = \tan^{-1} \frac{B_{rdg}}{A_{rdg}}$$

$$= \tan^{-1} \frac{-1.48}{-1.39} = 46.8° + 180°$$

$$= 226.8°$$

As discussed in Section III, the angle is determined to be between 180° and 270° by the sign convention adopted.

B. Measurement Run

Data Recorded:

Thrust, uncorr. :	26.4 lbs.
Thrust correction:	+0.7 lbs.
Press.column, H_1,:	184 mm.
RPM:	548
Gain Setting:	6
Resistance:	5000 ohms
$A_{reading}$:	-0.72
$B_{reading}$:	+1.92
α	327
Temperature:	80°F.

From this data we must determine the values of thrust, J, (advance coefficient) force on the bossing, and β_2.

Thrust, corrected = 26.4 + 0.7 = 27.1 lbs.

From propeller tunnel calibration data, the water velocity in the test section, in feet per second,

$$v = 0.41656\sqrt{H_1 \times C_{temp.}}$$

where H_1 is the measured height of the bromobenzine column, in mm.

and $C_{temp.}$ is a correction to the column reading to account for changes in atmospheric temperature. For 80°F., the value of $C_{temp.}$ is 0.985.

Thus,

$$v = 0.41656\sqrt{184 \times 0.985}$$

$$= 5.60 \text{ fps.}$$

By definition,

$$J = v/nd$$

where n = rev. per sec.
d = diameter in feet.
v = water velocity in ft/sec.

$$J = 4.60 \times \frac{60}{548} \times \frac{12}{11.82} = 0.622$$

For the determination of the force, the resultant reading is first determined as before,

$$R_{rdg}^{2} = (-0.72)^2 + (1.92)^2$$

$$R_{rdg} = 2.06$$

In the simplest case, the calibration curve for this arrangement of parameters is now entered with this resultant deflection, and the corresponding force read directly. This force, then, together with the corresponding thrust, is plotted.

As for the calibration data, by definition,

$$\beta_2 = \tan^{-1} \frac{B_{rdg}}{A_{rdg}}$$

$$= \tan^{-1} \frac{1.92}{-0.72} = 69.5°$$

In this particular instance, the sign convention determines that β_2 has a value between 90° and 180°. Thus,

$$\beta_2 = 180 - 69.5 = 110.5°$$

As previously discussed, the calibration data directly represents only forces between 0 and 1.1 lbs. For some combinations of nose pieces and clearances, the actual measured force exceeds this range. In such cases two methods of extrapolation were employed. The first, and simplest, was employed exclusively in reducing the data taken with the long nose piece. It consists of merely determining the slope of the calibration curve for the data taken, and thus obtaining a constant relationship between resultant deflection readings and force applied. This method involves the assumption of linear response of the bossing system to the applied forces over the full range of forces experienced. In general, the relationship is

$$\text{Force} = K + S \times R_{rdg}$$

where K = the base intercept of the calibration curve, and

S = slope of the calibration curve.

The second method, based precisely on the data taken, was employed in the analysis of a part of the short bossing data. Use is made of variable amplifier gain. A detailed description of this method may be found in the section on Detailed Procedure. See Section V for a discussion of the two methods.

C. Phase Determination.

The method of phase determination is discussed in detail in Appendix A. For the example given above,

$$\beta_1 = 226.8^\circ$$

$$\beta_2 = 110.5^\circ$$

$$\alpha = 327^\circ$$

$$360-\alpha = 33^\circ$$

In accordance with the development in Appendix A,

$$4\gamma = \beta_2 - (\beta_1 + \alpha)$$

$$= 110.5 - (226.8 + 33) = -149.3^\circ$$

$$\gamma = 37.3^\circ$$

where γ is defined as the phase angle between the time the generating line of an arbitrarily selected propeller blade coincides with the trailing edge of the bossing and the occurrence of the measured hydrodynamically induced force normal to the bossing.

APPENDIX C

Original Data and Calculations

TABLE I

Calibration Run No. 1

Nose Piece: Short
Resistance: 1000 ohms

Clearance 1"

RPM = 548
Amplifier Gain Setting: Variable

Spring Letter Designation	I.F. lbs + oz	W lbs + gms	F lbs	G.S. Amplifier Gain Setting	A rdg (+)	B rdg (+)	R rdg
N	2 - 11	4 + 200	1.10	6	0.55	1.00	1.14
				7	0.65	1.20	1.37
				8	0.82	1.67	1.86
				9	1.05	2.18	2.42
				10	1.25	2.61	2.89
				11	1.60	3.48	3.83
K	4 - 11	2.5 + 40	0.639	6	0.38	0.62	0.73
				7	0.41	0.75	0.86
				8	0.52	0.95	1.07
				9	0.61	1.20	1.35
				10	0.71	1.47	1.63
				11	0.89	1.90	2.10
P	3 - 11	4.0 + 125	1.06	6	0.50	0.92	1.05
				7	0.55	1.05	1.19
				8	0.70	1.55	1.70
				9	0.92	2.25	2.43
				10	1.12	2.48	2.72
				11	1.38	3.35	3.62

(continued)

TABLE I
(continued)

Calibration Run No. 1

Nose Piece: Short
Resistance: 1000 ohms

Clearance 1"

RPM = 548
Amplifier Gain Setting: Variable

Spring Letter Designation	I.F. lbs + oz	W lbs + gms	F lbs	G.S. Amplifier Gain Setting	A rdg (+)	B rdg (+)	R rdg
M	4 - 11	2 + 80	0.50	6	0.28	0.50	0.57
				7	0.30	0.58	0.65
				8	0.36	0.78	0.86
				9	0.45	0.97	1.07
				10	0.54	1.19	1.31
				11	0.65	1.55	1.68
V	4 - 11	3 + 140	0.82	6	0.40	0.69	0.80
				7	0.47	0.80	0.93
				8	0.62	1.15	1.31
				9	0.76	1.46	1.64
				10	0.90	1.79	2.00
				11	1.15	2.40	2.66
H	1.5 - 11	2.5 + 30	0.64	6	0.41	0.65	0.77
				7	0.45	0.75	0.87
				8	0.60	1.02	1.19
				9	0.70	1.29	1.47
				10	0.80	1.57	1.76
				11	1.05	2.05	2.30

TABLE II

Calibration Run No. 2

Nose Piece: Short
Resistance: 1000 ohms

Clearance 1"

RPM: 548
Amplifier Gain Setting: 10

Spring	I.F.	W	F	A rdg	B rdg	R rdg	* β_1
Letter Designation	lbs + oz	lbs. + gms.	lbs.	(+)	(+)		deg.
I	1 - 11	0.5 + 110	0.19	0.39	0.59	0.71	50.4
L	3 - 11	1.5 + 160	0.46	0.62	1.15	1.30	57.5
R	3 - 11	3.0 + 170	0.84	1.05	2.00	2.26	57.1
N	2 - 11	4.0 + 200	1.10	1.25	2.61	2.89	61.2
K	4 - 11	2.5 + 40	0.64	0.71	1.47	1.63	58.6
P	3 - 11	4.0 + 125	1.06	1.12	2.48	2.72	61.6
M	4 - 11	2.0 + 80	0.50	0.54	1.19	1.31	61.9
C	1.5 - 11	1.0 + 20	0.26	0.26	0.59	0.65	58.4
V	4 - 11	3.0 + 140	0.82	0.90	1.79	2.00	60.0
H	1.5 - 11	2.5 + 30	0.64	0.80	1.57	1.76	57.8

Average β_1 = 59.1°

* Note: β_1 is for an Amplifier Gain Setting of 6.

TABLE III

Measurement Run No. 1

Water Temperature: 77°F.
Nose Piece : Short
Thrust Correction: -2.0 lbs.
Clearance 1"
RPM : 548
Amplifier Gain Setting: 6
Resistance : 1000 ohms

T_{rdg}	T_{corr}	H_1	v	J	A_{rdg}	B_{rdg}	R_{rdg}	$F_{(10)}$	F	β_2	β_1	α_{rdg}	$360-\alpha$	4γ	γ
lbs.	lbs.	rdg	fps	v/nd				lbs.	lbs.	deg	deg	deg	deg	deg	(-)°
64.0	62.0	0	0	0	+0.90	-3.40	3.52	1.350	3.65	255.2	59.1°	288	72	124.1	31
63.0	61.0	13	1.46	0.162	-0.70	-3.25	3.32	1.272	3.44	257.8		290	70	128.7	32.1
56.8	54.8	42	2.68	0.297	-0.65	-2.85	2.93	1.125	3.04	257.7		288	72	128.6	31.7
51.6	49.6	79	3.68	0.408	-0.50	-2.45	2.50	0.958	2.60	258.5		288	72	127.4	31.9
45.7	43.7	117	4.47	0.495	-0.35	-2.15	2.18	0.833	2.26	260.6		287	73	128.5	32.1
39.3	37.3	165	5.32	0.591	-0.25	-1.90	1.92	0.733	1.99	362.5		284	76	127.4	31.9
33.3	31.3	220	6.13	0.682	-0.15	-1.60	1.62	0.617	1.67	264.7		287	73	132.6	33.1
26.5	24.5	279	6.90	0.767	-0.05	-1.50	1.51	0.575	1.56	268.0		285	75	133.9	33.4
23.1	21.1	314	7.33	0.814	+0.02	-1.35	1.35	0.515	1.40	270.8		285	75	136.7	34.1
17.9	15.9	377	8.03	0.892	+0.10	-1.25	1.26	0.480	1.30	274.5		287	73	142.4	35.6
13.1	11.1	433	8.60	0.954	+0.20	-1.20	1.22	0.465	1.26	279.5		290	70	150.4	37.6
8.9	6.9	491	9.16	1.018	+0.20	-1.15	1.17	0.443	1.20	280.0		288	72	148.9	37.2

TABLE IV

Calibration Run No. 3

Nose Piece: Short
Resistance: 1000 ohms
Clearance 1-1/2"
RPM: 548
Amplifier Gain Setting: 10

Spring	I.F.	W	F	A rdg	B rdg	R rdg	β_1
Letter Designation	lbs. + oz.	lbs. + gms	lbs.	(+)	(+)		deg.
P	4 - 11	3.5 + 200	0.88	1.85	3.55	4.00	62.5
				1.90	3.58	4.05	62.0
N	4 - 11	4 + 22	1.05	1.85	3.45	3.81	61.8
				1.85	3.55	4.00	62.5
V	4 - 11	3 + 40	0.77	1.35	2.52	2.96	61.8
				1.28	2.48	2.79	62.6
R	4 - 11	3 + 170	0.84	1.35	2.78	3.09	64.2
				1.35	2.70	3.02	63.5
L	4 - 11	2 + 0	0.50	0.72	1.55	1.71	65.0
				0.71	1.53	1.69	65.0
Q	4 - 11	2.5 + 50	0.66	1.04	2.04	2.39	63.0
				1.05	2.09	2.34	63.3
W	4 - 11	2.0 + 50	0.53	0.92	1.79	2.01	62.8
				0.93	1.78	1.99	62.5
X	4 - 11	1.5 + 190	0.48	0.82	1.60	1.80	62.8
				0.85	1.60	1.81	62.0
M	4 - 11	2.0 + 20	0.51	0.69	1.60	1.74	66.7
				0.75	1.60	1.77	65.0
C	3 - 11	1.0 + 20	0.26	0.39	0.80	0.89	64.0
				0.40	0.82	0.91	64.0
I	3 - 11	1.0 + 30	0.27	0.40	0.81	0.90	63.7
				0.42	0.82	0.92	63.0

Average $\beta_1 = 63.3^\circ$

TABLE V

Measurement Run No. 2

Water Temperature: 76°F.
Nose Piece : Short
Thrust Correction: -2.0 lbs.
Clearance 1-1/2"

RPM : 548
Amplifier Gain Setting: 10
Resistance : 1000 ohms

T_{rdg}	T_{corr}	H_1	v	J	A_{rdg}	B_{rdg}	R_{rdg}	F	β_2	β_1	α_{rdg}	$360-\alpha$	ΔY	$-Y$
lbs.	lbs.	rdg	fps	v/nd				lbs	deg	deg	deg	deg	deg	deg
51.0	49.0	23	1.99	0.221	-1.85	-4.30	4.68	1.31	247.3	63.3°	303	57	127.0	31.8
46.1	44.1	41	2.63	0.295	-1.95	-4.30	4.74	1.33	245.6		301	59	123.3	30.8
42.5	40.5	59	3.18	0.354	-1.85	-4.25	4.63	1.30	246.6		302	58	125.3	31.3
41.0	39.0	70	3.48	0.384	-1.80	-4.05	4.43	1.18	246.0		300	60	122.7	30.6
38.0	36.0	90	3.92	0.436	-1.70	-3.85	4.20	1.12	246.2		300	60	122.9	30.7
31.3	29.3	127	4.66	0.518	-1.50	-3.65	3.94	1.06	247.8		295	65	119.5	29.9
27.3	25.3	154	5.13	0.570	-1.32	-3.40	3.64	0.985	248.8		298	62	123.5	30.9
25.4	23.2	173	5.45	0.605	-1.19	-3.28	3.49	0.945	250.2		295	65	121.9	30.4
23.6	21.6	189	5.68	0.632	-1.15	-3.22	3.42	0.930	250.3		295	65	122.0	30.5
20.4	18.4	217	6.10	0.678	-1.02	-3.07	3.24	0.885	251.6		295	65	123.3	30.8
18.0	16.0	239	6.40	0.711	-0.98	-2.95	3.11	0.850	251.7		295	65	123.4	30.8
16.6	14.6	254	6.63	0.737	-0.98	-2.95	3.11	0.850	251.7		295	65	123.4	30.8
15.0	13.0	274	6.85	0.761	-0.89	-2.85	2.99	0.820	252.7		295	65	124.4	31.1
13.6	11.6	290	7.06	0.784	-0.80	-2.75	2.86	0.790	253.7		295	65	125.4	31.4
11.0	9.0	313	7.33	0.815	-0.75	-2.75	2.86	0.790	254.8		295	65	126.5	31.6
9.3	7.3	340	7.62	0.848	-0.62	-2.60	2.67	0.740	256.5		295	65	128.2	32.1
6.5	4.5	365	7.90	0.879	-0.55	-2.55	2.62	0.730	257.8		295	65	129.5	32.4
4.2	2.2	387	8.14	0.903	-0.40	-2.50	2.53	0.705	260.9		295	65	132.6	33.1

TABLE VI

Measurement Run No. 3

Water Temperature: 76°F.
Nose Piece: Short
Thurst Correction: -2.0 lbs.

Clearance 1-3/4"

RPM : 548
Amplifier Gain Setting: 10
Resistance : 1000 ohms

T_{rdg}	T_{corr}	H_1	v	J	A_{rdg}	B_{rdg}	R_{rdg}	F	β_2	β_1	α_{rdg}	$360-\alpha$	$\Delta\gamma$	$-\gamma$
lbs.	lbs.	rdg.	fps	v/nd				lbs.	deg.	deg.	deg.	deg.	deg.	deg.
55.1	53.1	1	0.414	0.046	-1.30	-4.10	4.30	1.097	252.4	64.3°	304	56	132.1	33.0
53.1	51.1	14	1.55	0.172	-1.65	-3.95	4.29	1.096	247.4		303	57	126.1	31.5
48.3	46.3	32	2.34	0.260	-1.45	-3.85	4.11	1.051	259.4		302	58	137.1	34.3
45.0	43.0	45	2.78	0.309	-1.45	-3.50	3.79	0.976	247.5		301	59	124.2	31.0
43.8	41.8	53	3.01	0.334	-1.45	-3.45	3.75	0.968	247.2		301	59	123.9	30.9
40.4	38.4	68	3.41	0.379	-1.32	-3.15	3.41	0.890	247.2		299	61	121.9	30.4
37.0	35.0	93	4.00	0.445	-1.20	-3.05	3.28	0.860	248.6		299	61	123.3	30.8
31.0	29.0	122	4.57	0.508	-1.12	-2.85	3.06	0.810	248.6		297	63	121.3	30.3
26.4	24.4	165	5.32	0.591	-0.99	-2.68	2.89	0.770	248.8		297	63	121.5	30.4
22.0	20.0	205	5.93	0.659	-0.85	-2.50	2.62	0.710	251.3		296	64	123.0	30.7
19.7	17.7	233	6.32	0.702	-0.75	-2.40	2.51	0.680	252.7		296	64	124.4	31.1
16.4	14.4	264	6.73	0.747	-0.65	-2.25	2.35	0.640	253.9		296	64	125.6	31.4
13.0	11.9	293	7.09	0.788	-0.55	-2.17	2.24	0.610	255.7		296	64	127.4	31.8
9.1	7.1	341	7.65	0.850	-0.35	-2.05	2.08	0.572	260.3		296	64	132.0	33.0
5.9	3.9	380	8.06	0.896	-0.20	-1.95	1.97	0.545	264.1		296	64	135.8	33.9
2.4	0.4	422	8.50	0.944	-0.15	-1.85	1.86	0.520	265.4		296	64	137.1	34.3

TABLE VII

Calibration Run No. 4

Nose Piece: Short
Resistance: 1000 ohms

Clearance 2"

RPM : Variable
Amplifier Gain Setting: 10

Spring	I.F.	W	F	A_{rdg}	B_{rdg}	R_{rdg}	β_1	RPM
Letter Design.	lbs. + oz.	lbs. + gms	lbs.	(+)	(+)		deg. *	
M	4.5 + 11	2.0 + 0	0.495	0.31	0.50	0.588		396
				0.35	0.59	0.686		426
				0.40	0.72	0.825		462
				0.47	0.85	0.972		482
				0.52	1.09	1.21		510
				0.61	1.49	1.61		536
				0.70	1.75	1.89		549
				0.80	2.19	2.33		560
				1.10	3.32	3.50		580
				1.22	3.90	4.08		584
Q	4.5 + 11	2.5 + 70	0.660	0.35	0.59	0.685		379
				0.36	0.63	0.726		391
				0.40	0.70	0.805		408
				0.44	0.79	0.904		425
				0.49	0.86	0.989		445
				0.50	0.95	1.075		458
				0.58	1.08	1.225		479
				0.60	1.25	1.39		496
				0.68	1.36	1.52		506
				0.85	1.91	2.09		535
				1.17	2.48	2.74		552
				1.30	3.80	4.00		569
				1.42	4.40	4.63		576

(continued)

TABLE VII
(continued)

Calibration Run No. 4

Nose Piece: Short
Resistance: 1000 ohms

Clearance 2"

RPM : Variable
Amplifier Gain Setting: 10

Spring Letter Design.	I.F. lbs. + oz.	W lb.s + gms.	F lbs.	A_{rdg} (+)	B_{rdg} (+)	R_{rdg}	β_1 deg. *	RPM
V	4.5 + 11	3.0 + 60	0.778	0.45	0.72	0.850		382
				0.49	0.78	0.92		396
				0.51	0.84	0.981		408
				0.51	0.90	1.037		416
				0.66	1.15	1.32		458
				0.75	1.30	1.50		474
				0.85	1.55	1.77		491
				1.15	2.10	2.40		522
				1.31	2.45	2.78		536
				1.41	2.75	3.09		546
				1.78	3.66	4.06		560
				1.90	4.85	5.20		570

* Note: β_1 not computed.

TABLE VIII

Calibration Run No. 4

Nose Piece: Short
Resistance: 1000 ohms

Clearance 2"

RPM : Variable
Amplifier Gain Setting: 10

Spring Letter Design.	I.F. lbs. + oz.	W lbs. + gms	F lbs.	A_{rdg} (+)	B_{rdg} (+)	R_{rdg}	β_1 deg. *	RPM
R	4.5 + 11	3.0 + 200	0.856	0.45	0.66	0.800		358
				0.55	0.72	0.905		368
				0.49	0.79	0.930		390
				0.55	0.91	1.062		410
				0.69	1.13	1.325		450
				0.76	1.34	1.54		468
				0.79	1.40	1.61		477
				0.89	1.59	1.82		492
				0.95	1.79	2.03		504
				1.09	2.03	2.30		515
				1.19	2.35	2.63		524
				1.41	3.11	3.42		544
				1.62	3.39	3.76		552
				1.68	3.85	4.20		555
				1.85	4.70	5.05		566
Q	4.0 + 11	4.0 + 50	1.021	0.59	0.85	1.035		365
				0.62	0.91	1.11		380
				0.65	1.00	1.19		394
				0.73	1.11	1.33		412
				0.84	1.28	1.53		432
				0.90	1.46	1.72		453
				1.04	1.70	1.99		471
				1.10	1.79	2.10		480
				1.35	2.25	2.62		502
				1.63	2.56	3.20		514
				1.70	2.85	3.32		522
				1.85	3.10	3.60		532
				2.10	3.95	4.47		545
				2.35	4.75	5.30		554

(continued)

TABLE VIII
(continued)

Calibration Run No. 4

Nose Piece: Short
Resistance: 1000 ohms

Clearance 2"

RPM : Variable
Amplifier Gain Setting: 10

Spring Letter Design.	I.F. lbs. + oz.	W lbs. + gms	F lbs.	A_{rdg} (+)	B_{rdg} (+)	R_{rdg}	β_1 deg. *	RPM
I	4.0 + 11	1.0 + 90	0.298	0.20	0.30	0.360		379
				0.25	0.33	0.413		395
				0.25	0.36	0.438		430
				0.25	0.45	0.515		461
				0.39	0.65	0.758		519
				0.48	0.86	0.985		545
				0.59	1.10	1.25		560
				0.62	1.42	1.55		576
				0.59	1.82	1.91		584
				0.55	1.73	1.81		583
				0.70	2.85	2.94		596
				0.65	4.35	4.40		602

* Note: β_1 not computed.

TABLE IX

Measurement Run No. 8

Water Temperature: 77°F.
Nose Piece : Short
Thrust Correction: -7.5 lbs.

Clearance 2"

RPM : 548
Amplifier Gain Setting: 10
Resistance : 1000 ohms

T_{rdg} lbs.	T_{corr} lbs.	H_1 rdg	v fps	J v/nd	A_{rdg} (+)	B_{rdg} (+)	R_{rdg}	F lbs	β_2 deg
59.5	52.0	26	2.11	0.234	4.10	1.30	4.29	0.950	17.6
55.0	47.5	45	2.78	0.308	3.85	1.20	4.03	0.910	17.3
52.2	44.7	59	3.2	0.355	3.75	1.02	3.89	0.885	15.2
50.7	43.2	74	3.58	0.398	3.60	1.00	3.74	0.860	15.5
45.2	37.7	105	4.26	0.473	3.30	0.98	3.44	0.805	16.5
40.1	32.6	144	5.00	0.555	3.05	0.92	3.18	0.760	16.8
30.5	23.0	217	6.13	0.681	2.70	0.88	2.83	0.695	18.0
34.8	27.3	183	5.63	0.626	2.85	0.90	2.99	0.725	17.5
28.4	20.9	248	6.56	0.730	2.50	0.88	2.65	0.660	19.3
25.5	18.0	278	6.95	0.772	2.41	0.88	2.57	0.640	20.0
22.3	14.8	315	7.40	0.820	2.29	0.89	2.45	0.620	21.4
19.3	11.8	347	7.75	0.862	2.20	0.92	2.39	0.605	22.7
15.7	8.2	386	8.19	0.910	2.04	0.96	2.26	0.580	25.3
13.9	6.4	417	8.50	0.945	2.00	0.95	2.22	0.570	25.5
11.5	4.0	444	8.76	0.975	1.92	0.93	2.13	0.550	26.0
9.1	1.6	478	9.10	1.011	1.87	0.95	2.09	0.545	27.0
8.0	0.5	491	9.24	1.025	1.82	0.95	2.05	0.525	27.6

Note: γ not computed for this run;

β_{rdg} = 42° for run and necessary information for calculation of γ is in thesis.

TABLE X

Calibration Run No. 5

Nose Piece: Short
Resistance: 1000 ohms

Clearance 2-1/4"

RPM = 548
Amplifier Gain Setting: 10

Spring Letter Designation	I.F. lbs. + oz.	W lbs. + gms	F lbs.	A rdg (+)	B rdg (+)	R rdg	β_1 deg.
O	4 - 11	2.5 + 70	0.66	1.21	2.47	2.75	64.0
				1.25	2.45	2.75	63.0
X	4 - 11	2.0 + 10	0.50	0.80	1.81	1.98	66.0
				0.83	1.79	1.97	65.2
G	3 - 11	1.0 + 40	0.27	0.40	1.02	1.10	68.5
				0.43	1.03	1.12	67.5
R	4 - 11	3.0 + 160	0.84	1.65	3.15	3.56	62.5
				1.59	3.15	3.52	63.2
M	4 - 11	1.5 + 250	0.51	0.78	1.85	2.01	67.2
				0.78	1.81	1.97	66.7
W	4 - 11	2.0 + 10	0.50	0.77	1.81	1.95	66.7
				0.79	1.85	2.01	66.8
L	4 - 11	1.5 + 220	0.49	0.70	1.77	1.90	68.3
				0.69	1.74	1.87	68.3
C	3 - 11	0.5 + 220	0.25	0.30	0.85	0.90	70.5
				0.31	0.84	0.90	69.7
N	4 - 11	4.0 + 100	1.05	2.05	4.05	4.53	63.0
				2.03	4.10	4.58	63.5
V	4 - 11	3.0 + 40	0.77	1.51	2.89	3.26	62.5
				1.51	2.86	3.24	62.2

Average β_1 = 65.3°

TABLE XI

Measurement Run No. 4

Water Temperature: 76°F.
Nose Piece : Short
Thrust Correction: -2.0 lbs. Clearance 2-1/4"

RPM : 548
Amplifier Gain Setting: 10
Resistance : 1000 ohms

T_{rdg} lbs.	T_{corr} lbs.	H_1 rdg	v fps	J v/nd	A_{rdg}	B_{rdg}	R_{rdg}	F lbs	β_2 deg	β_1 deg	α_{rdg} deg	$360-\alpha$ deg	4γ deg	$-\gamma$ deg
53.5	51.5	0	0	0	-1.05	-2.90	3.09	0.745	250.0	65.3°	303	57	127.7	31.9
53.0	51.0	17	1.71	0.190	-1.10	-2.90	3.10	0.752	249.3		302	58	126.0	31.5
52.5	50.5	21	1.90	0.211	-0.90	-2.85	2.95	0.720	252.5		302	58	129.2	32.3
47.7	45.7	36	2.48	0.276	-0.85	-2.70	2.83	0.695	252.5		302	58	129.2	32.3
45.5	43.5	45	2.78	0.309	-0.85	-2.60	2.73	0.675	252.0		301	59	127.7	31.9
42.5	40.5	62	3.26	0.362	-0.74	-2.40	2.51	0.630	252.8		301	59	128.5	32.1
39.5	37.5	78	3.65	0.406	-0.72	-2.28	2.39	0.600	252.5		299	61	126.2	31.6
36.4	34.4	101	4.16	0.462	-0.63	-2.15	2.24	0.570	253.7		298	62	126.4	31.6
30.2	28.2	133	4.77	0.530	-0.61	-2.05	2.14	0.550	253.5		298	62	126.2	31.6
26.3	24.3	168	5.36	0.596	-0.51	-1.87	1.94	0.500	254.7		298	62	127.4	31.9
24.9	22.9	179	5.53	0.614	-0.50	-1.87	1.93	0.495	255.0		299	61	128.7	32.1
21.8	19.8	208	5.96	0.663	-0.43	-1.85	1.90	0.490	257.0		299	61	130.7	32.6
19.5	17.5	230	6.26	0.697	-0.41	-1.65	1.70	0.445	256.0		299	61	129.7	32.4
16.3	14.3	263	6.72	0.746	-0.35	-1.60	1.64	0.435	257.7		300	60	132.4	33.1
12.5	10.5	305	7.23	0.804	-0.30	-1.51	1.54	0.410	258.7		301	59	134.4	33.6
8.8	6.8	347	7.70	0.856	-0.24	-1.40	1.42	0.380	260.3		301	59	136.0	34.0
5.2	3.2	388	8.15	0.906	-0.21	-1.30	1.32	0.355	260.8		302	58	137.5	34.4

TABLE XII

Measurement Run No. 5

Water Temperature: 76°F.
Nose Piece : Short
Thrust Correction: -2.0 lbs. Clearance 2-1/2"

RPM : 548
Amplifier Gain Setting: 10
Resistance : 1000 ohms

T_{rdg}	T_{corr}	H_1	v	J	A_{rdg}	B_{rdg}	R_{rdg}	F	β_2	β_1	α_{rdg}	$360-\alpha$	$\Delta\gamma$	$-\gamma$
lbs.	lbs.	rdg	fps	v/nd				lbs	deg	deg	deg	deg	deg	deg
52.5	50.5	2	0.585	0.065	-0.75	-2.50	2.61	0.615	253.3	67.0°	304	56	130.3	32.5
52.0	50.0	12	1.43	0.159	-0.75	-2.50	2.61	0.615	253.3		305	55	131.3	32.8
48.0	46.0	31	2.30	0.256	-0.60	-2.30	2.38	0.570	255.3		305	55	133.3	33.2
43.0	41.0	54	3.04	0.338	-0.52	-2.06	2.12	0.515	255.8		306	54	134.8	33.7
41.1	39.1	65	3.34	0.371	-0.50	-1.98	2.04	0.495	255.8		306	54	134.8	33.7
37.4	35.4	90	3.93	0.437	-0.43	-1.85	1.90	0.465	257.0		306	54	136.0	34.0
31.0	29.0	124	4.61	0.513	-0.39	-1.72	1.77	0.440	257.3		306	54	136.3	34.1
26.4	24.4	164	5.30	0.589	-0.31	-1.60	1.63	0.410	259.0		306	54	138.0	34.5
24.0	22.0	187	5.66	0.630	-0.28	-1.50	1.53	0.385	259.5		306	54	138.5	34.6
20.9	18.9	213	6.05	0.672	-0.25	-1.45	1.47	0.372	260.3		306	54	139.3	34.8
17.7	15.7	248	6.51	0.723	-0.22	-1.35	1.37	0.350	260.7		306	54	139.7	34.9
14.5	12.5	276	6.87	0.763	-0.16	-1.25	1.26	0.325	262.7		306	54	141.7	35.4
12.9	10.9	298	7.15	0.794	-0.13	-1.20	1.21	0.311	263.8		306	54	142.8	35.6
11.9	9.9	309	7.26	0.808	-0.13	-1.19	1.20	0.310	263.7		306	54	142.7	35.6
8.7	6.7	343	7.67	0.852	-0.09	-1.11	1.12	0.290	265.3		307	53	145.3	36.3
6.9	4.9	366	7.92	0.880	-0.05	-1.05	1.06	0.280	267.3		307	53	147.3	36.8
5.7	3.7	382	8.10	0.900	-0.05	-1.05	1.06	0.280	267.3		307	53	147.3	36.8
3.5	1.5	407	8.35	0.930	-0.03	-1.05	1.05	0.275	269.4		307	53	149.4	37.3

TABLE XIII

Calibration Run No. 6

Nose Piece: Short
Resistance: 1000 ohms
Clearance 2-3/4"
RPM = 548
Amplifier Gain Setting: 10

Spring	I.F.	W	F	A rdg	B rdg	R rdg	β_1
Letter Designation	lbs. + oz.	lbs. + gms	lbs.	(+)	(+)		deg.
L	4 - 11	1.5 + 200	0.48	0.80	2.05	2.20	68.7
R	4 - 11	3.0 + 200	0.86	1.87 1.89	3.65 3.62	4.10 4.08	62.8 62.5
M	4 - 11	2.0 + 60	0.53	0.79 0.81	2.11 2.15	2.25 2.30	69.5 69.3
V	4 - 11	2.5 + 220	0.74	1.51 1.55	3.28 3.38	3.61 3.71	65.3 65.3
X	4 - 11	2.0 + 50	0.53	0.81 0.82	2.05 2.05	2.20 2.21	68.5 68.5
W	4 - 11	1.5 + 230	0.50	0.76 0.78	2.15 2.11	2.28 2.25	70.5 69.7
Q	4 - 11	2.0 + 250	0.64	1.19 1.29	2.80 2.80	3.04 3.08	68.0 65.3
C	3 - 11	0.5 + 240	0.26	0.27 0.29	0.95 0.96	0.99 1.00	74.0 73.2

Average β_1 = 68.6°

TABLE XIV

Measurement Run No. 6

Water Temperature: 76°F.
Nose Piece : Short
Thrust Correction: -2.0 lbs.
Clearance 2-3/4"

RPM : 548
Amplifier Gain Setting: 10
Resistance :1000 ohms

T_{rdg} lbs.	T_{corr} lbs.	H_1 rdg	v fps	J v/nd	A_{rdg}	B_{rdg}	R_{rdg}	F lbs.	β_2 deg	β_1 deg	α_{rdg} deg	$360-\alpha$ deg	4γ deg	$-\gamma$ deg
54.4	52.4	18	1.76	0.196	-0.40	-2.30	2.34	0.520	260.2	68.6°	306	54	137.6	34.4
53.0	51.0	3	0.72	0.080	-0.90	-2.10	2.28	0.510	246.8		305	55	123.2	30.8
51.5	49.5	28	2.19	0.244	-0.40	-2.15	2.19	0.495	259.5		307	53	137.9	34.4
51.3	49.3	32	2.34	0.261	-0.40	-2.10	2.14	0.485	259.2		306	54	136.6	34.1
47.0	45.0	47	2.74	0.317	-0.45	-1.90	1.95	0.450	256.7		306	54	134.1	33.5
45.0	43.0	54	3.04	0.339	-0.40	-1.85	1.90	0.440	258.0		306	54	135.4	33.9
42.4	40.0	71	3.49	0.388	-0.40	-1.70	1.74	0.410	256.8		306	54	134.2	33.6
36.4	34.4	110	4.35	0.483	-0.26	-1.58	1.60	0.380	260.7		306	54	138.1	34.5
35.5	33.5	121	4.56	0.507	-0.25	-1.47	1.49	0.355	260.4		306	54	137.8	34.4
29.2	27.2	154	5.16	0.573	-0.25	-1.45	1.47	0.350	260.3		306	54	137.7	34.4
26.3	24.3	187	5.69	0.632	-0.21	-1.32	1.34	0.325	261.0		306	54	138.4	34.6
23.5	21.3	211	6.03	0.670	-0.20	-1.27	1.29	0.315	261.1		306	54	138.5	34.6
21.2	19.2	244	6.51	0.723	-0.15	-1.22	1.23	0.300	263.0		306	54	140.4	35.1
18.7	16.7	263	6.74	0.750	-0.12	-1.15	1.16	0.285	264.0		306	54	141.4	35.4
16.5	14.5	278	6.94	0.771	-0.09	-1.12	1.12	0.280	265.5		306	54	142.9	35.7
14.0	12.0	315	7.39	0.820	-0.05	-1.05	1.06	0.260	267.3		306	54	144.7	36.1
10.4	8.4	356	7.85	0.871	-0.05	-0.95	0.96	0.240	267.0		306	54	144.4	36.1
7.9	5.9	387	8.19	0.910	+0.05	-0.92	0.93	0.233	273.0		306	54	150.4	37.6
6.6	4.6	413	8.45	0.940	0.00	-0.95	0.95	0.235	270.0		306	54	147.4	36.9
4.3	2.3	430	8.65	0.960	+0.02	-0.85	0.86	0.220	271.5		306	54	148.9	37.2
2.0	0.0	466	9.00	1.00	0	-0.85	0.85	0.215	270.0		306	54	147.4	37.6

TABLE XV

Calibration Run No. 7

Nose Piece: Short
Resistance: 1000 ohms
Clearance 3"
RPM = 548
Amplifier Gain Setting: 10

Spring Letter Designation	I.F. lbs. + oz.	W lbs. + gms	F lbs.	A rdg (+)	B rdg (+)	R rdg	β_1 deg.
L	4 - 11	2.0 + 0	0.49	0.55	1.45	1.55	69.2
M	4 - 11	2.0 + 50	0.52	0.52	1.60	1.68	72.0
V	4 - 11	3.0 + 20	0.75	0.92	2.55	2.71	70.2
N	4 - 11	4.0 + 200	1.10	1.60 1.55	4.20 4.10	4.49 4.38	69.2 69.4
C	2.5 - 11	1.0 + 0	0.25	0.35	0.70	0.78	63.5
Q	3 - 11	2.5 + 90	0.67	0.82	2.25	2.39	70.0
R	4 - 11	3.5 + 30	0.88	1.20	2.95	3.19	68.0
P	4 - 11	4.5 + 90	1.16	1.70	4.10	4.34	67.5

Average β_1 = 68.8°

TABLE XVI

Measurement Run No. 7

Water Temperature: 76°F.
Nose Piece : Short
Thrust Correction: -2.0 lbs. Clearance 3"

RPM : 548
Amplifier Gain Setting: 10
Resistance : 1000 ohms

T_{rdg}	T_{corr}	H_1	v	J	A_{rdg}	B_{rdg}	R_{rdg}	F	β_2	β_1	α_{rdg}	$360-\alpha$	4γ	$-\gamma$
lbs.	lbs.	rdg	fps	v/nd				lbs	deg	deg	deg	deg	deg	deg
62.5	60.0	0	0	0	-0.40	-1.10	1.17	0.385	250.0	68.8°	302	58	123.2	30.8
55.2	53.2	23	1.99	0.221	-0.20	-1.05	1.07	0.360	259.3		301	59	131.5	32.9
50.9	48.9	35	2.45	0.272	-0.24	-0.95	0.98	0.335	255.8		301	59	128.0	32.0
48.8	46.8	45	2.77	0.308	-0.22	-0.95	0.97	0.330	257.0		301	59	129.2	32.3
43.4	41.4	71	3.49	0.388	-0.18	-0.77	0.79	0.280	257.8		301	59	130.0	32.5
39.5	37.5	95	4.03	0.448	-0.15	-0.71	0.73	0.262	258.0		301	59	130.2	32.6
36.4	34.4	124	4.61	0.512	-0.14	-0.65	0.67	0.245	257.8		298	62	127.0	31.8
30.3	28.3	144	4.97	0.552	-0.12	-0.66	0.67	0.245	259.7		298	62	128.9	32.2
26.6	24.6	173	5.44	0.605	-0.13	-0.60	0.61	0.225	257.7		297	63	125.9	31.5
22.9	20.9	207	5.94	0.660	-0.11	-0.51	0.52	0.200	257.8		297	63	126.0	31.5
19.3	17.3	242	6.44	0.716	-0.09	-0.50	0.51	0.190	259.8		297	63	128.0	32.0
17.2	15.2	261	6.68	0.743	-0.08	-0.50	0.51	0.190	261.0		298	62	130.2	32.5
15.7	13.2	282	6.94	0.772	-0.06	-0.46	0.46	0.175	262.5		298	62	131.7	32.9
12.0	10.0	327	7.48	0.830	-0.04	-0.40	0.40	0.155	264.0		298	62	133.2	33.3
7.6	5.6	372	7.97	0.885	0.00	-0.35	0.35	0.135	270.0		298	62	139.2	34.8
3.2	1.2	417	8.45	0.940	+0.02	-0.35	0.35	0.135	273.5		298	62	142.7	35.6

TABLE XVII

Measurement Run No. 9

Water Temperature: 79°F.
Nose Piece : Short
Thrust Correction: -7.5 lbs.

Clearance 2"

RPM : Variable
Amplifier Gain Setting: 10
Resistance : 1000 ohms

T_{rdg} lbs.	T_{corr} lbs.	H_1 rdg	v fps	J v/nd	A_{rdg} (+)	B_{rdg} (+)	R_{rdg}	F lbs	RPM
22.0	14.5	92	4.44	0.629	0.85	0.32	0.906	0.630	430
"	"	145	4.96	0.646	1.07	0.40	1.142	0.645	467
"	"	127	4.65	0.605	1.10	0.42	1.175	0.665	468
"	"	167	5.33	0.658	1.45	0.52	1.54	0.715	494
"	"	215	6.05	0.730	1.49	0.58	1.60	0.680	504
"	"	191	5.70	0.682	1.65	0.60	1.76	0.700	508
"	"	238	6.37	0.731	2.02	0.75	2.15	0.675	530
"	"	317	7.35	0.815	2.35	0.95	2.53	0.625	549
"	"	280	6.90	0.763	2.62	1.01	2.81	0.635	550
"	"	354	7.76	0.823	3.69	2.15	4.26	0.640	574
"	"	392	8.17	0.855	4.05	2.50	4.75	-----	582

TABLE XVIII

Measurement Run No. 10

Water Temperature: 78°F.
Nose Piece : Short
Thrust Correction: +0.5 lbs.

Clearance 2"

RPM : Variable
Amplifier Gain Setting: 10
Resistance : 1000 ohms

T_{rdg}	T_{corr}	H_1	v	J	A_{rdg}	B_{rdg}	R_{rdg}	F	RPM
lbs.	lbs.	rdg	fps	v/nd	(+)	(-)		lbs.	
24.9	25.4	250	6.53	0.696	2.70	3.70	4.58	0.680	572
22.0	22.5			0.719	1.45	2.40	2.80	0.635	554
17.4	17.9			0.756	0.87	1.30	1.57	0.540	526
13.0	13.5			0.785	0.65	0.85	1.07	0.465	506
7.4	7.9			0.854	0.41	0.42	0.586	0.355	464
3.6	4.1			0.940	0.35	0.14	0.376	0.280	423
0.6	1.1			1.00	0.29	0.05	0.294	0.250	397
26.4	26.9	200	5.84	0.655	1.12	2.10	2.37	0.650	543
21.6	22.1			0.683	0.82	1.35	1.58	0.580	520
15.4	15.9			0.731	0.55	0.75	0.93	0.475	486
11.5	12.0			0.768	0.42	0.45	0.615	0.375	463
5.7	6.2			0.854	0.33	0.18	0.376	0.280	416
29.1	29.6	150	5.05	0.575	1.02	1.95	2.20	0.670	534
24.7	25.2			0.605	0.72	1.30	1.49	0.575	508
18.3	18.8			0.647	0.50	0.71	0.867	0.473	475
9.1	9.6			0.767	0.29	0.15	0.326	0.270	401
33.2	33.7	100	4.13	0.481	0.96	1.85	2.08	0.730	522
26.3	26.8			0.518	0.59	1.09	1.24	0.620	486
20.9	21.4			0.556	0.40	0.59	0.711	0.460	452
14.7	15.2			0.620	0.29	0.25	0.382	0.290	406

TABLE XIX

Calibration Run No. 8

Nose Piece: Long
Resistance: 5000 ohms

Clearance 1"

RPM : 548
Amplifier Gain Setting: 6

Spring Letter Designation	I.F. lbs. + oz.	W lbs. + gms	F lbs.	A_{rdg} (-)	B_{rdg} (-)	R_{rdg}	β_1 deg.
L	4 - 11	2 - 20	0.505	0.35	0.44	0.561	231.6
I	2 - 11	1 - 30	0.265	0.15	0.22	0.266	235.9
V	4 - 11	2¼ - 220	0.740	0.52	0.65	0.830	231.5
C	3 - 11	½ - 190	0.228	0.13	0.21	0.246	238.4
R	4 - 11	3 - 150	0.821	0.58	0.75	0.945	232.5
N	4 - 11	4 - 40	1.007	0.72	0.90	1.150	231.5
Q	4 - 11	2¾ - 40	0.641	0.54	0.56	0.775	226.1
G	3 - 11	1 - 70	0.286	0.13	0.25	0.271	242.7
M	3 - 11	2 - 0	0.495	0.33	0.49	0.590	236.2
P	4 - 11	4 - 60	1.020	0.72	0.95	1.190	233.0
W	4 - 11	1¼ - 200	0.480	0.31	0.46	0.555	236.1
X	3 - 11	1½ - 180	0.470	0.28	0.45	0.529	238.3

TABLE XX

Nose Piece: Long

Calibration Run No. 9

Clearance 1-1/2"

RPM : 548
Amplifier Gain Setting: 6

Spring Letter Design.	I.F. lbs. + oz	W lbs. + gms	F lbs.	Resis. ohms	A_{rdg} (-)	B_{rdg} (-)	R_{rdg}	β_1 deg.
P	4 - 11	4 - 70	1.03	1000	1.83	1.65	2.45	221.9
				5000	0.45	0.72	0.85	238.1
M	4 - 11	2 - 0	0.496	1000	0.70	0.96	1.18	234.0
				5000	0.19	0.34	0.39	240.9
Q	4 - 11	2½ - 40	0.641	1000	1.05	1.22	1.61	229.4
				5000	0.29	0.45	0.53	237.4
L	4 - 11	2 - 10	0.500	1000	0.76	0.90	1.18	230.0
				5000	0.20	0.34	0.39	239.7
W	4 - 11	2 - 20	0.505	1000	0.76	0.94	1.20	231.2
				5000	0.21	0.35	0.41	239.2
G	4 - 11	1 - 40	0.270	1000	0.41	0.54	0.68	233.0
				5000	0.08	0.19	0.21	247.1
R	4 - 11	3 - 100	0.800	1000	1.39	1.48	2.04	226.9
				5000	0.35	0.59	0.69	239.5
I	3 - 11	1 - 10	0.254	1000	0.32	0.50	0.59	237.5
				5000	0.04	0.18	0.19	257.5
V	4 - 11	3 - 0	0.745	1000	1.18	1.40	1.82	230.0
				5000	0.32	0.52	0.61	238.5
X	3 - 11	2 - 0	0.495	1000	0.74	0.90	1.16	230.7
				5000	0.17	0.33	0.37	242.8
N	4 - 11	4 - 70	1.03	1000	1.65	1.85	2.28	228.4
				5000	0.45	0.70	0.83	237.4

TABLE XXI

Calibration Run No. 10

Nose Piece: Long
Resistance: 1000 ohms
Clearance 2"
RPM : 548
Amplifier Gain Setting: 6

Spring Letter Design.	I.F. lbs. + oz.	W lbs. + gms.	F lbs.	A_{rdg} (-)	B_{rdg} (-)	R_{rdg}	β_1 deg.
L	3 - 11	2 - 0	0.495	0.59	0.80	0.995	233.6
I	3 - 11	½ - 240	0.255	0.24	0.35	0.425	235.6
C	4 - 11	2½ - 50	0.648	0.83	1.04	1.33	231.4
M	4 - 11	2 - 0	0.495	0.55	0.72	0.910	232.6
W	4 - 11	1½ - 200	0.480	0.54	0.81	0.971	236.4
R	4 - 11	3 - 120	0.810	0.94	1.20	1.53	231.9
P	4 - 11	4 - 60	1.02	1.48	1.48	2.09	225.0
V	4 - 11	3 - 0	0.745	0.95	1.05	1.42	227.8
N	4 - 11	4 - 60	1.02	1.29	1.48	1.96	229.0
X	3 - 11	2 - 0	0.495	0.55	0.65	0.85	229.9
G	2 - 11	1 - 40	0.270	0.25	0.30	0.39	230.3

TABLE XXII

Calibration Run No. 11

Nose Piece: Long
Resistance: 1000 ohms

Clearance 2-1/2"

RPM: 548

Spring Letter Design.	I.F. lbs. + oz.	W lbs. + gms	F lbs.	Gain Setting	A_{rdg} (-)	B_{rdg} (-)	R_{rdg}	β_1 deg.
V	4 - 11	3 - 0	0.745	6	0.91	1.00	1.35	227.9
				8	1.80	2.10	2.76	229.4
N	4 - 11	4 - 50	1.01	6	1.27	1.45	1.93	228.9
				8	2.50	2.72	3.69	227.5
W	4 - 11	2 - 40	0.520	6	0.55	0.67	0.87	230.7
				8	1.10	1.42	2.10	232.3
X	3 - 11	1½ - 200	0.480	6	0.53	0.66	0.845	231.4
				8	1.06	1.33	1.70	231.5
L	4 - 11	2 - 10	0.500	6	0.55	0.67	0.870	230.6
				8	1.12	1.35	1.75	230.4
R	4 - 11	3 - 100	0.800	6	1.04	1.19	1.60	228.0
				8	2.00	2.30	3.05	229.0
G	3 - 11	1 - 40	0.270	6	0.26	0.35	0.435	233.5
				8	0.60	0.75	0.960	231.4
Q	4 - 11	2¼ - 0	0.620	6	0.75	0.96	1.22	232.1
				8	1.60	1.85	2.44	229.3
P	4 - 11	4 - 100	1.04	6	1.45	1.52	2.10	226.5
				8	2.67	2.92	3.97	228.0
C	3 - 11	¼ - 200	0.233	6	0.18	0.31	0.359	240.0
				8	0.50	0.71	0.869	235.0
I	3 - 11	1 - 20	0.260	6	0.23	0.32	0.393	234.4
				8	0.50	0.72	0.885	234.6

TABLE XXIII

Calibration Run No. 12

Nose Piece: Long
Resistance: 1000 ohms
Clearance 3"
RPM : 548
Amplifier Gain Setting: 8

Spring Letter Design.	I.F. lbs. + oz.	W lbs. + gms	F lbs.	A_{rdg} (-)	B_{rdg} (-)	R_{rdg}	β_1 deg.
M	4 - 11	2 - 0	0.495	0.75	1.25	1.46	239.0
G	3 - 11	1 - 40	0.270	0.35	0.72	0.80	244.2
W	3 - 11	2 - 40	0.520	1.05	1.40	1.74	233.3
C	3 - 11	½ - 200	0.233	0.25	0.65	0.695	249.0
V	4 - 11	2½ - 220	0.740	1.42	2.20	2.62	237.2
P	4 - 11	4 - 100	1.04	2.48	2.75	3.70	228.0
I	3 - 11	1 - 30	0.365	0.35	0.62	0.711	240.6
Q	4 - 11	2½ - 40	0.641	1.44	1.79	2.29	231.3
R	4 - 11	3 - 120	0.810	1.92	2.25	2.96	229.6
L	3 - 11	2 - 20	0.505	1.00	1.38	1.70	234.1
N	4 - 11	4 - 40	1.007	2.35	2.75	3.63	229.5

TABLE XXIV

Measurement Run No. 11

Water Temperature: 80°F.
Nose Piece : Long
Thrust Correction: +0.7 lbs.
Clearance 1"

RPM : 548
Amplifier Gain Setting: 6
Resistance :5000 ohms

T_{rdg} lbs.	T_{corr} lbs.	H_1 rdg	v fps	J v/nd	A_{rdg} (−)	B_{rdg} (+)	R_{rdg}	F lbs	β_2 deg	β_1 deg	α_{rdg} deg	$\Delta\gamma$ (−)°	γ (+)°
57.0	57.7	0	0	0	2.00	4.75	5.15	4.52	102.7	233.9	332	104.2	26.0
55.5	56.2	15	1.59	0.177	2.00	4.35	4.79	4.20	104.6		332	101.3	25.3
52.5	53.2	28	2.17	0.241	1.95	4.35	4.77	4.19	104.1		331	100.8	25.2
48.8	49.2	45	2.75	0.306	1.78	4.18	4.55	3.99	103.0		331	101.9	25.5
45.8	46.5	53	2.99	0.331	1.75	4.10	4.46	3.91	103.0		331	101.9	25.5
42.5	43.2	70	3.43	0.381	1.70	3.90	4.25	3.73	103.5		331	101.4	25.4
37.5	38.2	115	4.39	0.489	1.60	3.63	3.96	3.47	103.7		332	102.2	25.5
34.0	34.7	129	4.66	0.518	1.60	3.50	3.84	3.36	104.4		332	101.5	25.4
29.4	30.1	165	5.27	0.585	1.55	3.25	3.60	3.16	105.4		332	100.5	25.1
25.7	26.4	203	5.85	0.650	1.49	3.00	3.35	2.94	106.3		332	99.6	24.9
21.4	22.1	238	6.32	0.705	1.45	2.90	3.24	2.84	106.5		333	100.4	25.1
17.3	18.0	277	6.81	0.759	1.38	2.79	3.10	2.72	105.9		333	101.0	25.2
12.8	13.5	321	7.38	0.819	1.38	2.55	2.90	2.54	108.3		333	98.6	24.7
9.6	10.3	360	7.79	0.863	1.42	2.40	2.79	2.44	110.5		333	96.4	24.1
7.1	7.8	389	8.09	0.899	1.40	2.42	2.79	2.44	110.0		332	95.9	24.5
4.2	4.9	429	8.50	0.944	1.37	2.40	2.76	2.42	109.6		332	96.3	26.6
1.0	1.7	461	8.80	0.979	1.38	2.35	2.72	2.38	110.3		332	95.6	23.9

TABLE XXV

Measurement Run No. 12

Water Temperature: 80°F.
Nose Piece : Long
Thrust Correction: +0.7 lbs.
Clearance 1-1/4"
RPM : 548
Amplifier Gain Setting: 6
Resistance : 5000 ohms

T_{rdg}	T_{corr}	H_1	v	J	A_{rdg}	B_{rdg}	R_{rdg}	F	β_2	β_1	γ_{rdg}	$\Delta\gamma$	γ
lbs.	lbs.	rdg	fps	v/nd	(-)	(+)		lbs	deg	deg	deg	(-)°	(+)°
57.8	58.5	0	0	0	1.10	2.80	3.01	3.24	101.4	237.7	326	102.3	25.6
56.5	57.2	14	1.54	0.171	1.05	2.75	2.95	3.17	100.8			102.9	25.7
47.5	48.2	45	2.75	0.306	0.95	2.52	2.70	2.90	100.6			103.1	25.8
44.5	45.2	59	3.15	0.350	0.92	2.45	2.62	2.81	100.4		327	104.3	26.1
37.5	38.2	96	4.03	0.447	0.85	2.25	2.40	2.58	100.7			104.0	26.0
31.7	32.5	148	4.99	0.555	0.75	2.02	2.15	2.31	100.4			104.3	26.1
26.4	27.1	184	5.55	0.618	0.72	1.92	2.05	2.21	100.3			104.4	26.1
22.3	23.0	204	5.85	0.651	0.70	1.80	1.92	2.06	101.2		325	103.5	25.9
18.0	18.7	267	6.70	0.740	0.65	1.72	1.84	1.98	100.7			104.0	26.0
13.8	14.5	303	7.16	0.797	0.66	1.61	1.74	1.87	102.2			102.5	25.6
9.9	10.6	351	7.69	0.852	0.65	1.51	1.65	1.77	103.3			101.4	25.4
7.0	7.7	378	7.97	0.886	0.66	1.52	1.66	1.78	103.2		326	101.5	25.4
6.5	7.2	394	8.14	0.906	0.70	1.45	1.61	1.73	105.7			99.0	24.8
3.8	4.5	424	8.45	0.940	0.66	1.40	1.55	1.67	105.2			99.5	24.9
1.1	1.8	449	8.69	0.967	0.64	1.42	1.56	1.68	104.2			100.5	25.1

TABLE XXVI

Measurement Run No. 13

Water Temperature: 80°F.
Nose Piece : Long
Thrust Correction: +0.7 lbs.

Clearance 1-1/2"

RPM : 548
Amplifier Gain Setting: 6
Resistance : 5000 ohms

T_{rdg}	T_{corr}	H_1	v	J	A_{rdg}	B_{rdg}	R_{rdg}	F	β_2	β_1	α_{rdg}	4γ	γ
lbs.	lbs.	rdg	fps	v/nd	(-)	(+)		lbs	deg	deg	deg	(-)°	(+)°
56.3	57.0	3	0.71	0.08	0.55	1.80	1.89	2.34	107.1	241.6	323	97.5	24.4
54.5	55.2	15	1.54	0.171	0.62	2.00	2.09	2.59	107.3			97.3	24.3
52.0	52.7	25	2.05	0.228	0.60	1.75	1.85	2.29	109.0		322	94.5	24.4
46.7	47.4	45	2.75	0.306	0.50	1.71	1.79	2.21	106.4			97.1	24.3
40.0	40.7	79	3.64	0.405	0.41	1.55	1.61	1.99	104.8			98.7	24.7
36.5	37.2	102	4.15	0.461	0.39	1.48	1.53	1.89	104.8			98.7	24.7
31.5	32.2	131	4.70	0.522	0.37	1.40	1.45	1.80	104.8		325	101.7	25.4
28.4	29.1	169	5.32	0.592	0.35	1.37	1.42	1.76	104.3			102.2	25.5
23.6	24.3	205	5.88	0.652	0.28	1.29	1.32	1.63	102.2			104.3	26.1
19.1	19.8	246	6.42	0.715	0.28	1.22	1.26	1.56	102.9			103.6	25.9
16.4	17.1	288	6.97	0.772	0.31	1.19	1.23	1.52	104.6		324	100.0	25.2
11.7	12.4	329	7.45	0.828	0.30	1.13	1.17	1.45	104.8			100.7	25.2
9.0	9.7	354	7.73	0.859	0.32	1.10	1.16	1.42	106.2			99.3	24.8
5.6	6.3	394	8.14	0.907	0.30	1.03	1.08	1.34	106.2			99.3	24.8
1.7	2.4	441	8.61	0.959	0.29	0.99	1.04	1.29	106.2			99.3	24.8

TABLE XXVII

Measurement Run No. 14

Water Temperature: 80°F.
Nose Piece : Long
Thrust Correction: +0.7 lbs.
Clearance 1-3/4"

RPM : 548
Amplifier Gain Setting: 6
Resistance : 1000 ohms

T_{rdg}	T_{corr}	H_1	v	J	A_{rdg}	B_{rdg}	R_{rdg}	F	β_2	β_1	α_{rdg}	$\Delta\gamma$	γ
lbs.	lbs.	rdg	fps	v/nd	(-)	(+)		lbs	deg	deg	deg	deg	(+)°
56.5	57.2	0	0	0	1.0	5.0	5.1	2.30	101.3	230.7	322	91.4	22.9
54.0	54.7	16	1.64	0.183	1.0	4.8	4.9	2.21	101.8		323	91.9	23.0
49.0	49.7	35	3.43	0.270	0.88	4.6	4.68	2.12	100.8		323	92.9	23.2
46.8	47.5	45	2.75	0.307	0.80	4.40	4.48	2.03	100.3		324	94.4	23.6
41.0	41.7	77	3.60	0.400	0.70	3.95	4.01	1.82	100.0		324	94.7	23.7
34.5	35.2	116	4.42	0.592	0.60	3.75	3.80	1.72	99.1		324	95.6	23.9
29.0	29.7	150	5.01	0.559	0.55	3.50	3.55	1.62	98.9		324	95.8	23.9
26.0	26.7	180	5.50	0.611	0.50	3.35	3.39	1.54	98.5		323	95.2	23.8
21.6	22.3	220	6.09	0.676	0.48	3.15	3.19	1.45	98.7		323	95.0	23.8
17.0	17.7	260	6.61	0.736	0.48	3.00	3.05	1.39	99.1		323	94.6	23.7
13.0	13.7	303	7.16	0.979	0.44	2.82	2.86	1.31	98.9		323	94.8	23.7
8.6	9.3	346	7.61	0.849	0.45	2.65	2.69	1.23	99.6		322	93.1	23.2
5.0	5.7	375	7.95	0.882	0.46	2.55	2.60	1.20	100.2		322	92.5	23.1
3.0	3.7	402	8.23	0.916	0.45	2.50	2.55	1.17	100.2		322	92.5	23.1
1.2	1.9	416	8.36	0.930	0.53	2.42	2.48	1.14	102.3		322	90.4	22.6

TABLE XXVIII

Measurement Run No. 15

Water Temperature: 80°F.
Nose Piece : Long
Thrust Correction: +0.7 lbs.

Clearance 2"

RPM : 548
Amplifier Gain Setting: 6
Resistance : 1000 ohms

T_{rdg}	T_{corr}	H_1	v	J	A_{rdg}	B_{rdg}	R_{rdg}	F	β_2	β_1	α_{rdg}	$\Delta\gamma$	γ
lbs.	lbs.	rdg	fps	v/nd	(-)	(+)		lbs	deg	deg	deg	deg	(+) °
56.0	56.7	1	0.41	0.046	0.70	3.50	3.57	1.70	101.3	231.2	322	91.9	23.0
55.0	55.7	14	1.53	0.171	0.70	3.40	3.47	1.64	101.6		322	91.6	22.9
52.0	52.7	27	2.13	0.237	0.70	3.55	3.62	1.72	101.1		322	92.1	23.0
47.0	47.7	45	2.75	0.306	0.50	3.45	3.50	1.66	98.2		321	96.0	24.0
44.5	45.2	57	3.09	0.344	0.45	3.32	3.36	1.60	97.7		321	96.5	24.1
41.3	42.0	73	3.50	0.390	0.38	3.15	3.19	1.52	96.9		321	97.3	24.3
39.0	29.7	89	3.87	0.430	0.39	3.00	3.04	1.45	97.4		321	96.8	24.2
32.5	33.2	130	4.68	0.520	0.31	2.79	2.92	1.40	96.3		321	97.9	24.5
28.4	29.1	166	5.29	0.588	0.25	2.72	2.74	1.31	95.3		322	97.9	24.5
23.8	24.5	207	5.89	0.656	0.25	2.45	2.47	1.19	95.8		322	97.4	24.4
19.4	20.1	240	6.35	0.707	0.21	2.38	2.40	1.16	95.0		322	98.2	24.5
14.8	15.5	284	6.91	0.769	0.15	2.28	2.30	1.11	93.8		322	99.4	24.9
10.2	10.9	327	7.40	0.822	0.25	2.25	2.27	1.10	96.3		322	97.9	24.5
6.2	6.9	368	7.88	0.874	0.31	2.10	2.12	1.03	98.4		322	94.8	23.7
3.1	3.8	404	8.26	0.919	0.29	2.15	2.17	1.05	97.7		322	95.5	23.9
1.4	2.1	419	8.39	0.932	0.25	2.00	2.02	0.98	97.1		322	96.1	24.0

TABLE XXIX

Measurement Run No. 16

Water Temperature: 80°F.
Nose Piece : Long
Thrust Correction: +0.7 lbs.

Clearance 2-1/4"

RPM : 548
Amplifier Gain Setting: 6
Resistance : 1000 ohms

T_{rdg}	T_{corr}	H_1	v	J	A_{rdg}	B_{rdg}	R_{rdg}	F	β_2	β_1	α_{rdg}	4γ	γ
lbs.	lbs.	rdg	fps	v/nd	(-)	(+)		lbs	deg	deg	deg	deg	(+) °
55.5	56.2	1	0.410	0.046	0.50	2.55	2.60	1.295	101.0	231.3	325	95.3	23.8
55.6	56.3	15	1.54	0.171	0.75	2.25	2.38	1.195	108.4		325	87.9	22.0
52.2	52.9	28	2.17	0.241	0.65	2.45	2.54	1.265	104.8		321	87.5	21.9
47.7	48.4	45	2.75	0.306	0.54	2.35	2.42	1.215	102.9		321	89.4	22.4
42.3	43.0	72	3.47	0.387	0.41	2.12	2.17	1.095	100.9		321	91.4	22.9
38.7	39.4	97	4.04	0.449	0.40	2.00	2.04	1.040	101.3		323	93.0	23.2
34.4	35.1	125	4.59	0.505	0.34	1.88	1.92	0.980	100.2		323	94.1	23.5
25.5	26.2	193	5.70	0.635	0.30	1.73	1.75	0.900	99.8		323	94.5	23.6
21.2	21.9	228	6.20	0.690	0.24	1.65	1.67	0.865	98.3		323	96.0	24.0
17.8	18.5	255	6.55	0.729	0.25	1.60	1.62	0.840	98.9		325	97.4	24.3
13.9	13.6	294	7.04	0.783	0.25	1.55	1.57	0.815	99.1		325	97.2	24.3
10.5	11.2	325	7.40	0.822	0.24	1.46	1.48	0.775	99.3		325	97.0	24.2
8.4	9.1	348	7.64	0.849	0.22	1.44	1.46	0.765	98.7		324	96.6	24.1
7.1	7.8	364	7.82	0.870	0.25	1.37	1.39	0.730	100.3		324	95.0	23.8
3.1	3.8	404	8.25	0.918	0.24	1.36	1.38	0.725	100.0		324	95.3	23.8
2.5	3.2	419	8.39	0.932	0.24	1.31	1.34	0.705	100.4		324	94.9	23.7
1.0	1.7	431	8.51	0.945	0.25	1.31	1.34	0.705	100.8		324	94.5	23.6

TABLE XXX

Measurement Run No. 17

Water Temperature: 80°F.
Nose Piece : Long
Thrust Correction: +0.7 lbs.

Clearance 2-1/2"

RPM : 548
Amplifier Gain Setting: 8
Resistance : 1000 ohms

T_{rdg}	T_{corr}	H_1	v	J	A_{rdg}	B_{rdg}	R_{rdg}	F	β_2	β_1	α_{rdg}	$\Delta\gamma$	γ
lbs.	lbs.	rdg	fps	v/nd	(-)	(+)		lbs	deg	deg	deg	deg	(+) °
56.6	57.3	1	0.41	0.046	0.70	3.10	3.18	0.840	102.7	230.7	324	92.0	23.0
56.3	57.0	15	1.59	0.177	1.00	3.20	3.35	0.888	107.3		324	87.4	21.9
50.9	51.6	33	2.36	0.263	0.82	3.15	3.26	0.865	104.6		324	90.1	22.5
47.5	48.2	45	2.75	0.306	0.72	3.00	3.09	0.820	103.4		324	91.3	22.8
39.2	39.9	92	3.93	0.438	0.60	2.60	2.67	0.710	108.0		324	91.7	22.9
43.8	44.5	66	3.34	0.371	0.69	2.80	2.88	0.765	103.8		324	90.9	22.7
35.0	35.7	120	4.49	0.500	0.55	2.49	2.55	0.663	102.4		322	90.3	22.6
27.8	28.5	169	5.33	0.593	0.45	2.28	2.34	0.625	101.1		322	91.6	22.9
24.7	25.4	202	5.82	0.649	0.37	2.19	2.22	0.600	99.6		322	93.1	23.2
16.8	17.5	273	6.79	0.752	0.35	1.95	1.98	0.535	100.2		322	92.5	23.1
12.2	12.9	315	7.29	0.810	0.31	1.88	1.91	0.578	99.3		322	93.4	23.4
8.4	9.1	356	7.73	0.860	0.29	1.80	1.83	0.500	99.1		322	93.6	23.4
5.1	5.8	392	8.13	0.907	0.30	1.65	1.68	0.455	100.3		322	92.4	23.1
3.5	4.2	405	8.26	0.919	0.30	1.70	1.73	0.475	100.0		322	92.7	23.2
2.4	3.1	421	8.41	0.935	0.29	1.65	1.67	0.455	99.9		322	92.8	23.2
0	0.7	446	8.67	0.962	0.25	1.65	1.67	0.455	98.6		322	94.1	23.5

TABLE XXXI

Measurement Run No. 18

Water Temperature: 80°F.		RPM	: 548
Nose Piece : Long		Amplifier Gain Setting:	8
Thrust Correction: +0.7 lbs.	Clearance 2-3/4"	Resistance	: 1000 ohms

T_{rdg}	$T_{corr.}$	H_1	v	J	A_{rdg}	B_{rdg}	R_{rdg}	F	β_2	β_1	α_{rdg}	$\Delta\gamma$	γ
lbs.	lbs.	rdg	fps	v/nd	(-)	(+)		lbs	deg	deg	deg	deg	(+) °
55.5	56.2	3	0.71	0.079	0.85	3.00	3.11	0.864	105.7	233.3	325	92.6	23.1
55.5	56.2	18	1.74	0.194	1.10	2.75	2.97	0.824	111.7		325	86.6	21.6
47.2	47.9	45	2.75	0.306	0.60	2.60	2.67	0.774	103.0		325	95.3	23.3
40.1	40.8	85	3.78	0.421	0.45	2.28	2.32	0.655	101.2		325	97.1	24.3
34.9	35.6	119	4.48	0.598	0.37	2.15	2.18	0.620	99.8		325	98.5	24.6
31.2	31.9	140	4.85	0.539	0.33	2.11	2.14	0.600	98.9		324	98.4	24.6
27.9	28.6	170	5.34	0.593	0.29	1.99	2.02	0.578	98.3		324	99.0	24.7
23.2	23.9	210	5.94	0.661	0.22	1.88	1.90	0.548	96.7		324	100.6	25.1
17.5	18.2	260	6.61	0.735	0.21	1.75	1.77	0.513	96.8		324	100.5	25.1
13.5	14.2	293	7.02	0.782	0.15	1.68	1.69	0.492	95.1		324	102.2	25.5
10.8	11.5	328	7.41	0.824	0.15	1.64	1.66	0.485	95.2		324	102.1	25.5
7.4	8.1	363	7.82	0.869	0.15	1.55	1.56	0.460	95.5		324	101.8	25.4
2.9	3.6	412	8.32	0.926	0.15	1.50	1.52	0.450	95.7		324	101.6	25.4
1.6	2.3	428	8.49	0.943	0.15	1.45	1.46	0.433	95.9		324	101.4	25.3

TABLE XXXII

Measurement Run No. 19

Water Temperature: 80°F.
Nose Piece : Long
Thrust Correction: +0.7 lbs.

Clearance 3"

RPM : 548
Amplifier Gain Setting: 8
Resistance : 1000 ohms

T_{rdg}	T_{corr}	H_1	v	J	A_{rdg}	B_{rdg}	R_{rdg}	F	β_2	β_1	α_{rdg}	ΔY	Y
lbs.	lbs.	rdg	fps	v/nd	(-)	(+)		lbs	deg	deg	deg	deg	deg (+)
56.0	56.7	1	0.41	0.046	0.70	2.0	2.12	0.617	109.2	235.9	323	89.7	22.4
55.5	56.2	17	1.69	0.188	0.70	1.90	2.03	0.538	110.2		323	88.7	22.2
47.0	47.7	45	2.75	0.306	0.55	1.80	1.88	0.551	107.0		323	91.9	23.0
40.8	41.5	85	3.78	0.421	0.36	1.52	1.56	0.470	103.3		323	95.6	23.9
35.0	35.7	120	4.49	0.499	0.34	1.49	1.53	0.462	102.8		323	96.1	24.0
32.8	33.5	138	4.82	0.536	0.31	1.45	1.48	0.448	102.1		325	98.8	24.7
28.0	28.7	178	5.48	0.609	0.28	1.39	1.42	0.432	101.4		325	99.5	24.9
24.3	25.0	206	5.89	0.653	0.25	1.31	1.34	0.410	100.8		325	100.1	25.0
20.5	21.2	242	6.38	0.709	0.22	1.25	1.27	0.395	100.0		325	100.9	25.2
15.3	16.0	285	6.91	0.770	0.21	1.19	1.21	0.380	100.0		325	100.9	25.2
10.5	11.2	327	7.40	0.823	0.15	1.10	1.11	0.353	97.2		325	103.7	25.9
6.9	7.6	365	7.84	0.870	0.19	1.00	1.02	0.330	100.7		325	100.2	25.1
3.3	4.0	400	8.20	0.912	0.14	1.00	1.01	0.328	97.9		325	103.0	25.8
2.1	2.8	415	8.36	0.928	0.15	0.97	0.98	0.320	98.8		325	102.1	25.5
-1.8	-1.1	469	8.89	0.988	0.13	0.98	0.99	0.323	97.6		325	103.3	25.8

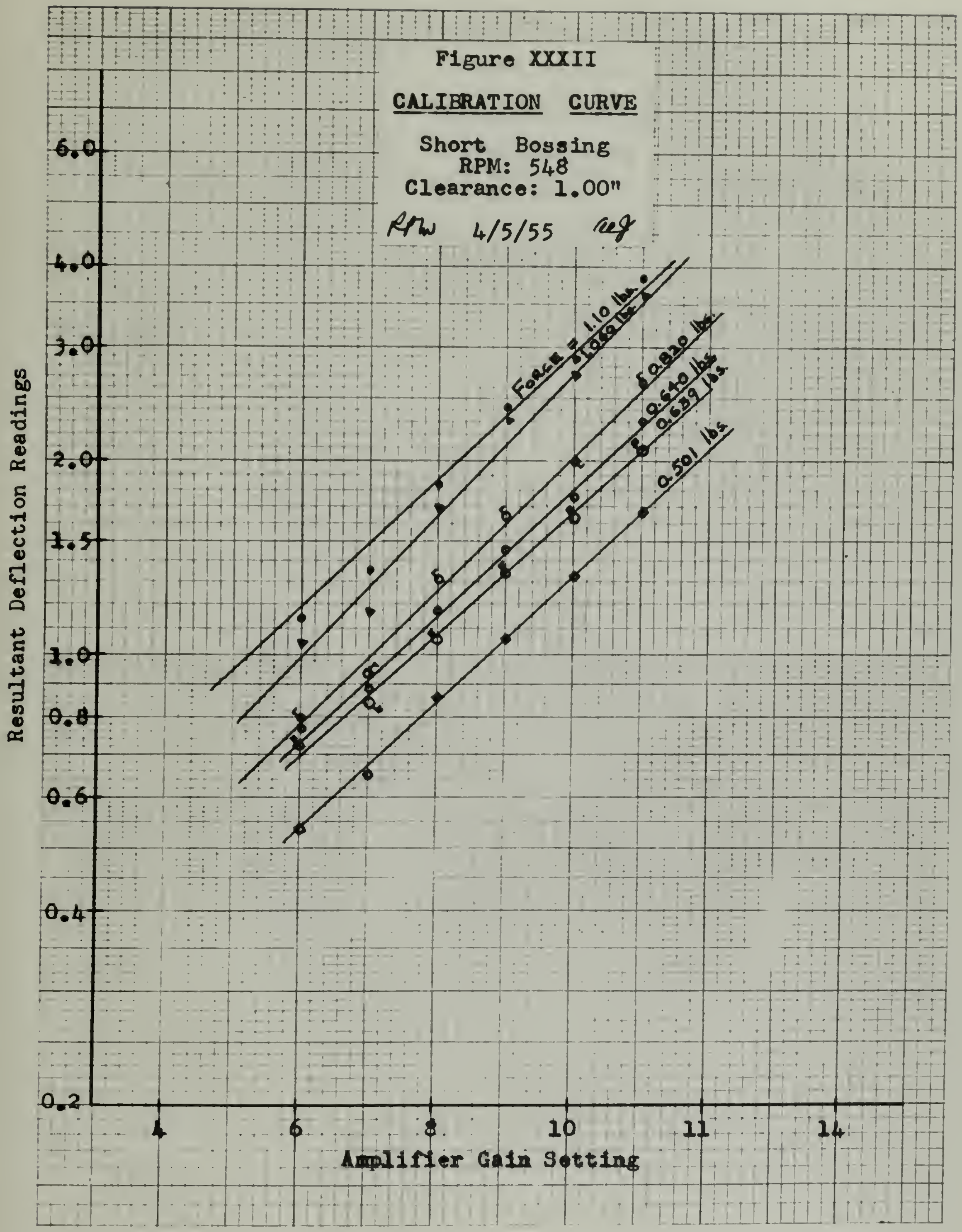

Figure XXXII

CALIBRATION CURVE

Short Bossing
RPM: 548
Clearance: 1.00"

RPW 4/5/55 ewj

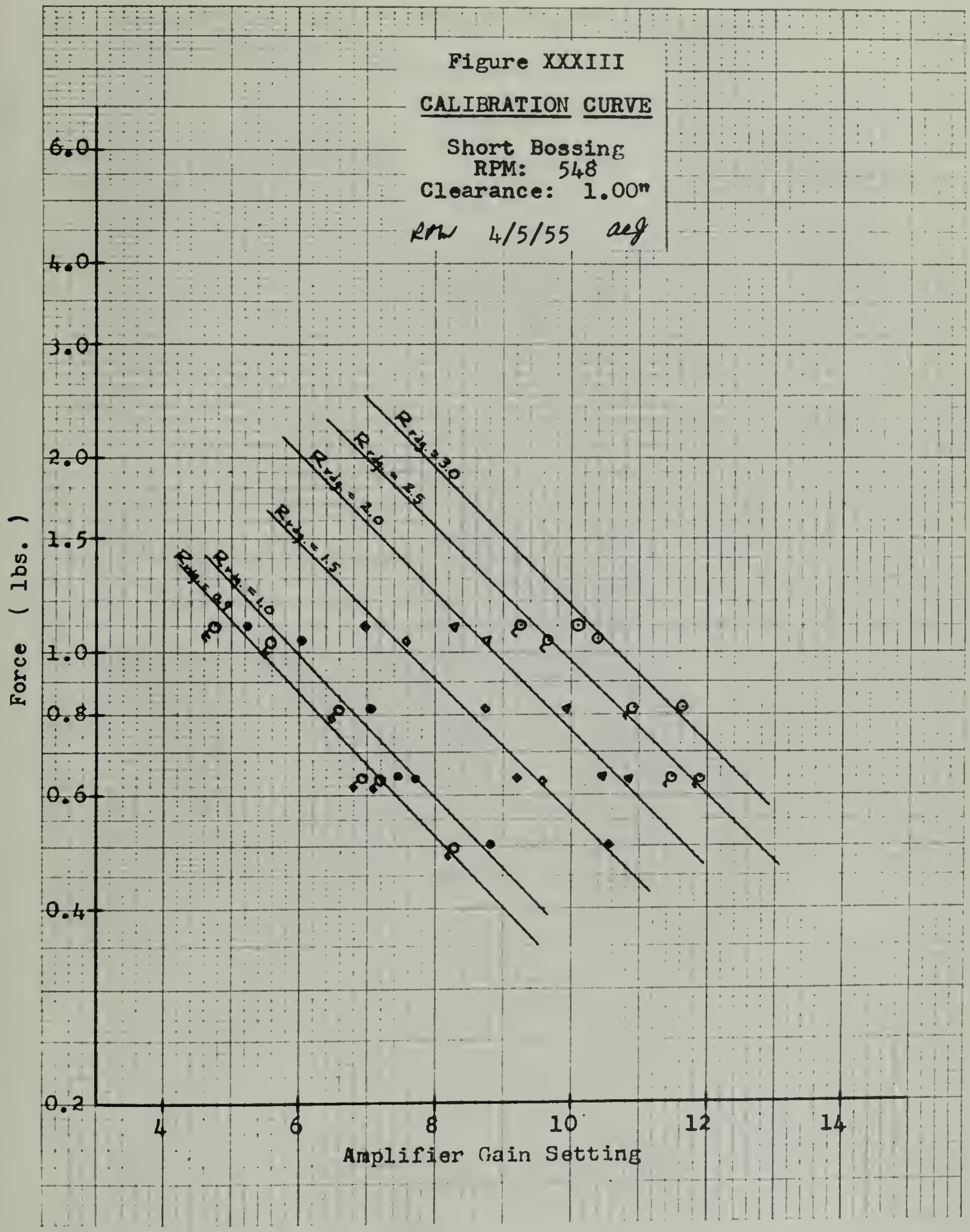

Figure XXXIII

CALIBRATION CURVE

Short Bossing
RPM: 548
Clearance: 1.00"

RRW 4/5/55 aeg

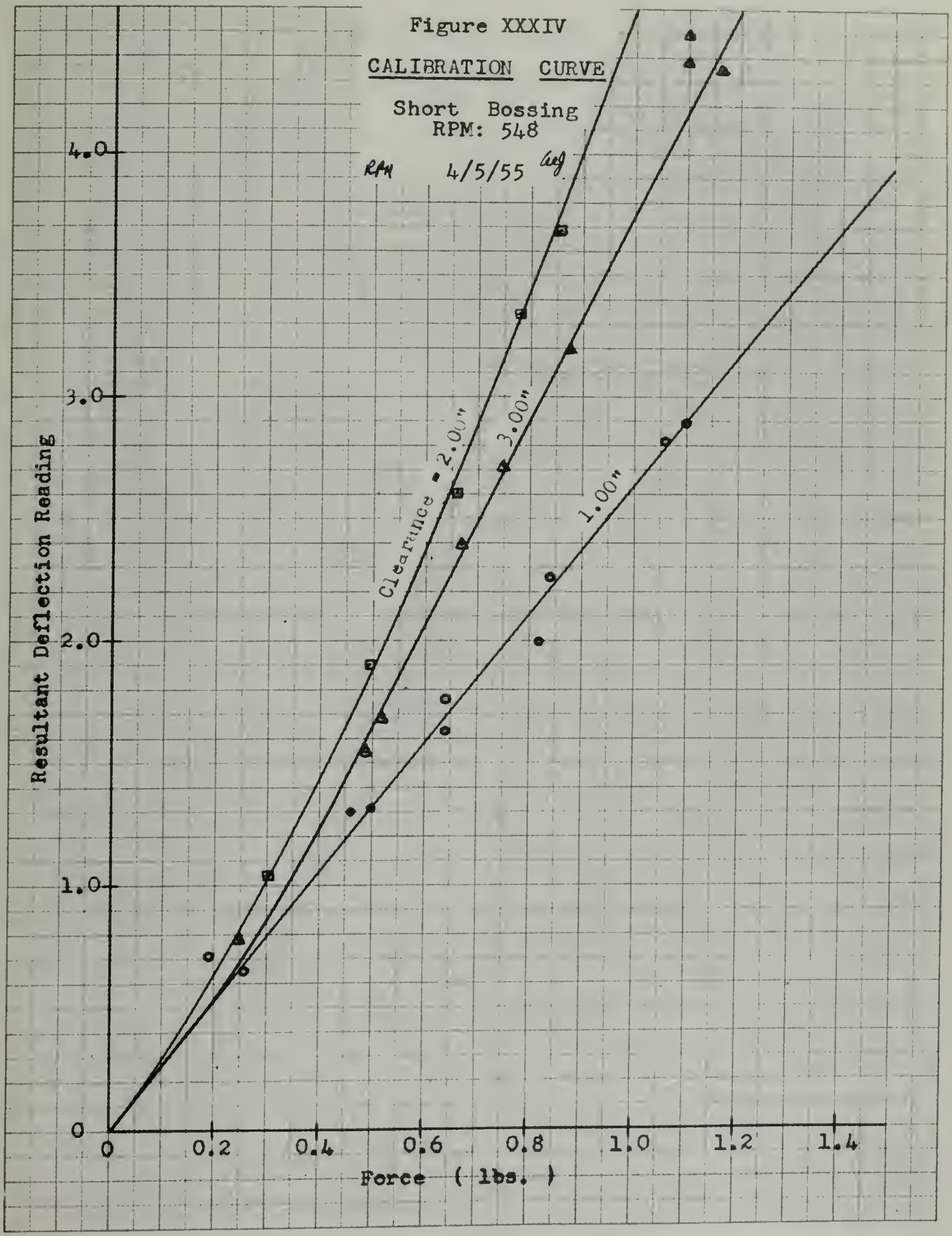

Figure XXXIV

CALIBRATION CURVE

Short Bossing
RPM: 548

RPH 4/5/55 ccg

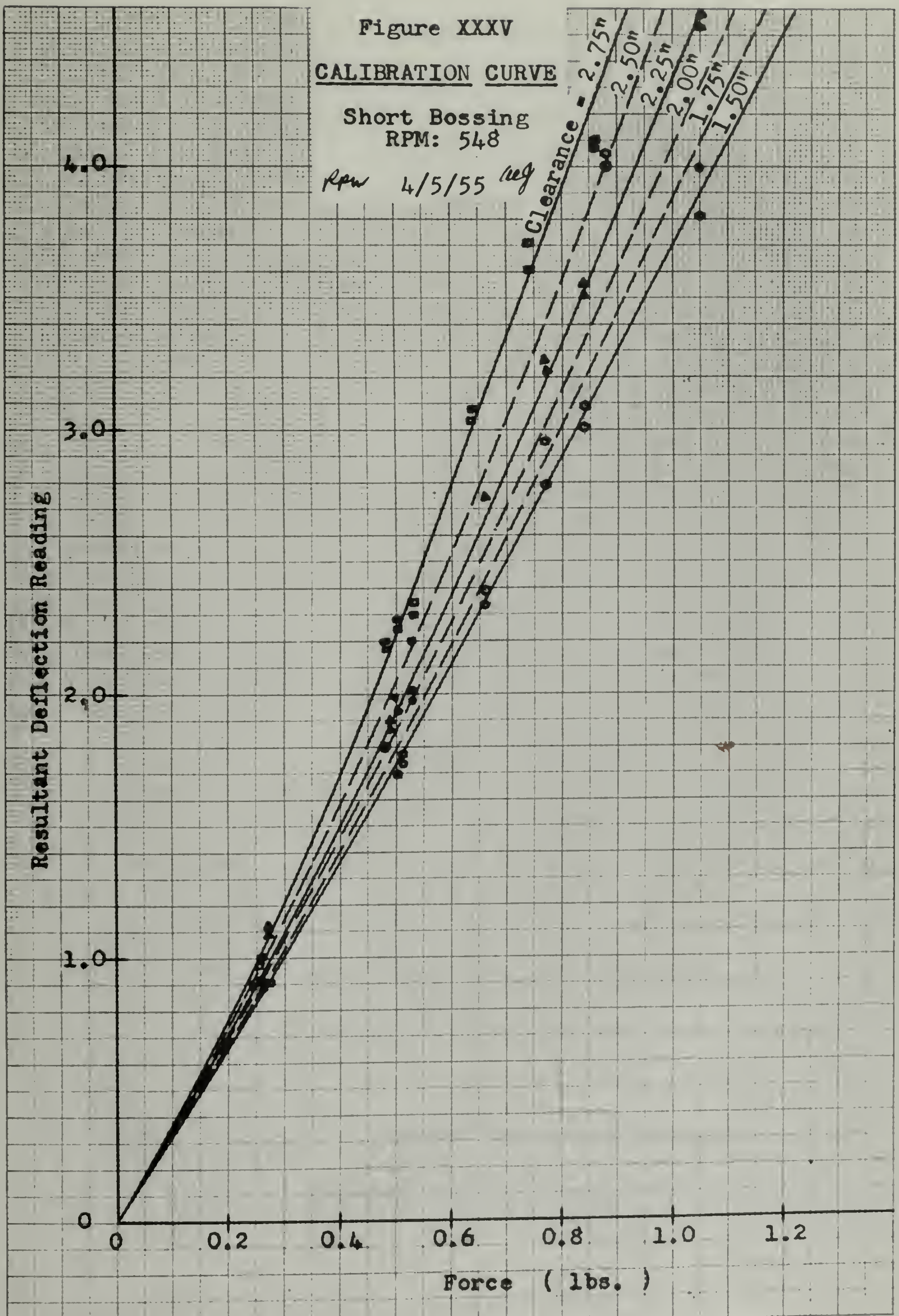

Figure XXXV

CALIBRATION CURVE

Short Bossing
RPM: 548

Rpw 4/5/55 ueg

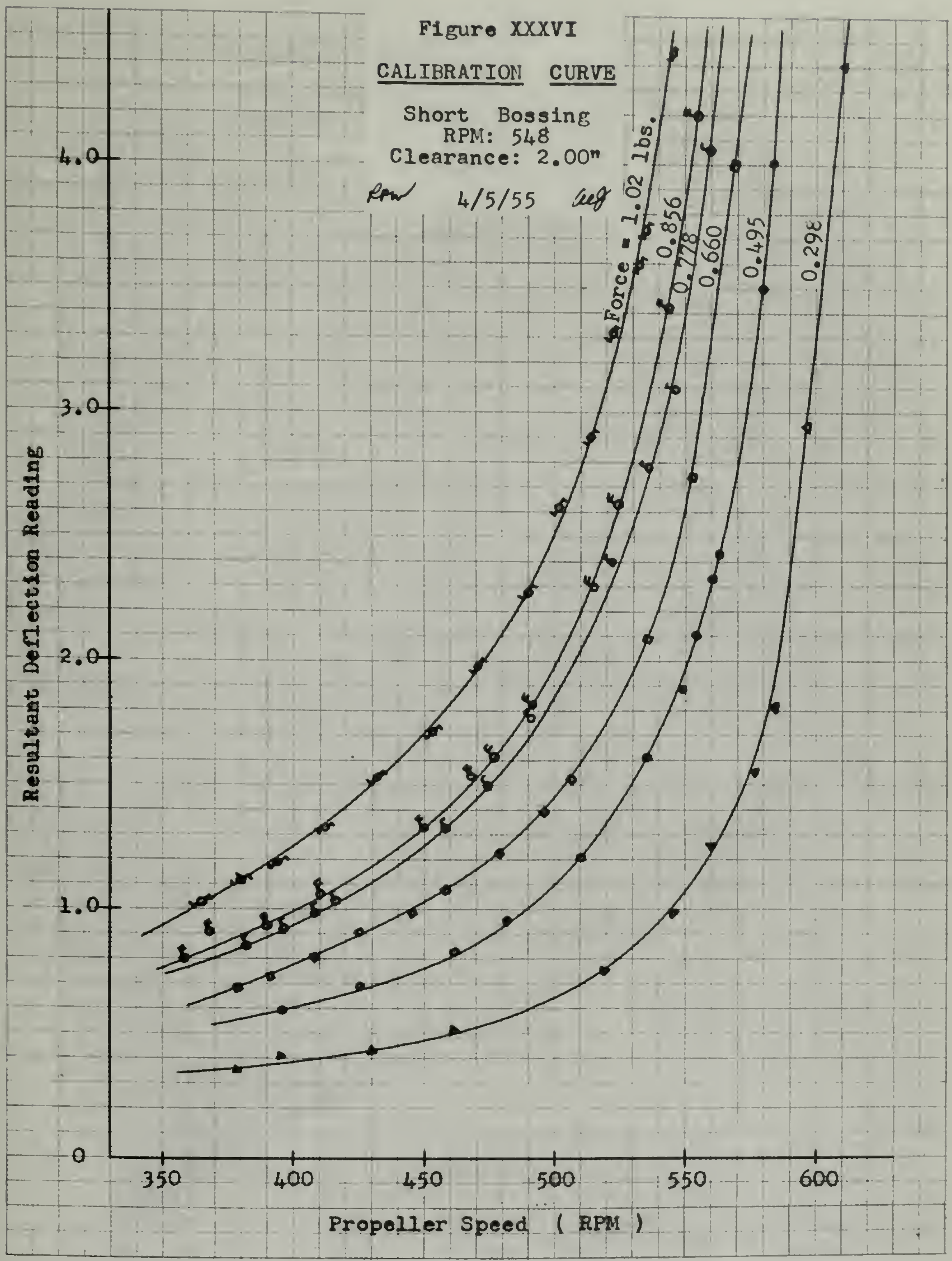

Figure XXXVI

CALIBRATION CURVE

Short Bossing
RPM: 548
Clearance: 2.00"

4/5/55

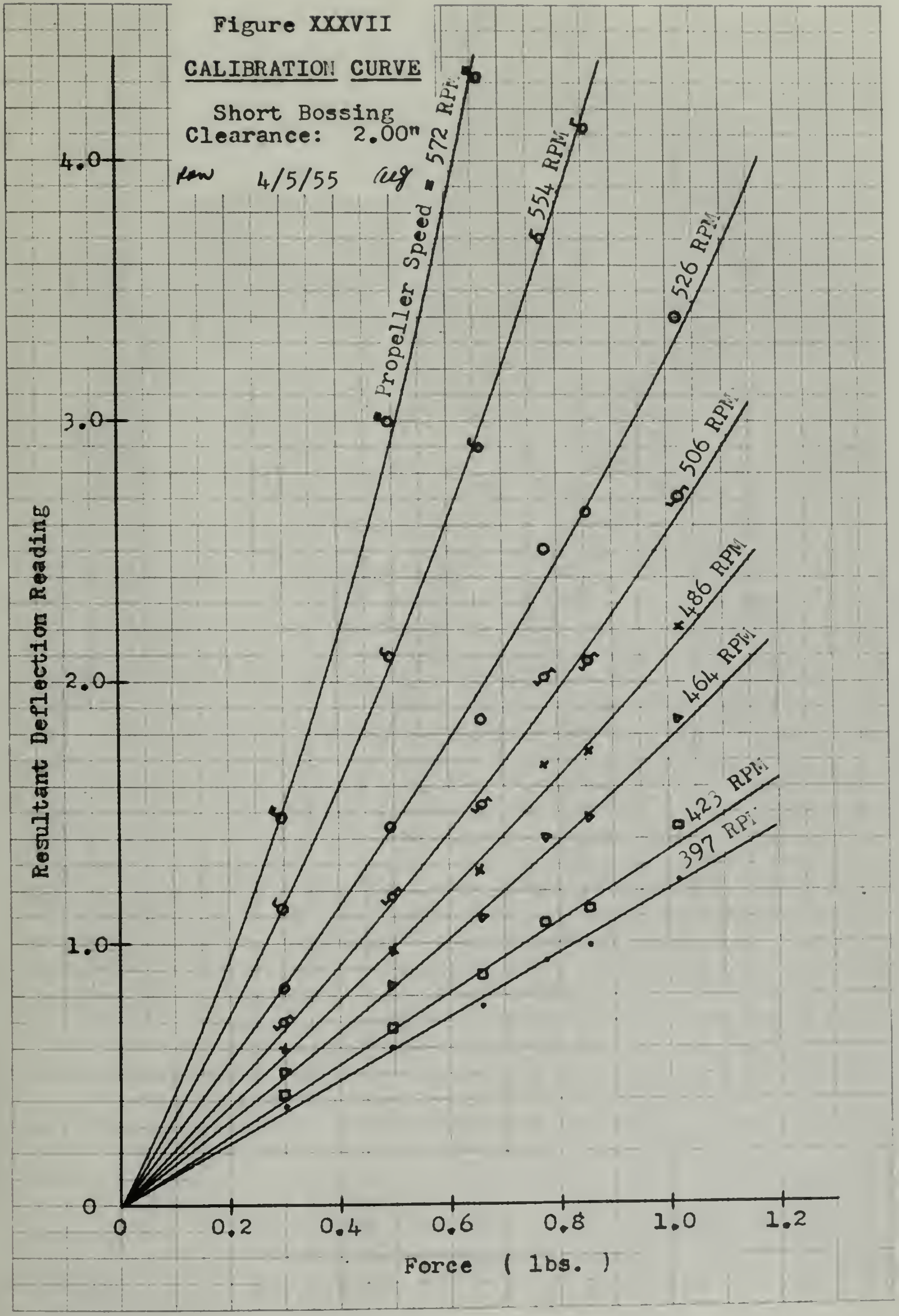

Figure XXXVII

CALIBRATION CURVE

Short Bossing
Clearance: 2.00"

4/5/55

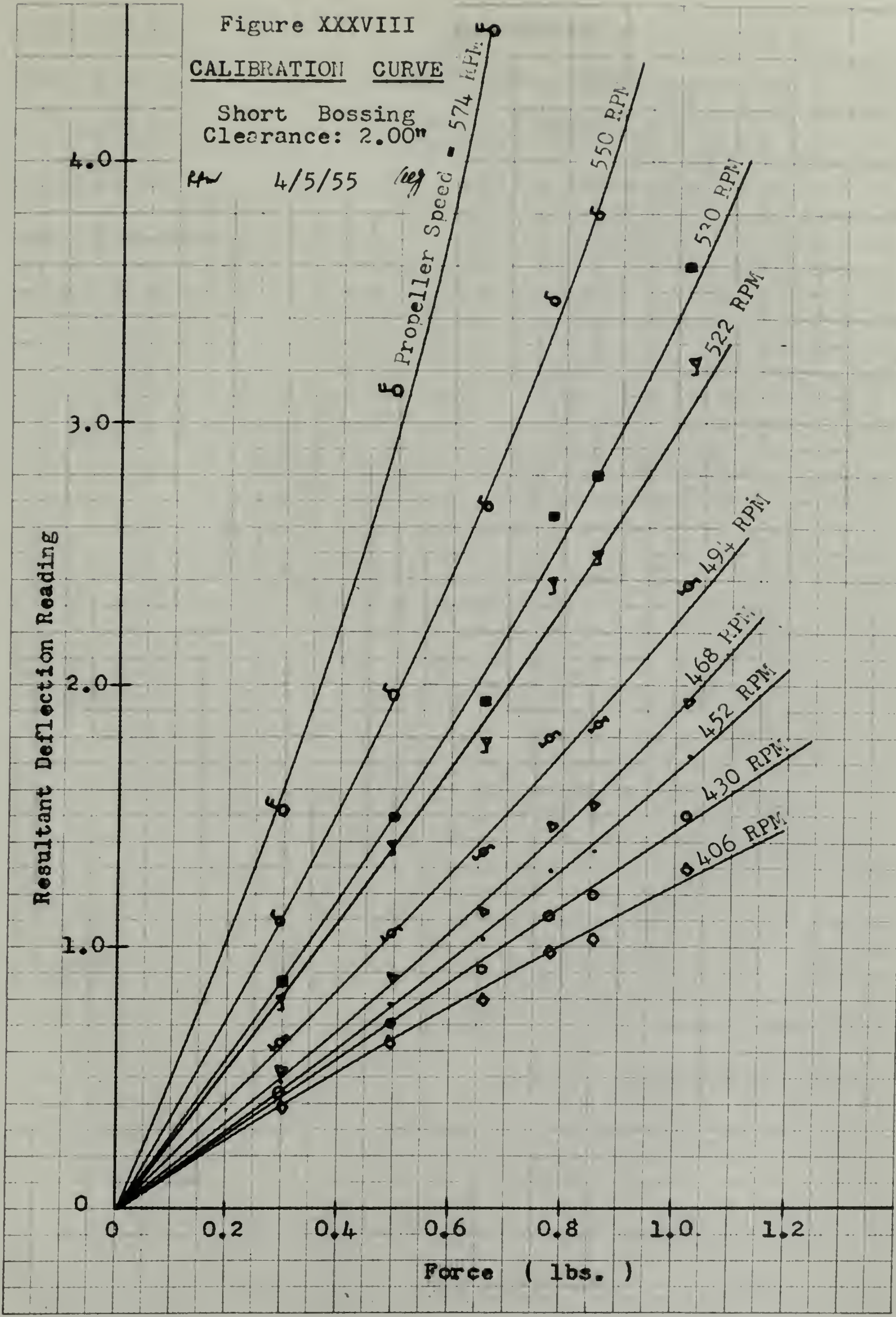

Figure XXXVIII

CALIBRATION CURVE

Short Bossing
Clearance: 2.00"

4/5/55

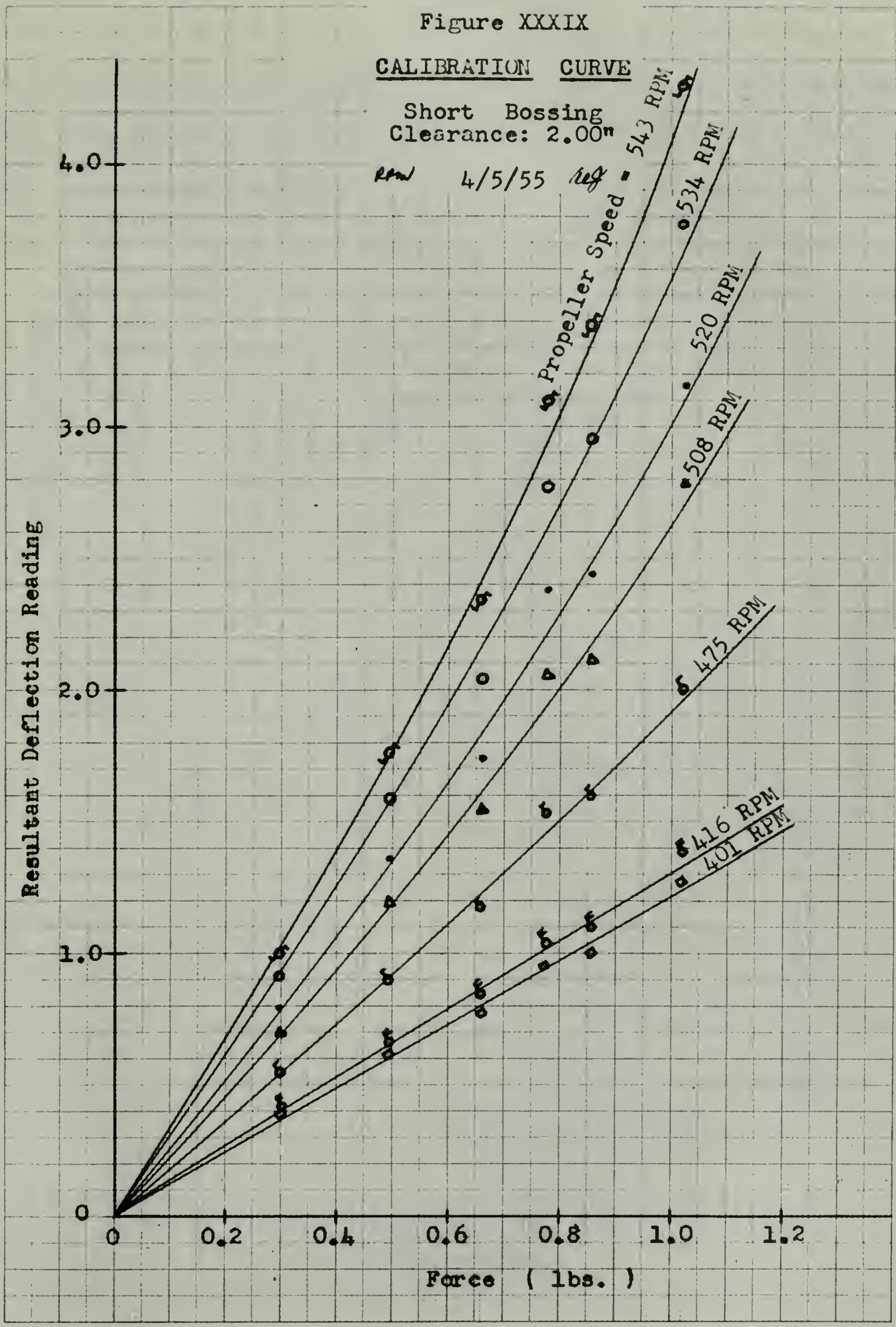

Figure XXXIX

CALIBRATION CURVE

Short Bossing
Clearance: 2.00"

4/5/55

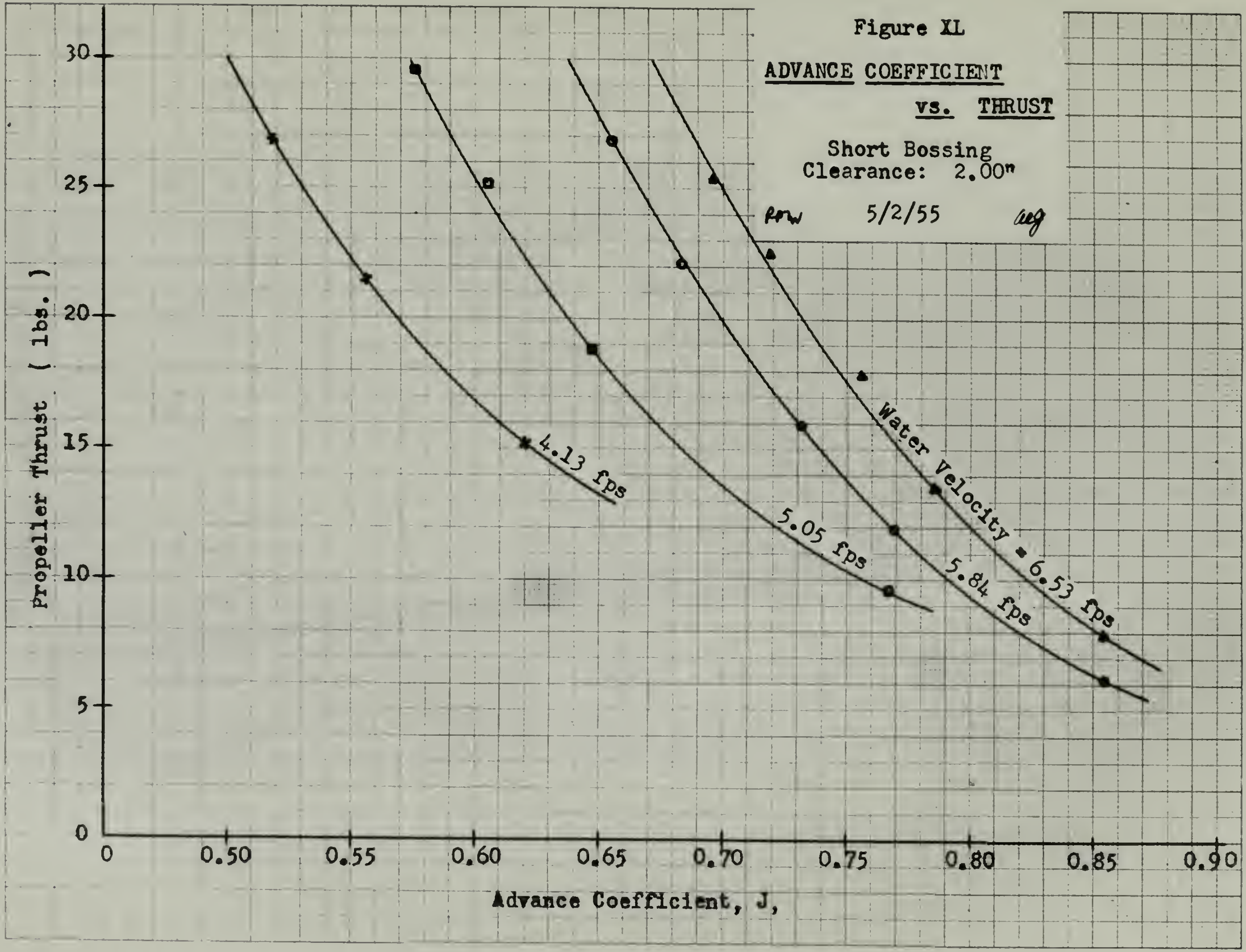

Figure XL

ADVANCE COEFFICIENT vs. THRUST

Short Bossing
Clearance: 2.00"

RPW 5/2/55 aeg

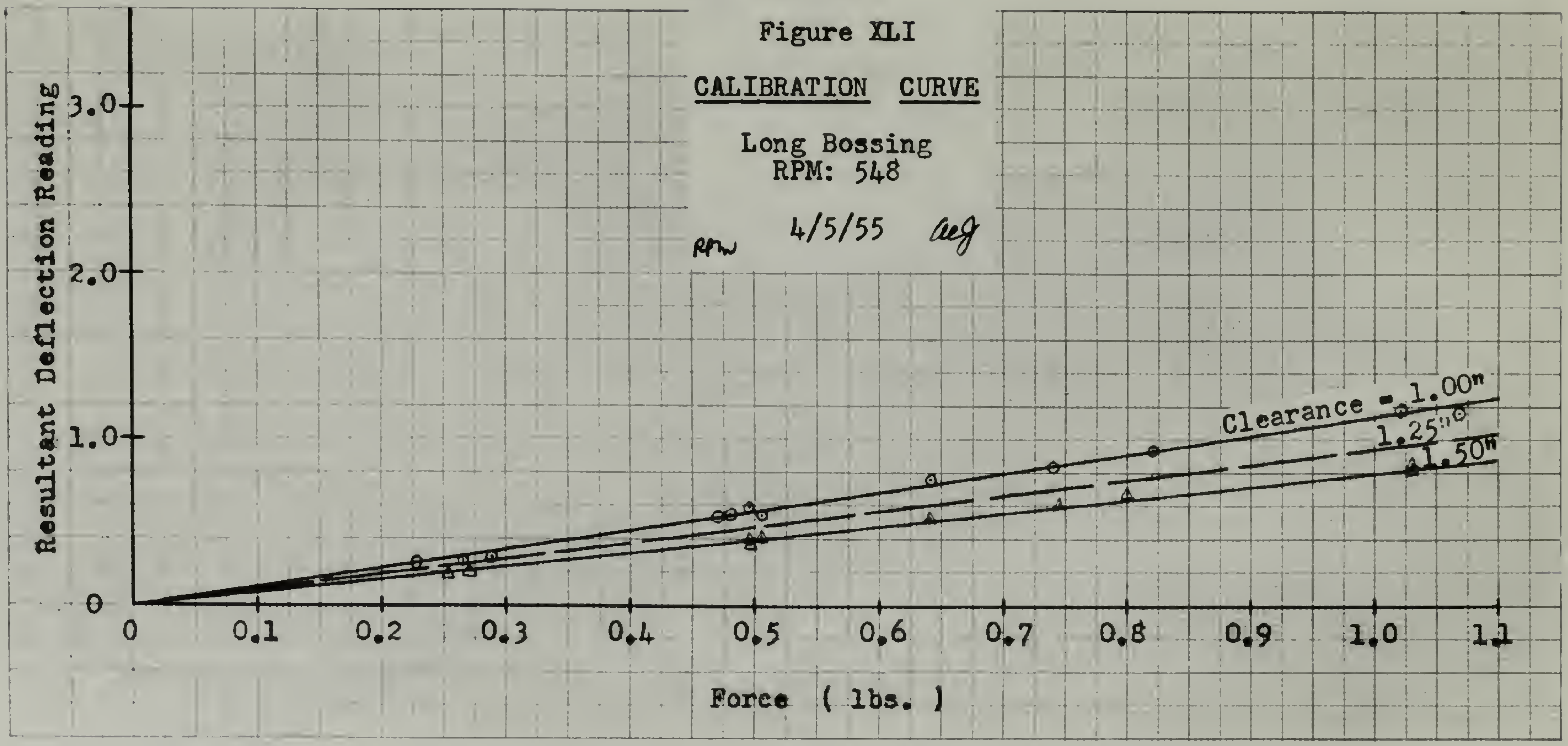

Figure XLI

CALIBRATION CURVE

Long Bossing
RPM: 548

RPW 4/5/55 aeg

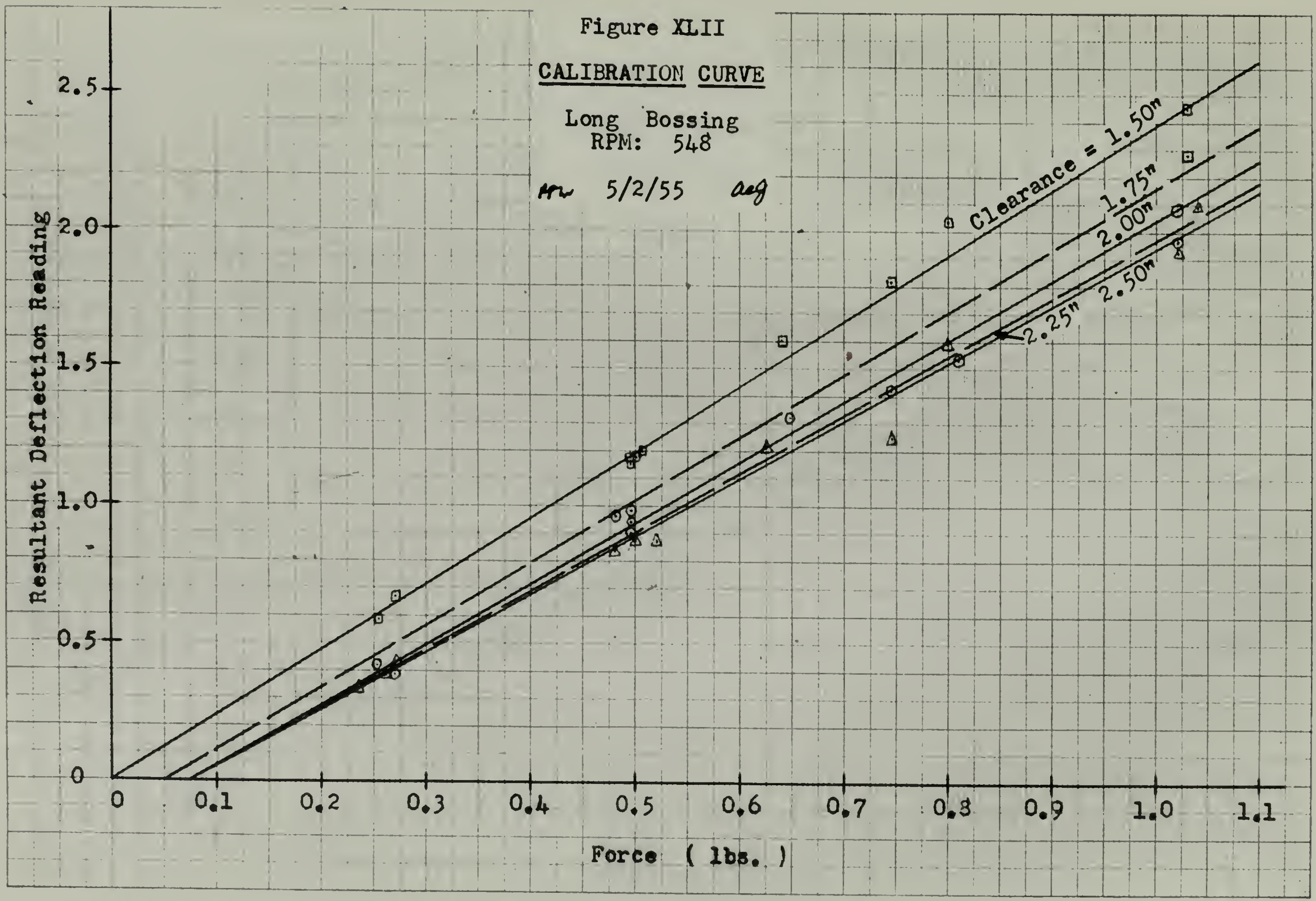

Figure XLII

CALIBRATION CURVE

Long Bossing
RPM: 548

Arw 5/2/55 aeg

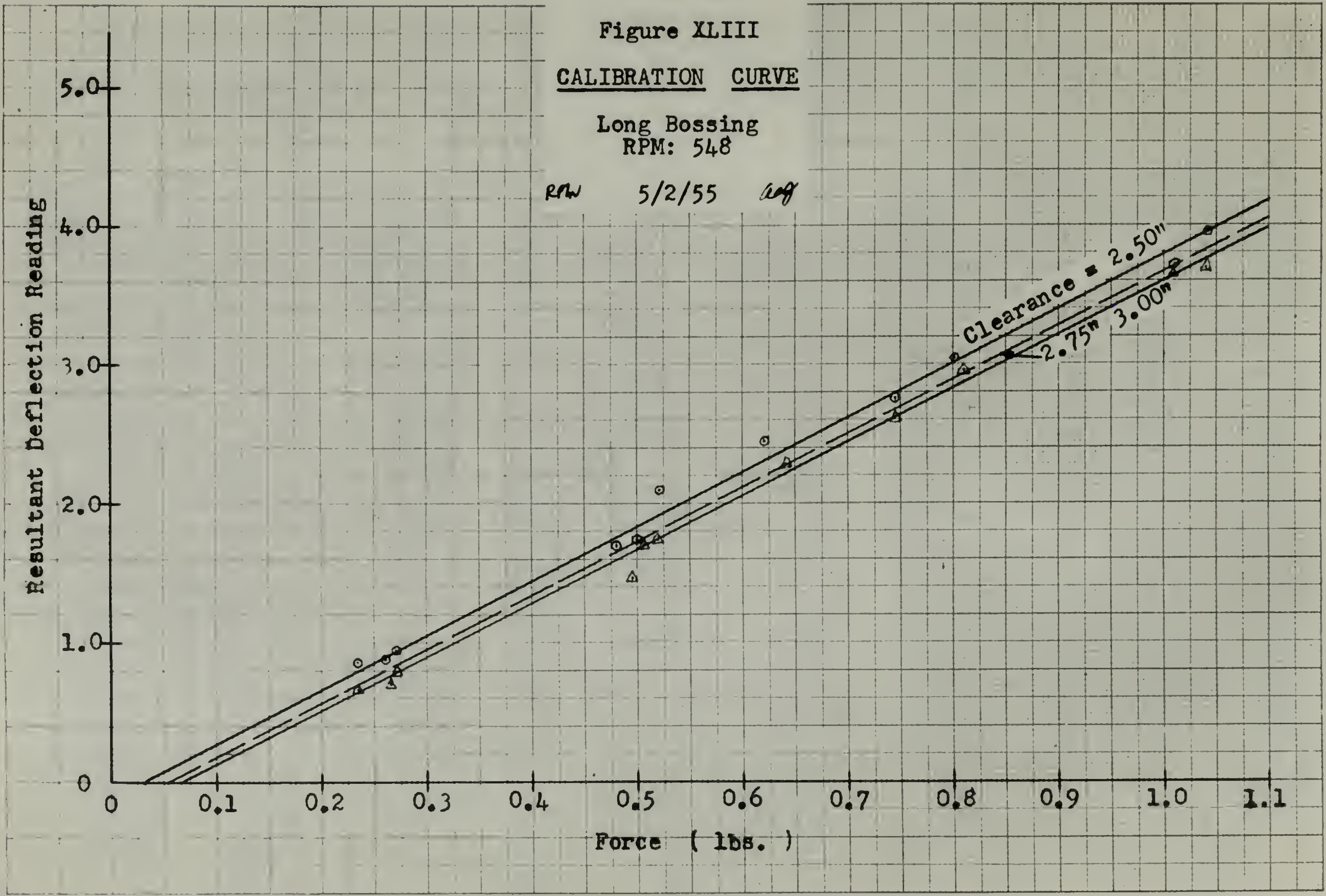

Figure XLIII

CALIBRATION CURVE

Long Bossing
RPM: 548

RAW 5/2/55

APPENDIX D

Bibliography

1. Brown, T.W.F., "Vibration Problems from the Marine Engineering Point of View," Transactions of the North East Coast Institution of Engineers and Shipbuilders, Vol. 55, 1938-1939.
2. Burrill, L.C., "Ship Vibration: Simple Methods of Estimating Critical Frequencies," Transactions of the North East Coast Institution of Engineers and Shipbuilders, Vol. 51, 1934-1935.
3. Calderwood, J., "Some General Observations on Vibration," Transactions of the North East Coast Institution of Engineers and Shipbuilders, Vol. 57, 1940-1941.
4. Constantini, "Vibration of Ships," Transactions of the Institution of Naval Architects, April 1938.
5. Coqueret, F., and Romano, P., "Some Particulars Concerning the Design of the 'Normandie' and the Elimination of Vibration," Transactions of The Society of Naval Architects and Marine Engineers, 1936.
6. Dinsmore, J.R., and Hooper, F.A., "Measurement of Hydrodynamic Vibratory Forces of a Model Propeller," Department of Naval Architecture and Marine Engineering Thesis, M.I.T., 1944.
7. Ellis, J.R., and Henderson, D.B., "Distribution of Hydrodynamic Vibratory Propeller Forces on a Model Propeller Bossing," Department of Naval Architecture and Marine Engineering Thesis, M.I.T., 1943.

8. Inglis, "A Suggested Method of Minimizing Vibration in Ships," *Transactions* of The Institution of Naval Architects, 1933.

9. Lewis, F.M., "Propeller Testing Tunnel at the Massachusetts Institute of Technology," *Transactions* of The Society of Naval Architects and Marine Engineers, 1939.

10. Lewis, F.M., "Propeller Vibration," *Transactions* of the Society of Naval Architects and Marine Engineers, 1935 and 1936.

11. Lewis, F.M., and Tachmindji, A.J., A paper presented at the Annual Meeting of The Society of Naval Architects and Marine Engineers, November 1954.

12. Mallock, A., "A Method of Preventing Vibration in Certain Classes of Steamships," *Transactions* of The Institute of Naval Architects, 1905.

13. McClure, A.C., and Mavor, J.W., "Hydrodynamic Vibratiory Forces Generated by a Ship's Propeller," Department of Naval Architecture and Marine Engineering Thesis, M.I.T., 1950.

14. Pinkerton, D.F., and Arnold, H.A., "Vibratory Hydrodynamic Forces from Ship's Propellers," Department of Naval Architecture and Marine Engineering Thesis, M.I.T., 1941.

15. Reece, H.B., and Lansdowne, F.M., "Further Investigation of Hydrodynamic Vibratory Propeller Forces," Department of Naval Architecture and Marine Engineering Thesis, M.I.T., 1941.

16. Taylor, J. Lockwood, "Vibration of Ships," *Transactions* of the Institution of Naval Architects, 1930.

17. Taylor, J. Lockwood, "Ship Vibration Periods," *Transactions* of the North East Coast Institution of Engineers and Shipbuilders, Vol. 44, 1927-1928.

18. Todd, F.H., "Some Measurements of Ship Vibrations," *Transactions* of the North East Coast Institution of Engineers and Shipbuilders, Vol. 48, 1931-1932.

19. Todd, F.H., "Ship Vibration--A Comparison of Measured with Calculated Frequencies," Transactions of the North East Coast Institution of Engineers and Shipbuilders, Vol. 49, 1932-1933.

[illegible] 28785

J46 Jenks

Propeller excited bossing forces.

Thesis 28785

J46 Jenks

Propeller excited bossing forces.

thesJ46
Propeller excited bossing forces /
3 2768 002 10744 3
DUDLEY KNOX LIBRARY